Bioenergy and its use to mitigate the climate impact of aviation

by

Mark Douglas Staples
B.Sc., Mechanical Engineering, University of Alberta, 2009
S.M., Technology & Policy, Massachusetts Institute of Technology, 2013

Submitted to the Institute for Data, Systems, and Society
in partial fulfillment of the requirements for the degree of

Doctor of Philosophy in Engineering Systems
at the
MASSACHUSETTS INSTITUTE OF TECHNOLOGY
February 2017

Author ..... Signature redacted
Institute for Data, Systems, and Society
December 16, 2016

Certified by ..... Signature redacted
Steven R.H. Barrett
Leonardo-Finmeccanica Associate Professor of Aeronautics and Astronautics, MIT
Thesis Supervisor, Committee Member

Certified by ..... Signature redacted
R. John Hansman
T. Wilson Professor of Aeronautics and Astronautics, MIT
Committee Chair

Certified by ..... Signature redacted
Robert Malina
Professor of Environmental Economics, University of Hasselt
Committee Member

Certified by ..... Signature redacted
James I. Hileman
Chief Scientific and Technical Advisor for Environment and Energy, US FAA
Committee Member

Accepted by ..... Signature redacted
John N. Tsitsiklis
Clarence J. Lebel Professor of Electrical Engineering, MIT
Graduate Officer, Institute for Data, Systems, and Society

Bioenergy and its use to mitigate the climate impact of aviation

by

Mark Douglas Staples

Submitted to the Institute for Data, Systems, and Society on December 16, 2016
in partial fulfillment of the requirements for the degree of
Doctor of Philosophy in Engineering Systems

Abstract

The use of modern bioenergy presents an opportunity to mitigate CO_2 emissions contributing to anthropogenic climate change by offsetting fossil fuel use, and the work presented in this thesis contributes to the literature on bioenergy and climate change mitigation in three areas.

First, this thesis quantifies the maximum potential reduction in global lifecycle greenhouse gas (GHG) emissions from the use of bioenergy to offset demand for fossil fuel-derived electricity, heat and liquid fuels in 2050. The findings indicate that bioenergy could reduce annual emissions from these end-uses by a maximum of 4.9-38.7 Gt CO_2e, or 9-68%. The range of results reflects different assumptions defining potential bioenergy availability, and fossil fuel demand that could by offset by bioenergy, in 2050. In general, assumptions leading to greater calculated bioenergy availability, and fossil fuel demand, correspond to larger reductions in anthropogenic GHG emissions. In addition, offsetting fossil fuel-fired electricity and heat with bioenergy is found to be 1.6-3.9 times more effective for emissions mitigation than offsetting fossil fuel-derived liquid fuel, on average. At the same time, liquid fuels make up 18-49% of global final bioenergy in the scenarios considered for 2050, demonstrating that a mix of bioenergy end-uses maximizes lifecycle emissions reductions. The analysis also finds that GHG emissions reductions are maximized by limiting deployment of total available primary bioenergy to 29-91%, showing that lifecycle emissions including land use change (LUC) are a constraint on the usefulness of bioenergy for mitigating global climate change.

Next, this thesis quantifies the environmental and economic performance of fermentation and advanced fermentation (AF) technologies for the production of renewable middle distillate (MD) fuels, including jet and diesel, in terms of lifecycle GHG emissions and minimum selling price (MSP). The attributional lifecycle GHG emissions of AF MD derived from sugarcane, corn grain and switchgrass are found to range from -27.0 to 19.7, 47.5 to 117.5, and 11.7 to 89.8 gCO_2e/MJ_{MD}, respectively, compared to 90.0 gCO_2e/MJ_{MD} for conventional petroleum-derived MD. These results are most sensitive to the co-product allocation method used, the efficiency and utility requirements of feedstock-to-fuel

conversion, and the co-generation technology employed. The MSP of MD fuel produced from sugarcane, corn grain and switchgrass AF is also calculated as a range from 0.61 to 2.63, 0.84 to 3.65, and 1.09 to 6.30 $USD_{2012}/liter_{MD}$. For comparison, the price of MD fuel was 0.80 $USD_{2012}/liter_{MD}$ when this analysis was initially carried out in 2013, and was \$0.38 $USD_{2012}/liter_{MD}$ at the time of writing. This analysis demonstrates that improvements in overall feedstock-to-fuel conversion efficiency, for example from more efficient sugar extraction, enzymatic hydrolysis, or metabolic conversion processes, could lead to reductions in both the lifecycle GHG emissions and MSP of AF MD fuels.

The final contribution of this thesis is a dynamic cost-benefit assessment (CBA) of a policy of large-scale alternative jet (AJ) fuel adoption, in terms of the societal climate damages and fuel production costs attributable to aviation. A system dynamics model is developed to capture time- and path-dependence of the environmental and economic performance of AJ technologies, as well as potential non-linearities and feedbacks associated with their adoption. The analysis finds that the large-scale use of AJ could result in a reduction in the net present value (NPV) of the societal costs of aviation, in terms of climate damages and fuel costs. However, even for the most promising feedstock-to-fuel production pathways considered, a net reduction in the societal costs of aviation has a probability of less than 50% if the initial societal opportunity cost of AJ feedstock exceeds 140 $USD_{2015}/t_{feedstock}$, or if land use change (LUC) emissions associated with incremental feedstock demand exceed 4.2 $t_{CO2}/t_{inc.\ feedstock}$. These results highlight the potential importance of waste- and residue-derived AJ for reducing the societal costs of aviation, as these feedstocks represent a lower risk of LUC emissions and potentially lower societal opportunity costs than commodity crops.

Thesis Supervisor: Steven R.H. Barrett
Title: Leonardo-Finmeccanica Associate Professor of Aeronautics and Astronautics, MIT

Committee Chair: R. John Hansman
Title: T. Wilson Professor of Aeronautics and Astronautics, MIT

Committee Member: Robert Malina
Title: Professor of Environmental Economics, University of Hasselt

Committee Member: James I. Hileman
Title: Chief Scientific and Technical Advisor for Environment and Energy, US FAA

Acknowledgments

I am very fortunate to have carried out the work presented in this thesis under the guidance of my committee. Thank you to Professor Barrett for giving me the opportunity, and encouragement, to pursue a PhD under your leadership; to Professor Hansman for the always honest, probing, and constructive criticism; to Professor Malina for your enthusiasm, and your academic, professional, and personal mentorship; and to Dr. Hileman for first hiring me back in 2011, and for always ensuring that I had interesting and impactful problems to work on thereafter.

Graduate school would not have been the same without the exceptional colleagues in the Laboratory for Aviation and the Environment with whom I have had the pleasure to work. Thank you to Akshay Ashok, Florian Allroggen, Seamus Bann, Fabio Caiazzo, Tim Galligan, Hakan Olcay, Matthew Pearlson, Cassie Rosen, Ray Speth, Pooja Suresh, Parth Trivedi, Philip Wolfe, and many others, for making work a place I looked forward to coming to each day.

My academic home at MIT was first TPP, then ESD, and finally IDSS, and the wonderful people that I have met and learned from over this scholarly journey are even more plentiful than the acronyms in this sentence. Lifelong friendships are more valuable to me than any academic credential, and I thank you all for your camaraderie. A special nod to those of you with whom I clicked with on day one, and who are still in the MIT/Cambridge orbit (more or less): Michael Chang, Morgan Edwards, Dara Fisher, Amanda Giang, Mac Hird, and Justin Stilwell.

Thank you to all of my dear friends at BT and in the BTYA community. Your support made Boston a home for Barbara and me, and has kept the struggles of completing a PhD properly in perspective.

None of my accomplishments, academic or otherwise, would be possible without my family. I cannot imagine better siblings to look up to, and to count on, than Maril and Bryn, John and Mara, and Lauren and Shawn. Our parents, Moira and Larry, deserve all of the credit for that. Thank you to Mom for being my biggest cheerleader, and to Dad for being the engineer I will always aspire to be.

Thank you to my wife, Barbara. You moved across an ocean to support me in getting this PhD, and for that I am forever grateful. I love you.

Finally, thank you to our unborn daughter. Your imminent arrival provided me with just the push I needed to finish this thing off.

Table of contents

List of abbreviations, acronyms and units

AEZ-EF	Agro-ecological zones emissions factor
AF	Advanced fermentation
AFEX	Ammonia fiber explosion
AJ	Alternative jet fuel
AnF	Anaerobic fermentation
APEC-WG	Asia-Pacific Economic Co-operation Energy Working Group
APMT	Aviation Portfolio Management Tool
APP	Aqueous phase processing
AR5	Assessment report 5
ASTM	American Society for Testing Materials
ASIA	Asia, excluding the Middle East, Japan and Former Soviet States
BCE	Before current era
CapEx	Capital expense
CBA	Cost-benefit assessment
CE	Current era
CH_4	Methane
CI	Confidence interval
CJ	Conventional jet fuel
CO_2	Carbon dioxide
CO_2e	Carbon dioxide equivalent
DCFROR	Discounted cash flow rate of return
DDGS	Distiller dry grains and solubles
EIA	Energy Information Agency
EJ	Exajoule
EtOH	Ethanol
ETP	Energy Technology Perspectives
EU	European Union
FAME	Fatty acid methyl ester

FAOSTAT	Food and Agriculture Organization Statistical programme
FP	Fast pyrolysis
FT	Fischer-Tropsch
FOG	Fats, oils and greases
GAEZ	Global agro-ecological zones
GDP	Gross domestic product
GHG	Greenhouse gas
GJ	Gigajoule
GREET	Greenhouse gases, regulated emissions, and energy use in transportation model
Gt	Gigatonne (metric)
GTAP	Global Trade Analysis Project
GWP_{100}	100-year global warming potential
HEFA	Hydroprocessed esters and fatty acids
HTL	Hydrothermal liquefaction
ICAO	International Civil Aviation Organization
ICE	Internal combustion engine
IGCC	Integrated gasification combined cycle
IEA	International Energy Agency
IEA ETP	International Energy Agency Energy Technology Perspectives
IIASA	International Institute for Applied Systems Analysis
IPCC	Intergovernmental Panel on Climate Change
IPCC AR5	Intergovernmental Panel on Climate Change Assessment Report 5
iBuOH	Isobutanol
K	Potassium
kg	Kilogram
KOH	Potassium hydroxide
kWh	Kilowatt hour
l	Liter
LAM	Latin America
LCA	Lifecycle analysis

LHV	Lower heating value
LUC	Land use change
LUH	Land use harmonization
MAF	Middle East and Africa
MD	Middle distillate
Mha	Megahectare
MJ	Megajoule
MSP	Minimum selling price
MSW	Municipal solid waste
N_2O	Nitrous oxide
N	Nitrogen
NG	Natural gas
NPV	Net present value
OECD	Organization for Economic Co-operation and Development
OpEx	Operating expense
P	Phosphorous
PDF	Probability density function
RCP	Representative concentration pathway
REF	Reforming economies of Eastern Europe and the Former Soviet Union
RFS2	Renewable Fuels Standard 2
RIN	Renewable Identification Number
SI	Sustainability index
SmF	Submerged fermentation
SSP	Shared socioeconomic pathways
t	Tonne (metric)
TAG	Triacylglycerol
TEA	Techno-economic analysis
US	United States
USD	United States dollar
WTP	Well-to-pump
yr	Year

1. Introduction

According to the Intergovernmental Panel on Climate Change (IPCC), *"warming of the climate system is unequivocal,"* and anthropogenic greenhouse gas (GHG) emissions are *"extremely likely to have been the dominant cause of the observed warming"* [1]. Carbon dioxide (CO_2) emissions are of particular importance, as increased atmospheric CO_2 concentrations account for approximately two thirds of radiative forcing contributing to climate change [2]. Furthermore, CO_2 emissions from fossil fuel combustion and other industrial processes make up approximately 60% of total anthropogenic GHG emissions since the pre-industrial era [1]. If unmitigated, climate change will have *"severe, pervasive, and irreversible impacts for people and ecosystems,"* including increased frequency and intensity of extreme weather events, ocean acidification, and sea-level rise [1]. Therefore, reducing CO_2 emissions from fossil fuel combustion is crucial for abating the adverse impacts of global climate change on society.

This thesis focuses on a means of mitigating fossil fuel CO_2 emissions that has historical precedent: the use of biomass to satisfy energy demand. As shown in Figure 1, biomass and charcoal constituted >90% of fuel consumption up until approximately 1700 Current Era (CE), and the dominance of fossil fuels as a source of primary energy source is a relatively new development on the timescale of human history.

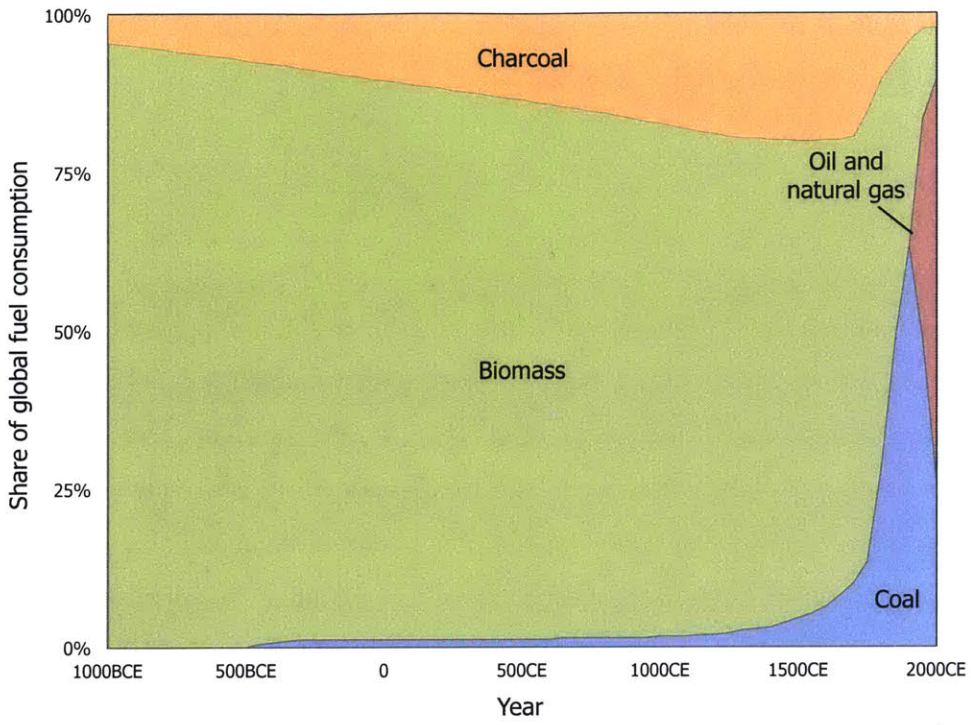

Figure 1: Approximate shares of global fuel consumption, adapted from Smil (2004) [3]. BCE stand for Before Current Era.

Traditionally, biomass has been used as a fuel for cooking, heating, and small-scale manufacturing. However, this thesis concerns the use of modern bioenergy for industrial-scale electricity and heat generation, and the production of liquid transportation fuels, particularly for use in aviation. CO_2 emissions from the combustion of biomass and biomass-derived fuels are biogenic, meaning that carbon in the fuel comes from atmospheric CO_2 recently sequestered during photosynthesis. As a result, bioenergy combustion does not add geologically sequestered carbon to the terrestrial biosphere-atmosphere carbon cycle in the same manner as fossil fuels. In addition to this CO_2 emissions benefit, the use of modern bioenergy is motivated by regionally- and context-dependent factors, including: the desire for domestically-sourced, secure, and diverse energy systems; the promotion of rural economic development; and the renewable nature of biomass resources [4,5].

This thesis quantifies the environmental and economic impacts of mitigating CO_2 combustion emissions from fossil fuels with the use of bioenergy, with an emphasis on

biomass-derived fuels suitable for use in aviation, and in doing so contributes to the field of environmental and economic technology assessment.

Key contributions

The first contribution of this thesis is to quantify the maximum potential reduction in anthropogenic GHG emissions from the use of bioenergy to offset demand for fossil fuels, accounting for lifecycle and land use change (LUC) emissions. The results show that bioenergy could mitigate GHG emissions from fossil fuel-derived electricity, heat and liquid transportation fuels by 9-68% in 2050, but that this potential is constrained by the lifecycle and LUC emissions attributable to bioenergy, as well as the lifecycle emissions of the fossil fuel it is offsetting. As a result, only 29-91% of available primary bioenergy is deployed in order to maximize emissions reductions. The range of scenario results calculated in this analysis show that the magnitude of anthropogenic GHG emission mitigation is a function of the potential availability of bioenergy resources, and the demand for fossil fuels that bioenergy could offset in 2050. In addition, although offsetting fossil fuel-fired electricity and heat with bioenergy is found to be more effective for GHG emissions mitigation on average, the results demonstrate that a mix of bioenergy end-uses, including liquid transportation fuels, is required to maximize to global GHG emissions reductions.

The second contribution is to quantify the lifecycle GHG emissions and minimum selling price (MSP) of renewable middle distillate (MD) fuels from fermentation and advanced fermentation (AF) production technologies. This thesis demonstrates that AF MD fuels could offer a reduction in attributional lifecycle GHG emission of 30-86%, but that this environmental benefit comes at a cost of production that is approximately 2-5 times the cost of conventional petroleum-derived MD fuels. This thesis also quantifies the influence of key technology choices and parameters, such as feedstock type, target platform molecule, and enzymatic and metabolic efficiencies, in order to identify opportunities for reductions in the lifecycle GHG emissions and production costs of AF MD fuels. This analysis shows that both the lifecycle GHG emissions and production costs of AF MD fuels can be reduced through increases in overall feedstock-to-fuel conversion efficiency.

Finally, this thesis presents a dynamic cost-benefit assessment (CBA) of a policy of large-scale adoption of alternative jet (AJ) fuel by quantifying the societal impact in terms of climate damages and fuel production costs. The findings show that large-scale AJ adoption could reduce the costs of aviation to society, but that this is contingent on a number of parameters. The lifecycle GHG emissions and production cost characteristics of the AJ feedstock-to-fuel pathway of interest, the societal opportunity cost of feedstock, the LUC emissions associated with incremental feedstock demand, and the assumed societal discount rate, are all found to drive the balance of the societal costs and benefits of a policy of large-scale AJ adoption. The results show that a net reduction in the climate damages and fuel production costs of aviation has a probability of less than 50% unless the initial societal opportunity cost of AJ feedstock is below 140 $USD_{2015}/t_{feedstock}$, and LUC emissions associated with incremental feedstock demand are less than 4.2 $t_{CO2}/t_{inc.\ feedstock}$. These results demonstrate that minimizing the risk of LUC emissions, and the societal opportunity costs of feedstock, maximizes the probability of a reduction in the societal climate and fuel production costs of aviation. The use of AJ derived from waste and residue feedstocks is identified an opportunity to achieve both of these objectives.

Thesis organization

The remainder of this thesis is organized as follows: Chapter 2 quantifies the limits of global bioenergy resources to mitigate fossil fuel GHG emissions; Chapter 3 presents a lifecycle and techno-economic analysis of AF production technologies; and Chapter 4 presents a dynamic CBA of large-scale AJ adoption. Chapters 2, 3 and 4 are each organized by Motivation and context, Methods and materials, Results and discussion, and Summary sections. Chapter 5 summarizes the conclusions of this thesis, and briefly discusses areas for future work.

2. The limits of bioenergy for mitigating global lifecycle greenhouse gas emissions from fossil fuels

Motivation and context

The use of bioenergy, in the form of biomass or biomass-derived fuels, represents an opportunity to reduce anthropogenic greenhouse gas (GHG) emissions from fossil fuels. This is due to the biogenic nature of combustion CO_2 emissions from bioenergy that, in contrast to fossil fuels, do not represent an addition of CO_2 to the terrestrial biosphere-atmosphere carbon cycle.

However, there are also GHG emissions associated with the cultivation, transportation, and conversion of bioenergy to final energy products, and lifecycle analysis (LCA) is a method that has been employed to quantify these emissions. For example, the Greenhouse Gases, Regulated Emissions, and Energy Use in Transportation (GREET) model, among others, has been used to quantify the lifecycle 100-year global warming potential (GWP_{100}) CO_2-equivalent (CO_2e) emissions attributable to biomass-derived transportation fuels [6-12], electricity, heat and other energy carriers [12-14], as well as their fossil fuel analogs. In addition, consequential LCA has been used to estimate the aggregate change in emissions to the environment due to specific policies or actions by employing partial- and general-equilibrium economic models of the market-mediated impacts of bioenergy use. A number of studies have demonstrated the importance of consequential lifecycle emissions associated with the large-scale adoption of bioenergy, specifically the contribution of CO_2 emissions from land use change (LUC) [15-17]. LUC emissions occur when a parcel of land is used in a different way than it had been used previously, resulting in a one-time change in the quantity of carbon stored in the soil and biomass on that land. For example, the conversion of natural grassland in the US to cropland for corn cultivation results in a reduction of the soil and biomass carbon stock of the land of approximately 37 Mg_C/ha [18], and this carbon is

emitted to the atmosphere as CO_2 through biomass burning or microbial decomposition [19,20].

A large body of work has also quantified the size of the global bioenergy resource. Early studies focused on estimating the land area available for cultivation and future biomass productivity, finding that many hundreds of exajoules of primary bioenergy are potentially available annually [21,22]. Subsequent studies have quantified bioenergy potentials that are cost-effective, avoid competition with food or feed production, or limit the environmental impacts of large-scale adoption [23-25]. Generally, these additional considerations result in lower estimates of primary bioenergy potential, on the order of approximately 100 EJ/yr.

Despite these advances, significant uncertainties remain in the literature regarding the determinants of global bioenergy availability. For example, a recent review of 90 studies indicates that by mid-century bioenergy crops, forestry, residues, and wastes could satisfy ~100-600 EJ of annual global primary energy demand, where the broad range of results are driven primarily by assumptions regarding future demand for food, agricultural productivity gains, and the availability of land for energy crop cultivation [26]. For context, the International Energy Agency (IEA) estimates that global demand for primary energy will be between 681 and 929 EJ/yr by 2050 [27] Although this continues to be an active area of research, no peer-reviewed analysis to date has quantified the potential for bioenergy to contribute to anthropogenic GHG emissions reductions, accounting for both the limits of bioenergy availability and lifecycle GHG emissions including LUC.

This chapter presents a model of future land availability, areal bioenergy yields, and lifecycle emissions including LUC, with the aim of establishing the relationship between global availability of bioenergy and the potential for GHG emissions reductions. The hypothesis behind this analysis is that the use of bioenergy for GHG emissions mitigation is constrained not only by growth in biomass productivity and the availability of land for energy crop cultivation in the future, as has been established in the literature [26], but also by the lifecycle emissions of final energy derived from biomass relative to the fossil fuels that bioenergy would replace. This hypothesis is tested by quantifying the maximum achievable reductions in lifecycle GHG emissions in 2050 from the allocation and deployment of bioenergy

resources to offset fossil fuels. The findings represent an estimate of the limits of the GHG mitigation potential of bioenergy, and of the degree to which bioenergy can contribute to climate stabilization goals by mid-century.

Methods and materials

In order to quantify the potential for bioenergy to mitigate lifecycle GHG emissions from fossil fuels, there are four major components to the analysis presented here: the availability of primary bioenergy; the availability of final energy carriers derived from primary bioenergy and the associated lifecycle GHG emissions; fossil fuel final energy that could potentially be offset by bioenergy and the associated lifecycle GHG emissions, and; the allocation of bioenergy resources amongst competing end-uses to maximize GHG emissions reductions.

Primary bioenergy availability

Energy crops

The potential availability of energy crops in 2050 is quantified by using data from three sources: Food and Agriculture Organization of the United Nations, Statistics Division (FAOSTAT) data is used to project average energy crop yields in future years based on empirical data [28]; maximum agro-climatically attainable yields from the Global Agro-ecological Zones model (GAEZ) are scaled to reflect geo-spatial heterogeneity in crop yields, and to provide a theoretical upper bound on areal yields of above ground biomass [29]; and the Land Use Harmonization (LUH) database is used to estimate land availability for energy crop cultivation in 2050 [30].

An example of the yield projection method is shown in Figure 2 for soybean oil in the countries of the Organization for Economic Co-operation and Development (OECD). FAOSTAT empirical yield data is collected for five world regions [28]: the Middle East & Africa (MAF); Latin America (LAM); Asia, excluding the Middle East, Japan and Former

Soviet States (ASIA); OECD countries, and; the reforming economies of Eastern Europe and the Former Soviet Union (REF). The yield data is then extrapolated in each world region under three different linear yield growth rate assumptions, corresponding to: the same rate as the slowest world region from 1995-2015; the same rate as the fastest world region from 1995-2015; and the same rate as the region of interest from 1995-2015. The extrapolated areal yields are limited on the high end by maximum agro-climatically attainable average yields in the region of interest from the GAEZ model [29], as can be seen for the high growth rate case in Figure 2. This procedure is repeated for 8 crop types in each world region. The resulting average yield projections are used to scale geo-spatially resolved data from the GAEZ model, in order to reflect location-specific heterogeneity in crop yields.

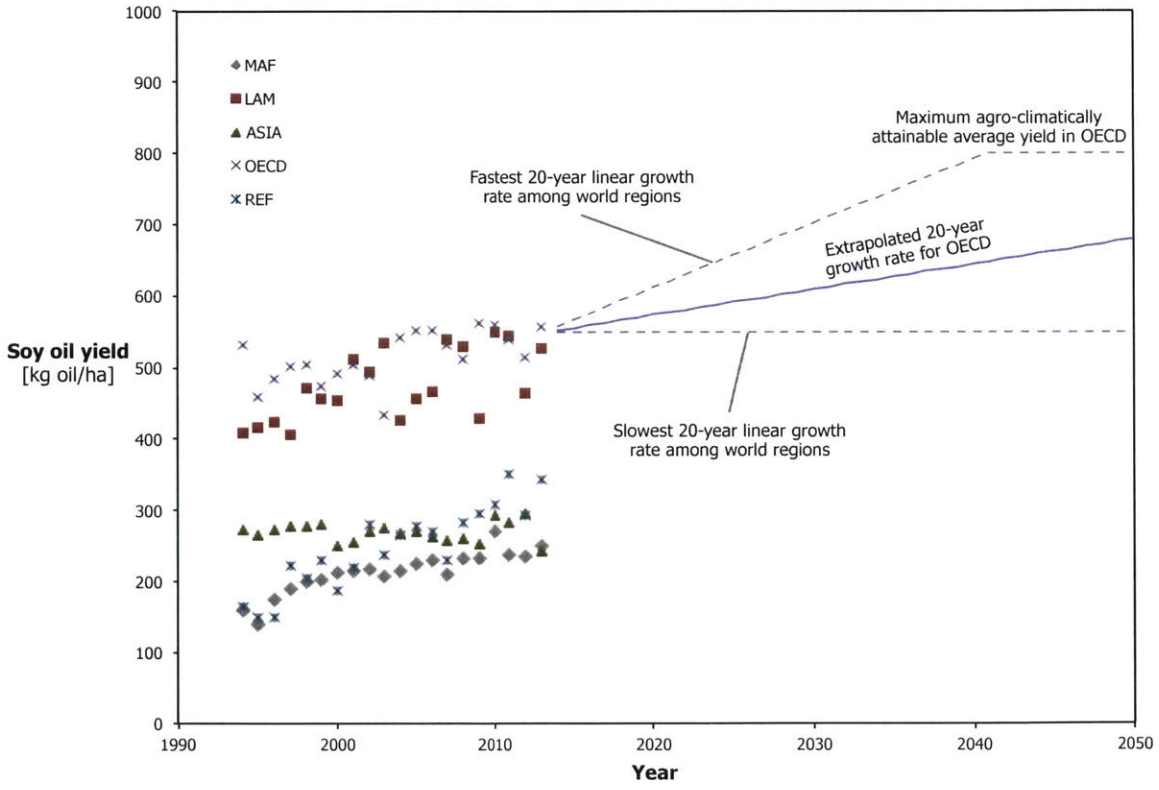

Figure 2: Extrapolation of soybean oil yields to 2050 in OECD countries.

The availability of arable land for energy crop cultivation is estimated based on LUH data, which describes projected 2050 land use patterns at 0.5° resolution in terms of five categories: cropland, pastureland, urban land, primary land and secondary land [30]. This analysis assumes the priority of land requirements for food and feed production, human

development, and eco-system protection in 2050, meaning that all land areas projected for these uses are assumed *a priori* to be unavailable for energy crop cultivation.

100 cm soil and biomass carbon stock data developed for Global Trade Analysis Project (GTAP) Agro-ecological Zones Emissions Factor (AEZ-EF) database is used to account for emissions from LUC to establish energy crops on forestland and pastureland [31]. LUC emissions factors are calculated in t_{CO2}/ha for the conversion of forested or pastureland to the cultivation of C3 crops (e.g. soybean, rapeseed, jatropha, cassava, sugarbeet, reed canary grass), C4 crops (e.g. switchgrass, corn grain, sorghum, miscanthus), palm oil, or sugarcane.

Combining the areal yield, land availability, and LUC emissions data described above results in a database of energy crop production potential and the associated LUC emissions in 2050 from starchy, sugary, vegetable oil and lignocellulosic energy crops, globally resolved at 0.083°. Note that, although this analysis does not explicitly consider primary bioenergy availability from forestry (other than residues), the potential availability of bioenergy from the establishment of energy crop cultivation (including lignocellulosic crops) on forestlands is included.

Residue and waste feedstocks

Primary bioenergy from crop residues is calculated from the potential availability of energy crops, as described above, coupled with a range of food crop production projections that reflect the Shared Socio-economic Pathways (SSP) from the Intergovernmental Panel on Climate Change (IPCC) [32]. Residue to primary crop ratios are estimated from Lal (2005), and a range of net residue availability of 14.0% to 47.5% is assumed [33-36].

The availability of primary energy from forestry residues is quantified from estimates of industrial roundwood and woodfuel production in 2050 [37], combined with estimates of the net availability of logging and wood processing residues that range from 8.0% to 35.5% and 1.0% to 26.3%, respectively [36-38].

The availability of waste fats, oils and greases (FOG) is estimated from livestock production projections scaled to the SSP scenarios [39], together with a range of estimates of livestock species-specific net waste FOG availability [40-42].

Scenario definition for primary bioenergy availability

In order to capture variability in the underlying assumptions, three scenarios (low, mid, and high) are defined for the availability of primary bioenergy in 2050. The parameter assumptions that correspond to the three scenario definitions can be found in Table 1.

Table 1: Parameter definition for 2050 primary bioenergy availability scenarios

		Low	Mid	High
Energy crops	Energy crop yield growth	Low	Mid	High
	2050 land use scenario from LUH database	RCP 8.5	RCP 6.0	RCP 4.5
	Pastureland availability	0.0%	10.0%	20.0%
	Agro-climatic suitability threshold	SI > 70 [IIASA 2012]	SI > 55 [IIASA 2012]	SI > 40 [IIASA 2012]
Residue & waste	Socio-economic scenario from SSP database	SSP3	SSP4	SSP5
	Net crop residue availability	14.0%	28.9%	47.5%
	Net forest residue availability	Logging: 8.0% Processing: 1.0%	Logging: 19.8% Processing: 8.1%	Logging: 35.5% Processing: 26.3%
	Net waste FOGs availability	30.0%	50.0%	70.0%

Further detailed information about the methods and data used to model 2050 primary bioenergy availability, as well as derivation of the parameters and assumptions defined in Table 1, can be found in Appendix A.

Final bioenergy availability and associated lifecycle GHG emissions

The availability of final energy derived from biomass, and the associated lifecycle GHG emissions per unit of final energy, is calculated by considering four potential end-uses for bioenergy: biomass combustion for electricity generation; biomass combustion for heat generation; production of renewable liquid fuels interchangeable with light distillate petroleum-derived fuels (such as ethanol or renewable gasoline); and production of renewable liquid fuels interchangeable with middle and heavy distillate petroleum-derived fuels (such as renewable diesel). It is important to note that biomass resources could also be allocated to end-uses beyond those studied here in order to mitigate GHG emissions, such as bio-chemicals or the use of plant-based foods to offset demand for livestock production. However, this analysis focuses on these four end uses because energy-related emissions currently make up approximately 68% of total annual anthropogenic GHG emissions [43].

In order to capture these different feedstock end-uses, 35 representative biomass-to-final energy carrier pathways are modeled. The conversion efficiencies, attributional lifecycle GHG emissions factors, and energy allocation factors for LUC emissions associated with each conversion pathway, are derived from the GREET1 2015 database. Lifecycle GHG emissions factors are reported in grams of GWP_{100} CO_2e per MJ of final energy, according to IPCC AR5 [44]. This data is given in Table 2.

Because this analysis is carried out for 2050, and the infrastructure required to produce the calculated quantities of final bioenergy would need to be newly constructed, the highest efficiency feedstock-to-final energy conversion factors in the GREET1 2015 database are assumed. In the case of bio-heat and bio-electricity generation, these are industrial boiler and integrated gasification combined cycle (IGCC) technologies, with thermal efficiencies of 80% and 45%, respectively. The allocation ratios reported in Table 2 correspond to an assumption of energy allocation at all steps of the LCA. Note here that the lifecycle GHG emissions factors listed in Table 2 do not include LUC emissions associated with the establishment of energy crop cultivation on pastureland and forestland, and that LUC emissions are accounted for in a subsequent step using the GTAP AEZ-EF database [28].

Table 2: Feedstock-to-final energy conversion factors, LUC allocation ratios and attributional lifecycle GHGs.

Final fossil carrier offset	Final energy carrier	Feedstock	Feedstock-to-final energy conversion technology	Feedstock-to-final energy conversion [$MJ_{final\ energy}/kg_{feedstock}$]	Feedstock units	Energy allocation factor for LUC emissions	Attrib. LCA GHG of final energy carrier [$gCO_2e/MJ_{final\ energy}$]	Source
Middle & heavy distillate fuels	Renewable diesel	Soybean	Hydroprocessed esters and fatty acids (HEFA)	39.6	Oil	42.1%	31.5	GREET1 2015
		Rapeseed				68.7%	39.1	
		Jatropha				70.2%	38.8	
		Palm oil				92.9%	23.7	
		Switchgrass	Fischer-Tropsch gasification and synthesis	8.4	Dry biomass	100.0%	8.9	
		Miscanthus		8.9			6.6	Derived from miscanthus renewable diesel
		Reed canary grass						
		Agricultural residue		10.1			5.5	GREET1 2015
Light distillate fuels	EtOH	Corn grain	Fermentation	9.3	Corn grain (15.5% mst.)	60.9%	40.9	GREET1 2015
		Grain sorghum			Sorghum grain (12.4% mst.)		50.4	
		Cassava		3.3	Cassava root (59.7% mst.)		40.9	Derived from corn grain ethanol on the basis of starch content
		Sugarcane		1.7	Wet sugarcane (50% mst.)	82.7%	24.5	GREET1 2015
		Sugarbeet		2.4	Sugarbeet root (75% mst.)			Derived from sugarcane ethanol on the basis of sugar content
		Switchgrass	Enzymatic hydrolysis and fermentation	7.5	Dry biomass	90.8%	17.7	GREET1 2015
		Miscanthus		8.0			11.9	Derived from miscanthus renewable ethanol
		Reed canary grass						
		Agricultural residue		9.0			9.2	GREET1 2015
	Renewable gasoline	Soybean	Fischer-Tropsch gasification and synthesis	36.6	Oil	42.1%	29.3	GREET1 2015
		Rapeseed				68.7%	35.9	
		Jatropha				70.2%	35.5	
		Palm oil				92.9%	17.7	
		Waste FOG				100.0%	34.4	
		Switchgrass		8.3	Dry biomass		8.8	
		Miscanthus		8.9			6.5	Derived from miscanthus renewable gasoline
		Reed canary grass						
		Agricultural residue		10.0			5.5	GREET1 2015
Fossil fuel-fired heat	Bio-fired heat	Switchgrass	Industrial boiler (η=80%)	16.8	Dry biomass	100%	11.2	GREET1 2015
		Miscanthus		17.8			7.3	Derived from miscanthus-fired heat generation
		Reed canary grass						
		Agricultural residue		17.1			13.8	GREET1 2015
Fossil fuel-fired electricity	Bio-fired electricity	Switchgrass	Integrated gasification combined cycle (IGCC) (η=45%)	7.6	Dry biomass	100%	27.5	GREET1 2015
		Miscanthus		8.0			18.7	Derived from miscanthus-fired electricity generation
		Reed canary grass						
		Agricultural residue		7.7			18.8	GREET1 2015
		Forestry residue		9.1			12.8	

Fossil fuel-derived final energy and associated lifecycle emissions

The GHG emissions mitigation potential of bioenergy depends upon the quantity and lifecycle emissions of the fossil fuels that it could offset. Therefore, 2050 projected demands for fossil fuel-derived transportation fuels, electricity, and heat are taken from the 2DS, 4DS and 6DS scenarios of the 2014 International Energy Agency Energy Technology Perspectives (IEA ETP) report and database [27]. These scenarios reflect three possible futures for the global energy system in 2050, resulting in projected mean global temperature changes of 2°C, 4°C and 6°C by 2100. In addition, a distribution of the lifecycle GHG emissions associated with each of the end uses is estimated in order to reflect the global distribution of fossil fuel-to-final energy pathways with differing lifecycle GHG emissions.

Crude oil-derived transportation fuels

The proportion of crude oil from conventional (including natural gas liquids for the purposes of lifecycle GHG emissions) and unconventional sources (oil sands and tight oil for the purposes of lifecycle GHG emissions) is estimated from the IEA World Energy Outlook (2014) [45]. The resulting demand for light, middle, and heavy distillate fuels, and the crude oil mix is shown in Table 3.

Table 3: Summary of 2050 petroleum-derived light- and middle & heavy distillate final energy demand, and crude oil mix.

Mean global temperature change by 2100 [IEA ETP 2014]	Global light distillate fuel final energy demand [EJ/yr]	Global middle & heavy distillate fuel final energy demand [EJ/yr]	Proportion of crude oil from conv. sources [%]	Proportion of crude oil from unconv. sources [%]
2°C	14.3	28.6	89.1%	10.9%
4°C	60.6	54.7	83.9%	16.1%
6°C	74.8	60.1	82.7%	17.3%

A truncated triangular distribution of emissions factors is fit to the 2050 projections for global final energy demand for transportation fuels. The maximum and minimum emissions factors for light- and middle- & heavy-distillate fuels are defined by the values for gasoline and diesel derived from Canadian oil sands and conventional crude production, respectively,

from GREET1 2015, and the average value is the weighted average of the unconventional and conventional values, defined by the proportions shown in Table 3 [44]. The resulting distribution parameters are shown in Table 4.

Table 4: Triangular distribution parameters for light- and middle- & heavy-distillate transportation fuel final energy demand in 2050.

Mean global temperature change by 2100 [IEA ETP 2014]	Light distillate fuel [gCO_2e/MJ_{LD}]			Middle & heavy distillate fuel [gCO_2e/MJ_{MD}]		
	Min	Max	Peak	Min	Max	Peak
2°C			97.6			91.2
4°C	95.2	117.0	98.7	88.9	109.9	92.3
6°C			99.0			92.6

Fossil fuel-fired electricity

2050 demand for combustion-generated electricity, and the proportions of electricity generated from coal, oil and natural gas, is estimated from the IEA ETP temperature change scenarios [27], and global average thermal efficiency of electricity generation is estimated for each fuel by dividing final energy demand by primary energy demand in each scenario. Average thermal efficiency is used to estimate the average lifecycle GHG emissions factor of electricity generated from each fuel source, and the lowest and highest efficiency technologies for that fuel source define the maximum and minimum emissions factors from GREET1 2015 [44]. These parameters are used to fit a truncated triangular distribution of emissions factors to the 2050 projections for global final energy demand from coal, oil and natural gas-fired electricity generation. This data is given in Table 5, broken out by scenario and fuel source.

Table 5: Summary of 2050 fossil fuel-fired electricity demand and triangular distribution parameters.

Fuel source	Mean global temperature change by 2100 [IEA ETP 2014]	Final energy electricity demand [EJ/yr]	Average thermal efficiency [%]	LCA emissions factor [gCO_2e/MJ_{elec}]			Note
				Min	Max	Average	
Coal	2°C	16.8	38.4%	240.2	284.4	282.0	Min - IGCC Max - steam cycle
	4°C	44.5	41.7%			261.1	
	6°C	71.3	39.8%			272.8	
Oil	2°C	0.4	40.0%	249.0	292.9	249.0	Min - ICE Max - oil-fired gas turbine
	4°C	0.9	40.0%				
	6°C	1.6	40.0%				
Natural gas	2°C	21.3	50.5%	119.1	228.4	162.6	Min - IGCC Max - NG-fired ICE
	4°C	44.8	53.0%			151.1	
	6°C	52.8	53.1%			150.7	

Fossil fuel-fired heat

2050 demand for combustion-generated heat, and the proportional mix of fossil fuels, is also defined by the IEA ETP temperature change scenarios [27]. A range of lifecycle GHG emissions factors for each fossil fuel is estimated from GREET1 2015, and is used to fit a truncated triangular distribution of emissions factors to the 2050 projections for global final energy demand from coal, oil and natural gas-fired heat generation, given in Table 6.

Table 6: Summary of 2050 fossil fuel-fired heat demand and triangular distribution parameters.

Fuel source	Mean global temperature change by 2100 [IEA ETP 2014]	Final energy heat demand [EJ/yr]	LCA emissions factor [gCO_2e/MJ_{heat}]			Note
			Min	Max	Average	
Coal	2°C	37.4	95.0	107.3	101.2	Average defined by fuel combustion in an industrial boiler
	4°C	49.1				
	6°C	54.6				
Oil	2°C	22.7	81.1	107.0	94.2	
	4°C	33.3				
	6°C	38.8				
Natural gas	2°C	73.4	56.5	78.7	67.6	
	4°C	87.2				
	6°C	94.3				

The data shown above demonstrates that the 6°C scenario from the IEA ETP (2014) corresponds to the greatest projected demand, and the 2°C scenario corresponds to the lowest projected demand for fossil fuels. Therefore, for the remainder of this Chapter, the IEA ETP (2014) scenarios are referred to as low, mid and high fossil fuel demand scenarios [27].

Maximization of GHG emissions mitigation

In cases where multiple energy crop types could potentially be grown on the same parcel of land, and those different primary bioenergy carriers could be used for different end uses, the feedstock and conversion pathway that results in the greatest annual reduction in GHG emissions is selected. This accounts for the lifecycle GHG and LUC emissions associated with the bioenergy pathway, as well as the lifecycle GHG emissions of the unit of fossil fuel energy that would be offset. For a given original land use type k in each 0.083° grid cell g, the maximum reduction in GHG emissions $R_n(k,g)$ via bioenergy pathway n is defined by Equation 1.

Equation 1: Maximization of GHG emissions reduction from offsetting fossil fuels with bioenergy.

$$R_n(k,g) = \max_{n \in [N]} \left\{ [LC_{fossil}(n) \cdot y(n) \cdot c(n) \cdot a(k)] - \left[\left(LC_{bio}(n) \cdot y(n) \cdot c(n) \cdot a(k) \right) + \left(\frac{\omega(n) \cdot LUC(k) \cdot a(k)}{m} \right) \right] \right\}$$

where

$R_n(k,g)$ = max. GHG emissions reduction on land type k (pasture or forestland) in cell g [gCO_2e/yr]

$[N] = \left\{ \begin{matrix} \text{veg. oil to ren. gas or diesel} \\ \text{sugary or starchy crop to EtOH, ren. gas or dies} \\ \text{lignocell. crop to elec, heat, EtOH, ren. gas or dies.} \end{matrix} \right\}$; set of 35 bioenergy pathways

$LC_{fossil}(n)$ = attrib. LC emissions from fossil fuel analog to bioenergy pathway n [$gCO_2e/MJ_{final\ energy}$]

$LC_{bio}(n)$ = attrib. LC emissions from bioenergy pathway n [$gCO_2e/MJ_{final\ energy}$]

$y(n)$ = grid cell specific areal yield of bioenergy crop n [$kg_{crop}/ha/yr$]

$c(n)$ = conversion efficiency of bioenergy crop n to final energy [$MJ_{final\ energy}/kg_{crop}$]

$a(k)$ = grid cell specific area available for bioenergy crop cultivation on land type k [ha]

$\omega(n)$ = energy allocation factor of feedstock emissions to final energy carrier [%]

$LUC(k)$ = grid cell specific LUC emissions from conv. of land type k to bioenergy cultivation [gCO_2/ha]

m = LUC emissions amortization period [yr]

The primary energy, final energy, and specific lifecycle GHG emissions per unit of final energy (including LUC emissions), corresponding to bioenergy pathway n that maximizes GHG reductions, is calculated for each land use type k, in each grid cell g. Similarly, each waste and residue feedstock type (for which there are no k, y(n), a(k), ω(n), LUC(k) or m parameters) is allocated to the conversion pathway that results in the greatest annual reduction in GHG emissions from offsetting fossil fuel use, using a simplified version of the above $R_n(k,g)$ formula.

Energy allocation is used at all stages of the LCA, and LUC emissions are amortized evenly over a 30-year period with no discounting (parameter m) [46]. Results are also calculated assuming a 20-year amortization period to demonstrate the sensitivity of results to this particular assumption. [47]. The feedstock-to-fuel specific value of parameters $LC_{bio}(n)$, c(n) and ω(n) are defined in Table 2.

The maximization routine shown in Equation 1 is performed iteratively, beginning with the highest values of $LC_{fossil}(n)$ from the distributions defined in the previous section, and decreasing as greater final bioenergy deployment corresponds to lower lifecycle GHG emissions fossil fuel final energy remaining to be offset. This is done in increments of 5 EJ/yr of final bioenergy, requiring between 7 and 73 iterations to achieve convergence in all scenarios.

The resulting maximum GHG emissions reduction of final bioenergy allocation and deployment R_{tot} is calculated by summing all positive values of $R_n(k,g)$ over all land types k and grid cells g, given by Equation 2.

Equation 2: Maximum reduction in GHG emissions from offsetting fossil fuels with bioenergy.

$$R_{tot} = \sum_{g\in[G]} \sum_{k\in[K]} R_n\,(k, g),$$

where

R_{tot} = total max. GHG emissions reduction from final bioenergy [gCO_2e/yr]

[G] = set of all grid cells

[K] $= \left\{ \begin{matrix} \text{pasture} \\ \text{forestland} \end{matrix} \right\}$; set of all original land use types

for

$R_n(k, g)$ > 0.

Payback period

Payback period is defined as the time required for the difference in attributional lifecycle GHG emissions (excluding LUC emissions) between bioenergy pathway n and the fossil fuel analog to make up for a one-time pulse of LUC emissions. This metric is also calculated for the results presented below, and is given by Equation 3.

Equation 3: LUC emissions payback period.

$$PB_n(k) = \frac{\omega(n) \cdot LUC(k) \cdot a(k)}{[LC_{fossil}(n) \cdot y(n) \cdot c(n) \cdot a(k)] - [LC_{bio}(n) \cdot y(n) \cdot c(n) \cdot a(k)]},$$

where

$PB_n(k)$ payback period for bioenergy pathway n on land type k [yr].

The methods and materials described above are also depicted schematically in Figure 44 in Appendix A, in order to augment the written description.

Results and discussion

Primary bioenergy availability and land requirements

Table 7 shows the calculated values for primary bioenergy and required land area for three scenarios in 2050: low, mid and high bioenergy availability. The results show a range of 112-794 EJ/yr of primary bioenergy, requiring 634-2807 Mha of land for biomass cultivation. For context, global oilseed and maize harvested areas were 291 Mha and 186 Mha,

respectively, and total global arable agricultural land area was 1408 Mha, in 2013 [48]. These results are consistent with the recent meta-analysis of studies that seek to quantify the potential size of the global bioenergy resource by Slade, Bauen & Gross (2014), and the low and mid scenario results shown here are within the envelope of estimates defined by those authors as *"plausible"* (between 100 EJ/yr requiring <500Mha land area, and 600 EJ/yr requiring >1500 Mha land area) [26].

Table 7: Results of 2050 primary bioenergy scenarios.

Bioenergy availability scenario	Low		Mid		High	
	Primary energy [EJ/yr]	**Land [Mha]**	**Primary energy [EJ/yr]**	**Land [Mha]**	**Primary energy [EJ/yr]**	**Land [Mha]**
Vegetable oil energy crops	17	216	43	500	32	688
Sugary & starchy energy crops	33	204	60	498	100	802
Lignocellulosic energy crops	43	214	210	664	561	1317
Energy crop subtotal	93	634	312	1662	693	2807
Agricultural residues	15	-	46	-	81	-
Forestry residues	4	-	9	-	19	-
Waste fats, oils & greases (FOG)	1	-	1	-	1	-
Residue & waste subtotal	19	-	56	-	101	-
Total	**112**	**634**	**368**	**1662**	**794**	**2807**

The results in Table 7 are also disaggregated by energy crop, and residue and waste feedstocks. The land areas required for energy crop cultivation imply average areal biomass yields that are congruent with the literature (8.1-13.7 oven dry tonnes (odt)/ha, assuming a lower heating value (LHV) of 18 GJ/odt) [26]. The calculated availability of primary bioenergy from residue and waste is 19-101 EJ/yr, which also agrees with previous analyses: Daioglou et al. (2015) projected global residue availability of 48 EJ/yr by 2050, and reported estimates of 20-86 EJ/yr from similar peer-reviewed studies [49].

In order to identify the parameters driving variability between the low, mid, and high scenarios, a sensitivity analysis of primary bioenergy availability is carried out, shown in Figure 3. The three variables contributing to the greatest variation from the mid scenario

results are: the minimum threshold for agro-climatic suitability of lands for energy crop cultivation; growth in energy crop yields; and the assumed 2050 land use scenario.

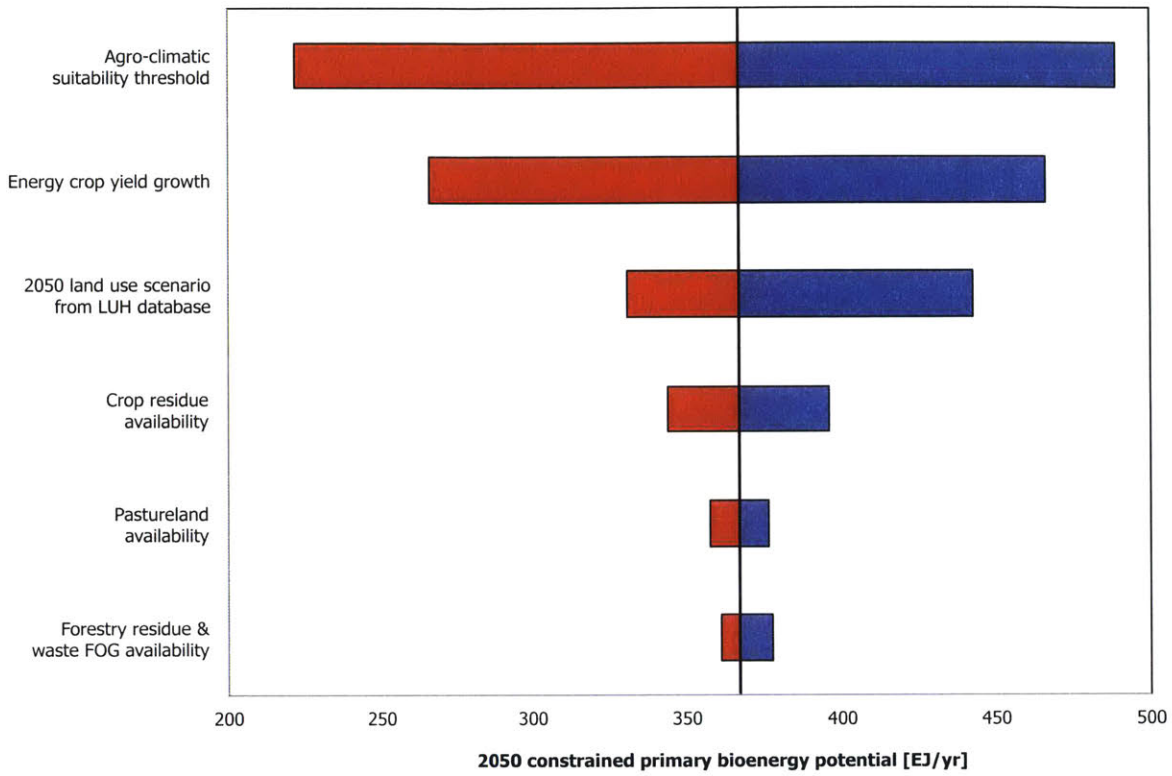

Figure 3: Sensitivity analysis of primary bioenergy availability scenarios. The baseline results correspond to the mid scenario, and the bars represent the change in results due to change in an individual parameter as defined for the low and high scenarios in Table 1.

Bioenergy allocation and deployment to maximize GHG emissions reductions

Based on the primary bioenergy results above, curves of final bioenergy availability are established for the four competing end-uses (middle and heavy distillate fuels; light distillate fuels; heat; and electricity), versus their specific lifecycle GHG emissions including location- and pathway-specific LUC emissions. This is done according to the maximization routine described in Equation 1, whereby each unit of available primary bioenergy is allocated amongst these four mutually exclusive end-uses in order to maximize total annual GHG emissions reductions compared to fossil fuels. The resulting curves of final bioenergy

availability and specific lifecycle GHG emissions are shown in Figure 4, broken out by middle and heavy distillate fuels, light distillate fuels, heat, and electricity, for each of the three bioenergy availability scenarios.

The curves consist of discrete units of available final bioenergy, rank-ordered from lowest to highest specific lifecycle GHG emissions ($gCO_2e/MJ_{final\ energy}$), with lifecycle GHG emissions per unit of final bioenergy monotonically increasing with greater final bioenergy deployment. The four uses of final bioenergy shown in Figure 4 (middle and heavy distillate fuels; light distillate fuels; heat; and electricity) have non-LUC lifecycle GHG emissions ranging from 5.5-39.1, 5.5-50.4, 7.3-13.8, and 12.8-27.5 $gCO_2e/MJ_{final\ energy}$, respectively. The share of lifecycle GHG emissions above these values corresponds to the contribution of LUC emissions for a given unit of biomass-derived final energy, and therefore LUC accounts for a greater proportion of total lifecycle emissions from final bioenergy moving to the right along the colored curves. The horizontal sections of the curves reflect final energy derived from residue and waste feedstocks, for which specific lifecycle GHG emissions are constant because there are no associated LUC emissions.

The final bioenergy results are compared to three scenarios of projected 2050 global demand for combustion-generated electricity and heat and liquid transportation fuels, derived from fossil fuels, shown in black and adapted from the IEA ETP temperature change scenarios [27]. These curves are rank-ordered in terms of decreasing specific lifecycle GHG emissions, with emissions per unit of fossil fuel-derived final energy monotonically decreasing with greater deployment of bioenergy to offset fossil fuel demand.

The results shown in Figure 4 are used to compare the specific lifecycle GHG emissions of biomass-derived final energy, allocated to maximize GHG emissions reductions, to its fossil fuel analog at a given level of bioenergy deployment. By doing so, the change in lifecycle GHG emissions from offsetting the marginal unit of fossil fuel with the marginal unit of bioenergy can be determined. This implies that, for any given pairing of bioenergy and fossil fuel curves for each of the end-uses shown in Figure 4, bioenergy deployment beyond the point of intersection of the two curves represents a net increase in GHG emissions. Therefore, the level of bioenergy deployment to offset fossil fuel demand that maximizes

GHG emissions reductions is the point of intersection of the two curves, where the lifecycle GHG emissions of the bioenergy and fossil fuel pathways are equivalent.

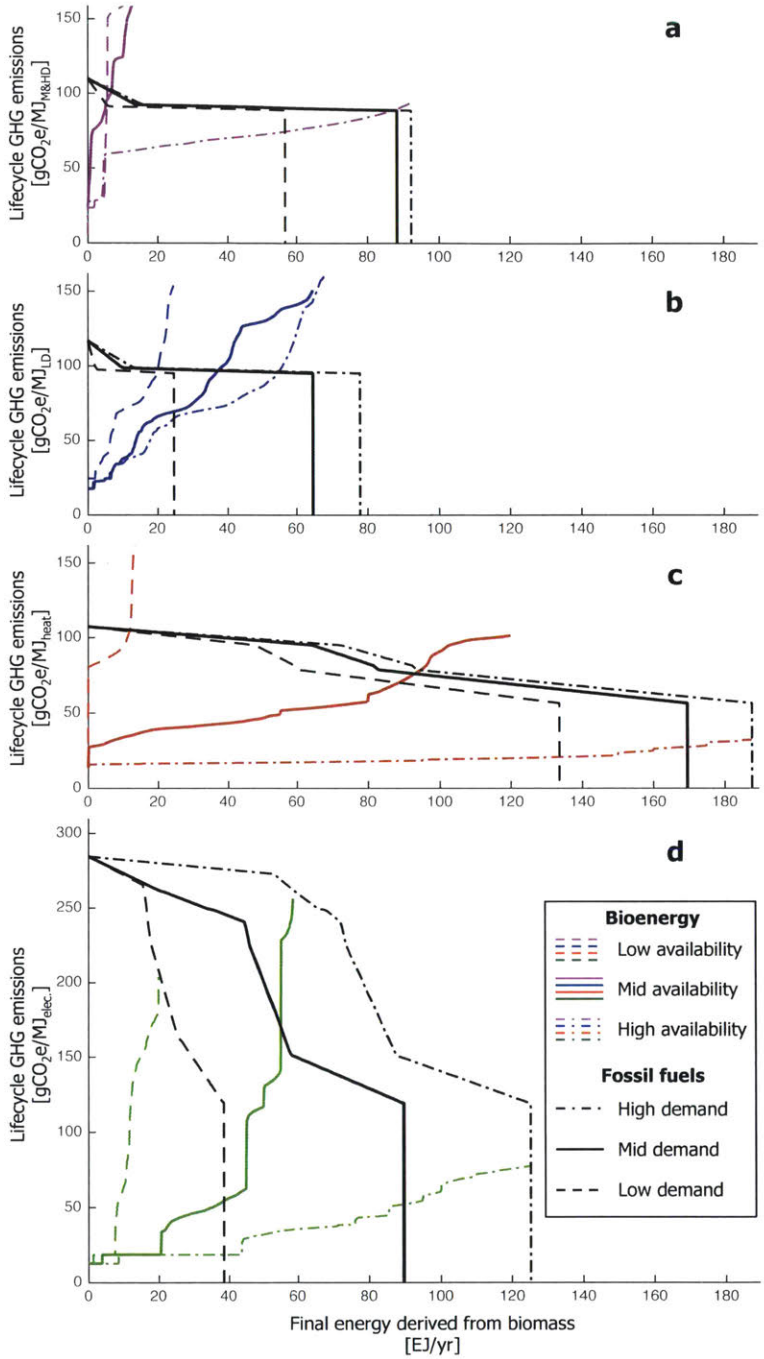

Figure 4: Availability and specific lifecycle GHG emissions of final bioenergy compared to fossil fuel-derived final energy demand and emissions in 2050, allocated to maximize GHG emissions reductions. Panel a shows biomass-derived (magenta) and petroleum-derived (black) middle and heavy distillate (M&HD) liquid fuels. Panel b shows biomass-derived (blue) and petroleum-derived (black) light distillate (LD) liquid fuels. Panel c shows biomass-derived heat final energy (red), compared to coal-, oil-, and natural gas-derived heat (black). Panel d shows biomass-derived electricity (green), compared to for coal-, oil-, and natural gas-derived electricity (black). The colored bioenergy curves in each panel correspond to the three bioenergy availability scenarios, and the black fossil fuel curves correspond to the three fossil fuel demand scenarios (low, mid and high corresponding to 2°C, 4°C and 6°C temperature change scenarios from IEA ETP, respectively [27]).

Figure 5 shows final bioenergy deployment plotted against cumulative mitigation of GHG emissions, calculated as the integrated area between the curves from Figure 4. The results are disaggregated by bioenergy end-use, and the curves for each end-use are stacked in order to indicate the total final bioenergy deployment associated with the maximum reduction in GHG emissions across all four end-uses. These results are calculated for all nine combinations of bioenergy and fossil fuel curves (shown in Table 8), and three scenarios are shown in Figure 5 to represent a broad range of the final bioenergy deployment (57-460 EJ/yr), and maximum GHG emissions reduction (4.9-38.7 Gt_{CO2e}/yr) results. The results of the mid bioenergy availability and fossil fuel demand scenario combination indicate final bioenergy deployment of 192 EJ/yr, leading to maximized GHG emissions reductions of 17.2 Gt_{CO2e}/yr. The three scenarios correspond to 88, 273 and 721 EJ/yr of primary bioenergy deployment in the low, mid and high bioenergy availability scenarios.

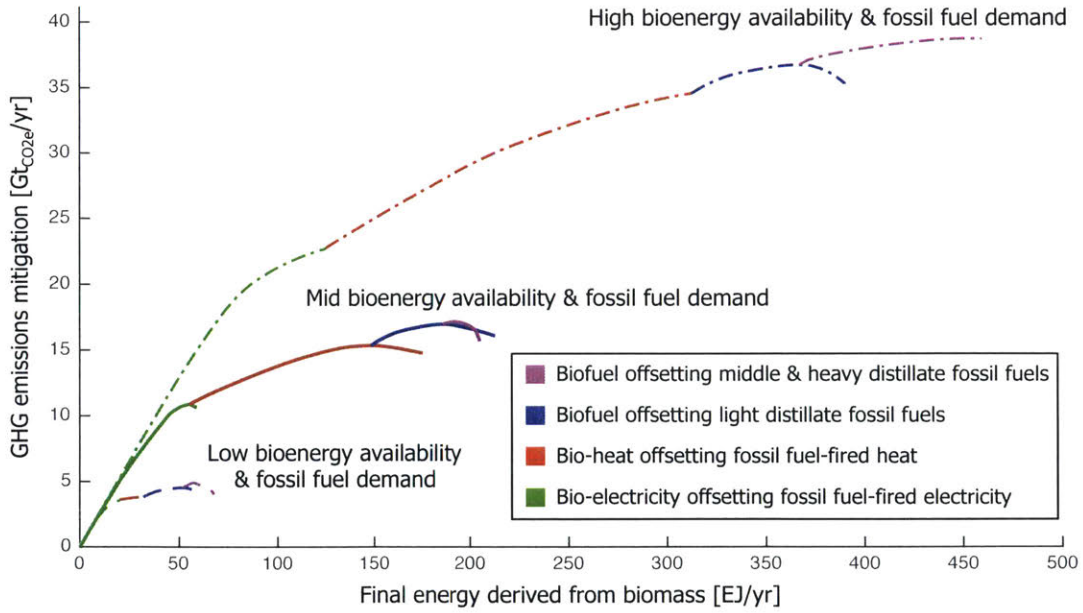

Figure 5: Deployment of biomass-derived final energy versus cumulative GHG emissions mitigation. The maximum of each curve represents the level of final bioenergy deployment for the indicated final energy end-use that maximizes GHG emissions reductions. The dashed lines denote the combination of the low bioenergy availability and fossil fuel demand scenarios, the solid lines denote the combination of the mid bioenergy availability and fossil fuel demand scenarios, and the dash-dot lines denote the combination of the high bioenergy availability and fossil fuel demand scenarios.

Table 8 shows tabular results for all nine scenario combinations, compared to total primary bioenergy availability, global final energy demand for combustion-generated electricity and heat, and liquid transportation fuels, and the total associated lifecycle GHG emissions if this demand were to be satisfied completely with fossil fuels. This comparison indicates that bioenergy allocated and deployed to maximize GHG emissions reductions could satisfy 10-97% of projected 2050 final energy demand for fossil fuel-derived electricity, heat, and liquid fuels, leading to a reduction in GHG emissions from these sources of 9-68%. This coincides with deployment of 29-91% of the total available primary bioenergy reported in Table 7. In the mid bioenergy availability and fossil fuel demand scenario combination, final bioenergy deployment is 47% of final energy demand for electricity, heat, and liquid fuels, requiring 74% of available primary bioenergy, and resulting in a maximized reduction of 36% of lifecycle GHG emissions.

Table 8: Bioenergy allocation and deployment to maximize GHG emissions reductions. Primary bioenergy availability, final bioenergy deployment, and the reduction in lifecycle (LC) GHG emissions are compared against 2050 final energy demand for combustion-generated electricity and heat, and liquid transportation fuels from fossil fuels, and the associated LC GHG emissions.

2050 scenario					Bioenergy allocation & deployment													
					Primary energy		Final energy						Maximum GHG emissions reduction					
Fossil fuel demand scenario	Global demand for fossil fuel elec., heat, and liquid transp. fuels	LC GHG emissions from fossil fuels	Primary bioenergy avail.		Total	Propoortion of total avail.	Elec.	Heat	LD fuels	M&HD fuels	Total	Offset of final energy demand	Elec.	Heat	LD fuels	M&HD fuels	Total	Reduction in LC GHG emissions
	[EJ/yr]	[Gt_{CO2e}/yr]		[EJ/yr]	[EJ/yr]	[%]	[EJ/yr]					[%]	[Gt_{CO2e}/yr]					[%]
Low	253	26.8	Low	112	88	79%	20	12	20	5	57	22%	3.6	0.2	0.7	0.4	4.9	18%
			Mid	368	239	65%	35	121	25	8	188	74%	5.8	5.9	1.1	0.4	13.3	49%
			High	794	230	29%	23	134	25	14	195	77%	5.5	8.8	1.3	0.7	16.4	61%
Mid	412	47.1	Low	112	90	80%	26	0	25	0	51	12%	4.0	0.0	1.2	0.0	5.2	11%
			Mid	368	273	74%	55	93	37	7	192	47%	10.9	4.5	1.6	0.2	17.2	36%
			High	794	613	77%	90	170	54	88	401	97%	15.6	11.1	2.1	3.3	32.2	68%
High	483	59.6	Low	112	89	79%	26	0	24	1	50	10%	4.4	0.0	1.2	0.0	5.6	9%
			Mid	368	286	78%	75	62	37	7	181	37%	15.8	2.3	1.7	0.2	19.9	33%
			High	794	721	91%	125	188	55	92	460	95%	22.8	11.8	2.2	2.0	38.7	65%

GHG mitigation effectiveness and mix of bioenergy end-uses

In order to compare between the different bioenergy end-uses considered in this analysis, average GHG mitigation effectiveness is defined as the ratio of maximum GHG emissions reduction to total final bioenergy deployment. This is shown in Table 9, broken out by all four bioenergy end-uses, as well as aggregated to biomass-fired electricity and heat, and liquid biofuels. In the nine scenario combinations, the average GHG mitigation effectiveness of biomass-fired electricity and heat, and liquid biofuels, range from 0.08-0.17 Gt_{CO2e}/EJ and 0.03-0.05 Gt_{CO2e}/EJ, respectively. The average GHG mitigation effectiveness of biomass-fired electricity and heat is 1.6-3.9 times higher than that of liquid biofuels across all scenario combinations. This indicates that, from a GHG mitigation perspective, biomass combustion to generate electricity or heat is, in aggregate, a more effective end-use for bioenergy resources than liquid biofuel production. This is in line with previous studies that identify power and heat generation as a more environmentally beneficial use of scarce biomass resources than the production of liquid fuels [50-54].

Table 9: Average GHG mitigation effectiveness of bioenergy end-uses in 2050. This is defined as the ratio of maximum GHG emissions reduction, and total final energy, from biomass-derived electricity, heat, light distillate (LD) fuels, and middle & heavy distillate (M&HD) fuels. The ratio of effectiveness of electricity and heat to liquid fuels is shown in the rightmost column.

Fossil fuel demand scenario	Bioenergy availability	Average effectiveness [Gt_{CO2e}/EJ]						Ratio of elec. & heat to liquid fuels effectiveness
		Elec.	Heat	Biomass-fired elec. & heat	LD fuels	M&HD fuels	All liquid biofuels	
Low	Low	0.18	0.02	0.12	0.04	0.07	0.04	2.7
	Mid	0.17	0.05	0.08	0.04	0.05	0.05	1.6
	High	0.24	0.07	0.09	0.05	0.05	0.05	1.7
Mid	Low	0.16	-	0.16	0.05	0.02	0.05	3.3
	Mid	0.20	0.05	0.10	0.04	0.03	0.04	2.5
	High	0.17	0.07	0.10	0.04	0.04	0.04	2.7
High	Low	0.17	-	0.17	0.05	0.02	0.05	3.4
	Mid	0.21	0.04	0.13	0.04	0.03	0.04	3.1
	High	0.18	0.06	0.11	0.04	0.02	0.03	3.9

Despite having a lower average effectiveness of GHG mitigation, however, 18-49% of the calculated total deployed final bioenergy comes from liquid biofuels in all scenarios investigated. The reason for this can be observed in Figure 5. The initial marginal effectiveness (or slopes) of offsetting fossil fuel-fired electricity and heat with bioenergy (the beginning of the green and red curves) is greater than that of offsetting petroleum-derived liquid fuels (the beginning of the blue and magenta curves). This indicates that, initially, biomass-fired electricity and heat production maximizes GHG emission reductions per unit of final bioenergy. However, as the level of deployment of these bioenergy end-uses increases along the curves, the marginal effectiveness of offsetting electricity and heat decreases and eventually becomes equivalent to the initial marginal effectiveness of offsetting petroleum-derived liquid fuels. Beyond this point a switch occurs between competing bioenergy end-uses, and using the next unit of final bioenergy to offset petroleum-derived fuels maximizes GHG emissions reductions. This is because the fossil fuel-fired electricity and heat with the highest specific lifecycle GHG emissions has already been offset, and the greatest subsequent reduction in GHG emissions can be achieved by using liquid biofuels to offset petroleum-derived fuels with relatively high specific lifecycle GHG emissions.

This finding is particularly relevant for sectors with few technical options beyond the use of bioenergy to reduce GHG emissions, but where the use of scarce bioenergy resources may not be justified as the most effective among competing end-uses. One such example is the aviation industry, for which it is technically infeasible to make use of other forms of renewable energy or vehicle electrification, and will therefore require the use of energy-dense liquid fuels (potentially including biomass-derived fuels) for the foreseeable future [55-58]. At the same time, Trivedi et al. (2015) demonstrate that using lignocellulosic feedstocks to produce drop-in middle distillate fuels (including jet fuel) is less societally beneficial than alternative bioenergy uses on average [50].

In contrast, this analysis here shows that the allocation and deployment of bioenergy resources to maximize GHG reductions requires a mix of bioenergy end-uses. Notably, this mix consists of uses that are not necessarily the most effective, initially or on average, including drop-in middle distillate fuels such as jet fuel. Note that this analysis has

considered renewable ethanol, gasoline, and diesel pathways as representative proxies of liquid biofuel pathways, and that these fuels are not suitable for use in aviation [59]. However, a number of technologies exist to convert biomass to renewable jet fuel, with feedstock-to-fuel conversion efficiencies and lifecycle GHG emissions comparable to the pathways that we have considered here [9, 11, 60-65]. These technologies will be the subject of the subsequent chapters of this thesis.

LUC emissions amortization and payback period

LUC emissions are included in total lifecycle GHG emissions by amortizing evenly over a 30-year time horizon without discounting, consistent with the United States Environmental Protection Agency (US EPA) approach to treatment of LUC emissions from biofuel production [46]. To test the sensitivity of the findings to this assumption, results are also generated for a 20-year amortization period, consistent with the European Union Renewable Energy Directive [47]. The results indicate that, when assuming a 20-year amortization period, the maximum GHG emissions reductions are 5-26% smaller than those calculated when assuming a 30-year amortization period. The full results of this sensitivity are available in Appendix A.

Alternatively, the payback period can be calculated for LUC emissions associated with a given unit of final bioenergy. This is shown aggregated for all four end-uses in Figure 3. LUC is assumed to result in a one-time pulse of CO_2 emissions, and the payback period is defined as the number of years required for the difference in the attributional lifecycle GHG emissions of a unit of final bioenergy (excluding LUC emissions) and its fossil fuel analog to make up for the LUC emissions pulse. The payback period of the last unit of final bioenergy deployment is shown as a function of cumulative final bioenergy deployment in Figure 3, for the three scenarios combinations of bioenergy and fossil fuel curves from Figure 2. The calculated LUC emissions payback increases with increasing bioenergy deployment up to 39, 35 and 31 years for optimal final bioenergy deployment in the low bioenergy availability and fossil fuel demand, mid bioenergy availability and fossil fuel demand, and high bioenergy availability and fossil fuel demand scenario combinations, respectively. The end point of

each curve represents the level of optimal final bioenergy deployment, and corresponding payback period, for each scenario combination.

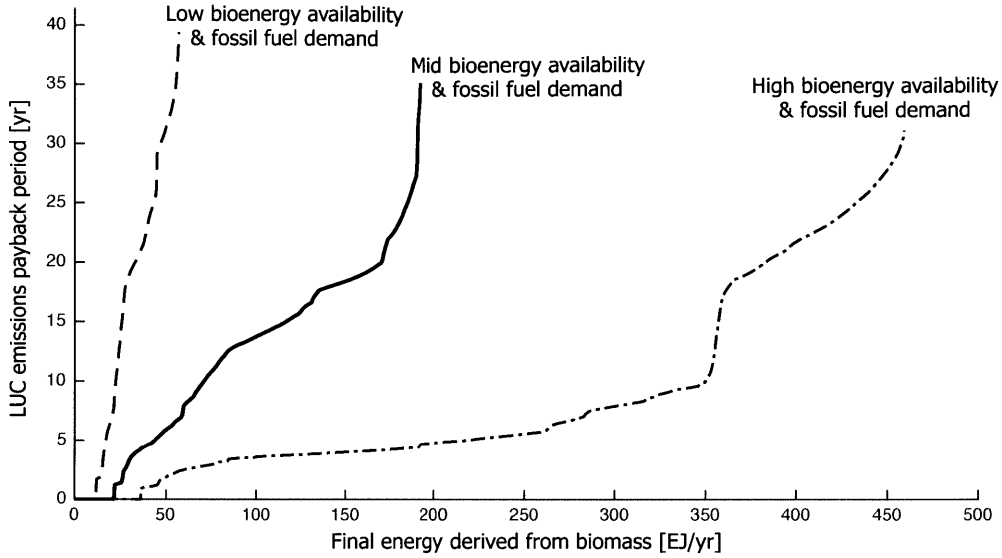

Figure 6: Deployment of biomass-derived final energy versus payback period for LUC emissions. The end point of each curve in the figure represents the level of final bioenergy deployment that maximizes GHG emissions reductions for that scenario combination of bioenergy and fossil fuel curves.

Limitations and areas for future work

Several additional factors could impact the results that have been calculated here. For example, energy crop cultivation is considered only on lands where irrigation is not a prerequisite for agro-climatic suitability, and potentially disruptive innovations in biomass cultivation, such as the intensification of agricultural production using multi- or intercropping, are not captured in the results presented above [66]. These assumptions could result in an underestimate of agricultural production at the intensive margin. In order to quantify the magnitude of the potential for intensification, a sensitivity analysis is carried out for the three scenarios shown in Figure 5, where the land requirements of bioenergy cultivation are reduced by 50%. This assumption implies that for each unit of biomass cultivated on new land brought into agricultural production, a second unit of comes from intensified production on existing agricultural lands. The result is an increased proportion of fossil fuel final energy demand offset by bioenergy, from between 22-95% to 48-96% for the

three scenarios considered. Correspondingly, the range of reductions in LC GHG emissions from electricity, heat and liquid fuels grows from between 18-65%, to 39-76%. These results are available in Appendix A. Although this is a simplified example for the purposes of sensitivity analysis, the results demonstrate the potential importance of intensification for the GHG emissions mitigation potential of bioenergy.

Industrial aquaculture of feedstocks, such as algae, could represent a large additional source of primary bioenergy because they are not limited by the availability of land area for cultivation and the associated GHG emissions impact of LUC. In practice, the production potential of these feedstocks is constrained by local availability of solar insolation, concentrated CO_2, and water as a growth medium, among other factors [67]. Consideration of these parameters is beyond the scope of the work presented here, however future work in this field would benefit from the inclusion of aquaculture feedstocks, focusing on the lifecycle emissions tradeoffs between total feedstock production potential and appropriate siting of cultivation facilities.

A lack of regionally specific data for 2050 necessitates a simplified approach for quantifying the lifecycle GHG emissions of fossil fuel and biomass-derived final energy: this analysis adopts point estimates of lifecycle emissions to represent 35 biomass feedstock-to-final energy conversion pathways, and 24 fossil fuel-derived final energy carriers. In reality, the range of lifecycle GHG emissions of different energy sources exist on a location- and time-dependent continuum that is not fully represented here. Furthermore, the large-scale use of emerging feedstock-to-final energy technologies that are not considered in this work could offer greater opportunities for GHG emissions mitigation, or even net sequestration, such as electricity generation from biomass coupled with carbon capture and storage (CCS) [68-70]. A more complete global assessment of the GHG mitigation potential of bioenergy could build upon the work presented here by accounting for technological development, and regional and temporal heterogeneity in lifecycle GHG emissions, as reliable data becomes available. In addition, inclusion of the use of bioenergy to offset additional sources of GHG emissions, such as chemicals manufacturing from fossil fuels, or livestock production, would improve the analysis presented here.

There are also economic feedbacks associated with bioenergy deployment and availability that could be the subject of future research. For example, the valorization of waste and residues might drive up their commodity prices, such that these feedstocks are no longer considered wastes and residues. This could influence the allocation of resources, production patterns, and ultimately feedstock availability. However, the focus of this work is the physical limits of global GHG emissions reductions from the use of bioenergy, and therefore the economic impacts and feedbacks described above have not been captured here.

Finally, it is important to note that GWP_{100} has been used as the *de facto* standard for LCA climate metrics in the past, including in GREET1 2015 and in this analysis. Future work in this area could benefit from the use of alternative metrics. For example, a metric that reflects physical impacts, such as global temperature potential (GTP), may be more relevant for policy-making. In addition, accounting for LUC emissions in the context of LCA requires comparison of an emissions pulse at time zero to other lifecycle GHG emissions in subsequent time steps. Therefore, a dynamic metric that reflects the physical processes of climate change, such as annual radiative forcing (RF) impact, would more accurately account for the time-dependent emissions profiles of large-scale bioenergy deployment.

Summary

The final bioenergy deployment to maximize GHG emissions reductions calculated in this analysis represents 10-97% of projected annual demand for combustion-generated electricity and heat, and liquid transportation fuels in 2050, across the nine scenarios considered. This corresponds to a reduction in annual lifecycle GHG emissions from these sources of 9-68%, if this demand were otherwise satisfied with fossil fuels. Each of the scenarios reported here reflects a different state of the world in 2050 in terms of two distinct but interdependent domains: the availability and allocation of primary bioenergy resources amongst competing end uses; and the types and quantities of fossil fuels used to satisfy final energy demand. These scenarios are defined in order to capture the limits of GHG emissions mitigation potential from bioenergy under a range of potential future conditions, and therefore there is not necessarily any predictive or probabilistic meaning to any specific scenario combination

over the others. In general, the range of results shown here demonstrate that assumptions corresponding to greater availability of bioenergy resources (such as the availability of arable land, and projected growth in crop yields), and greater fossil fuel demand in 2050, leads to higher calculated maximum GHG emissions reductions.

It is also important to highlight that this analysis minimizes GHG emissions by assuming that the next available unit of bioenergy is used for the lowest lifecycle GHG emissions intensity end-use, and to offset the unit of fossil fuel energy with the highest remaining lifecycle GHG emissions intensity. This implies a frictionless matching of final bioenergy supply to the fossil fuel use that will result in the greatest reduction in GHG emissions globally, without incurring additional GHG emissions from transportation or transmission. This is a simplifying assumption, and therefore the results should be interpreted as an upper bound on GHG mitigation potential via the uses of bioenergy considered here to 2050. In reality, decisions about bioenergy resource allocation, fossil fuel use, and land use planning are not made solely on the basis of GHG emissions. Practical limitations that are not represented here, such as existing investments in fossil fuel resources and infrastructure, the challenges of biomass transportation logistics, path dependency of energy and environmental policy, economic considerations, and other factors, will guide decisions about bioenergy deployment and the sources of energy it will replace or offset in the future. These factors are beyond the scope of this analysis; however, they represent additional constraints on bioenergy adoption, and on the potential reductions in GHG emissions that have been calculated here.

In summary, this chapter quantifies the allocation and deployment of bioenergy resources to maximize reductions in GHG emissions from fossil fuel-fired electricity and heat, and petroleum-derived liquid transportation fuels, to 2050. The findings provide evidence for the hypothesis that GHG emissions mitigation via the use of bioenergy is constrained not only by the availability of biomass, as considered in previous assessments of bioenergy potential, but also by the lifecycle GHG emissions of final bioenergy when LUC is taken into account: the analysis finds that GHG emissions reductions are maximized when deployment is limited to 29-91% of total primary bioenergy availability, where the range of results is defined primarily by the potential availability of bioenergy resources, and the fossil fuel energy

demand that bioenergy could be used to offset in 2050. In addition, the results show that while biomass-fired electricity and heat generation are, on average, more effective means of GHG mitigation than the production of biomass-derived liquid fuels, the allocation and deployment of global bioenergy resources that maximizes total GHG emissions reductions requires a mix of end-uses, including biomass-derived transportation fuels. This is of particular interest for the subsequent Chapters of this thesis, which concern the use of alternative fuels for aviation derived from biomass and other non-petroleum feedstocks.

The work contained in this Chapter has been published in *Nature Energy,* with co-authors Robert Malina and Steven Barrett.

Staples, M.D., Malina, R. & Barrett, S.R.H. (2017). The limits of bioenergy for mitigating global life-cycle greenhouse gas emissions from fossil fuels. *Nature Energy*. DOI: 10.1038/nenergy.2016.202

3. Lifecycle greenhouse gas emissions and minimum selling price of renewable jet and diesel fuel from fermentation and advanced fermentation production technologies

Motivation and context

Transportation is an energy and greenhouse gas (GHG) intense activity, which predominately relies on the use of fossil fuels: in 2014 the transportation sector accounted for approximately 121 EJ, or 21%, of global annual primary energy demand and 23% of global CO_2 emissions from fossil fuel combustion [71].

In order to address the climate change impact of transportation, as well as the sector's dependence on non-renewable sources of energy, a number of jurisdictions have enacted policies that encourage the production and use of liquid fuels derived from biomass. For example, in the United States (US) the Renewable Fuels Standard 2 (RFS2) mandates the use of 36 billion gallons of renewable transportation fuels per year, approximately 9% of current US liquid fuel consumption, by 2022 [72,73], and in the European Union (EU) the Renewable Energy Directive requires that 10% of all transport fuels come from renewable sources such as biofuels [47]. Together, these two jurisdictions account for 62% of global biofuel production [74]. To date, the vast majority of fuels produced under these policies have been ethanol and fatty acid methyl ester (FAME) biodiesel, to be blended with petroleum-derived gasoline and diesel for use in conventional internal combustion and compression-ignition engines, respectively. Of the total renewable fuel volumes reported under RFS2 in 2015, 87% was ethanol and 9% was biodiesel [75].

Within the transportation sector, commercial aviation accounts for approximately 2.0% of global annual primary energy demand and 2.6% of CO_2 emissions from fossil fuels [71,76]. Although it is currently a relatively small contributor, Owen, Lee & Lim (2010) estimate that aviation's share of global CO_2 emissions could grow to 4.2% by 2050 [77]. This is in part

because aviation is growing more quickly than other sectors of the economy. For example, average annual growth in global GDP was 2.9% from 2004-2015 [78], whereas annual average growth in aviation revenue-passenger kilometers was 6.5% over the same period [79].

The use of renewable alternatives to petroleum-derived fuels is of particular interest for aviation because other means of reducing reliance on fossil fuels and mitigating CO_2 emissions, especially in the face of increasing aviation activity, are limited. Operational efficiency gains are incremental in nature, offering only marginal emissions reductions during the unavoidable takeoff, cruise and landing stages of flight. And while airframe and engine technology improvements have resulted in consistent reductions in specific fuel consumption over the past two decades of approximately 1.9% per year, this rate of improvement has been insufficient to offset absolute growth in aviation activity. Furthermore, the acceleration of airframe and engine technology improvements is limited by long development and certification cycles for new aircraft, and the long service lives (25-30 years) of the existing stock of aircraft [55-57,80]. In contrast, renewable alternative jet fuels could potentially offer large, near-term reductions in the climate impact of aviation by virtue of their biogenic CO_2 combustion emissions, and compatibility with existing aircraft and infrastructure. As a result, the International Civil Aviation Organization (ICAO), the intergovernmental body that develops international standards and practices for aviation, has identified alternative jet fuels as one of a "basket of measures" to mitigate the climate impact of aviation [81].

Jet A and Jet A-1 fuels adhering to ASTM specification D1655 currently make up ~99% of aviation fuel burn [82,83], however this demand cannot be offset by existing biofuel production because these fuels are not suitable for use in aviation. Blending of ethanol with jet fuel results in higher vapor pressure and an increased risk of fire or explosion, and the use of biodiesel for aviation is limited by its poor thermal stability and high freezing point [59,84]. Therefore, in order to be compatible with the existing fleet of turbojet and turboprop aircraft, and fuel transportation and refueling infrastructure, alternative jet fuels must have chemical properties similar petroleum-derived jet fuel. These are referred to as "*drop-in*" fuels.

One class of technologies for the production of renewable drop-in middle distillate (MD) fuels, including jet and diesel fuel, involves the micro organic metabolism, or fermentation, of biomass-derived sugars. Typically, polymer sugars are extracted from a biomass feedstock and decomposed to monomer sugars using mechanical, chemical or biological means. The monomer sugars are then metabolized by a microorganism to produce an energy carrying platform chemical, which is chemically upgraded to a drop-in MD fuel or blend-stock specification. This class of production technologies is referred to as fermentation and advanced fermentation (AF). AF production technologies make up a subset of techniques for the valorization of biomass resources, which are defined by ElMekawy et al. (2013, 2014) as submerged fermentation (SmF) and anaerobic fermentation (AnF) [85,86].

A number of private corporations are in varied stages of commercialization of technologies that could be categorized as AF, such as TerraVia, Inc. (formerly Solazyme), Amyris, Inc., Byogy Renewables, Inc., and Gevo, Inc. As of the writing of this thesis, two of these technologies have received ASTM certification for use in turbine engines under D7566: synthesized iso-paraffinic (SIP) fuel such as that produced by Amyris, and alcohol-to-jet (ATJ) fuel such as that produced by Gevo and Byogy [87]. Despite commercial and regulatory interest in AF technologies, the environmental and economic feasibility of AF MD fuel has not been comprehensively addressed in the literature. Therefore, the aim of this Chapter is to quantify the lifecycle GHG emissions and minimum selling price (MSP) of AF MD fuel, in order to assess their feasibility relative to conventional petroleum-derived MD fuel.

AF MD fuels have not yet been produced at commercial or industrial scale because significant technical challenges remain to be resolved. These include: variable feedstock composition and quality; the recalcitrance of lignocellulosic biomass; and the efficiency and costs of sugar extraction, hydrolysis and fermentation processes [86,88]. As a result of these remaining challenges, it is not yet known empirically how these technologies will develop and perform commercially. In order to capture the spectrum of potential outcomes, a wide range of feedstock-to-fuel conversion technology parameters are considered here. Sugarcane, corn grain and switchgrass feedstocks, as well as a number of feedstock-to-intermediate

chemical-to-fuel conversion pathways, are examined to estimate the mass and energy balances associated with n^{th} plant, commercial-scale production of AF MD fuels.

The resulting mass and energy balances are used in conjunction with the Greenhouse Gases Regulated Emissions, and Energy Use in Transportation (GREET) model (.NET v1.0.0.8377), developed by Argonne National Laboratory, to calculate their attributional lifecycle GHG emissions of the fuels produced. In addition, the material balances of AF MD fuel production are used together with petroleum industry heuristics and empirical biofuel industry data, in a discounted cash flow rate of return (DCFROR) model, to calculate the MSP of AF MD fuels. Sensitivity analysis is carried out on the lifecycle GHG emissions and MSP results in order to quantify the importance of critical engineering parameters. The results of this study are used to characterize the potential for AF MD fuels to reduce the lifecycle GHG emissions compared to petroleum-derived diesel and jet fuel, and to evaluate their economic viability.

Methods and materials

Lifecycle GHG emissions

The methodological challenges associated with the calculation of the lifecycle GHG emissions of renewable fuels are addressed extensively in the literature. For example, Limayem & Ricke (2012) and Singh et al. (2013,2010) identify the major issues as functional unit definition, system boundary definition, spatial and temporal variability, data availability and quality, and co-product allocation [88-90].

This analysis employs a lifecycle analysis (LCA) methodology for GHG emissions quantification consistent with Stratton et al. (2011), which uses a functional unit of grams of 100-year global warming potential (GWP100) CO2-equivalent (CO2e) emissions per megajoule of total MD fuel, including jet and diesel fuel [9]. The system boundary of interest includes biomass feedstock cultivation, recovery and transportation; feedstock-to-fuel conversion; transportation and distribution of finished MD; and MD fuel combustion. Low,

baseline and high lifecycle GHG emissions scenarios are defined in order to capture spatial, temporal and data quality variability. This is achieved by identifying key parameters affecting lifecycle GHG emissions, and then combining a survey of the academic and technical literature with the engineering judgment of the author. In particular, a broad range of AF feedstock-to-fuel conversion pathways are considered. The assumptions that result in the low, baseline and high attributional lifecycle GHG scenarios are summarized in Table 10, and these assumptions are discussed in detail in the following sections.

The resulting calculated mass and energy balances are then integrated into the GREET model (.NET v1.0.0.8377) in order to quantify the lifecycle GHG emissions attributable to MD fuel products. In order to allocate emissions among fuel and non-fuel co-products, market-based allocation is used. This means that at the point where the fuel-destined product stream is physically separated from the non-fuel stream, emissions are allocated amongst the process streams in proportion to their contributions to total product market value [91,92]. Market-based allocation is used in this analysis in order to assign emissions to diverse co-products in proportion to a measure of their relative societal values (where market price is used as a proxy for societal value). The analysis also quantifies the sensitivity of the findings to the emissions accounting method that is chosen by recalculating selected results using the displacement method, also known as system expansion [93]. This is done because although the issue has been discussed extensively, the appropriate choice of allocation method remains largely unresolved in the literature [94,95]. In all cases, emissions are further allocated amongst all finished fuel products according to their relative energy contents [91].

Table 10: Scenario definition for low, baseline and high lifecycle GHG emission cases. Data sources are listed for each step of the feedstock-to-fuel conversion pathway.

Pathway	Case	Pretreatment	Saccharification efficiency (% of theor. max. from polymer to monomer sugar)	Target platform molecule, theor. max. mass conversion efficiency of sugars to platform molecules	Metabolic efficiency (% of theor. max.)	Extraction /purification technology	Upgrading to drop-in fuel	Excess biomass co-generation technology
Sugarcane AF	Low	State-of-the-art milling (Lobo et al. 2007, Dias et al. 2009)	100%	EtOH, 51% (from stoich., Dugar & Stephanopoulos 2011)	90% C6 sugars	Distillation (Mei 2006, MnTAP 2008)	Dehydration, oligomerization and hydroprocessing (Byogy 2012)	Gasification η_{elec}=27% , η_{heat}=24% (Murphy & McKeogh 2004)
	Base	Conventional milling (Lobo et al. 2007, Dias et al. 2009)	97.50%	Fatty acids, 34% (US PAP 2013, Dugar & Stephanopoulos 2011)	85% C6 sugars	Centrifugation (Vasudevan et al. 2012)	66% of hydroprocessing requirements (Pearlson et al. 2013)	Incineration η_{elec}=15% , η_{heat}=43% (Murphy & McKeogh 2004)
	High	Conventional milling (Lobo et al. 2007, Dias et al. 2009)	95%	TAG, 31% (US PAP 2011)	80% C6 sugars	Hexane (Sheehan et al. 1998)	100% of hydroprocessing requirements (Pearlson et al. 2013)	Incineration η_{elec}=15% , η_{heat}=43% (Murphy & McKeogh 2004)
Corn grain AF	Low	Dry milling (Wang et al. 1999, Mei 2006, Mueller 2008)	100%	Alkanes, 34% (US PAP 2013, Dugar & Stephanopoulos 2011)	90% C6 sugars	KOH steam extraction and centrifugation (Vaswani 2009)	33% of hydroprocessing requirements (Pearlson et al. 2013)	n/a
	Base	Dry milling (Mei 2006, Kwiatkowski et al. 2006)	97.50%	Fatty acids, 34% (US PAP 2013, Dugar & Stephanopoulos 2011)	85% C6 sugars	Centrifugation (Vasudevan et al. 2012)	66% of hydroprocessing requirements (Pearlson et al. 2013)	
	High	Dry milling (Mei 2006, Shapouri et al. 2002, Phillips et al. 2007)	95%	iBuOH, 41% (from stoich., Dugar & Stephanopoulos 2011)	80% C6 sugars	Distillation (Mei 2006, MnTAP 2008)	Dehydration, oligomerization and hydroprocessing (Gevo 2012)	
Switchgrass AF	Low	Dilute acid (Wyman et al. 2005)	n/a (Saccharification efficiency is included in pretreatment references, in the form of raw feedstock to sugar monomers)	EtOH, 51% (from stoich., Dugar & Stephanopoulos 2011)	90% C6 sugars 70% C5 sugars	Distillation (Mei 2006, MnTAP 2008)	Dehydration, oligomerization and hydroprocessing (Byogy 2012)	Gasification η_{elec}=27% , η_{heat}=24% (Murphy & McKeogh 2004)
	Base	Dilute alkali (Kumar & Murthy 2011)		Fatty acids, 34% (US PAP 2013, Dugar & Stephanopoulos 2011)	85% C6 sugars 60% C5 sugars	Centrifugation (Vasudevan et al. 2012)	66% of hydroprocessing requirements (Pearlson et al. 2013)	Incineration η_{elec}=15% , η_{heat}=43% (Murphy & McKeogh 2004)
	High	Aq. ammonia (Tao et al. 2011)		iBuOH, 41% (from stoich., Dugar & Stephanopoulos 2011)	80% C6 sugars 50% C5 sugars	Distillation (Mei 2006, MnTAP 2008)	Dehydration, oligomerization and hydroprocessing (Gevo 2012)	Incineration η_{elec}=15% , η_{heat}=43% (Murphy & McKeogh 2004)

Sugarcane feedstock pretreatment

In order to extract sucrose from raw sugarcane, the feedstock is cleaned, chopped, shredded and crushed, and the resulting juice is concentrated and sterilized. The mass and energy balances of these processes are calculated based on Lobo et al. (2007) [96], which compares conventional and optimized milling technologies, and Dias et al. (2009) [97]. The lower heating value (LHV) of the bagasse remaining after juice extraction (7.54 MJ/kg, 50% moisture content) is taken from Ensinas et al. (2007) [98]. This analysis considers incineration and gasification technologies for the co-generation of heat and power from biomass co-products (sugarcane bagasse in this case) to meet the utility requirements of the bio-refinery, using LHV-to-process heat and electricity conversion efficiencies estimated from Murphy & McKeogh [98].

Corn grain feedstock pretreatment

Starch is typically extracted from corn grain using the dry mill process (approximately 90% of corn ethanol plants in the US use dry milling, as opposed to wet milling [99]), during which corn kernels are fed to electric-powered hammermills that grind corn into a flour. The corn flour is liquefied by slurrying with process water and is exposed to high pressure steam to break down starches and kill bacteria. The starch extraction efficiency, utility requirements, and co-production of distiller dry grains and solubles (DDGS) from the corn grain milling and liquefaction processes are estimated from Wang et al (1999), Mei (2006), Shapouri et al. (2002), Mueller (2008), Kwiatkowski et al. (2006) and Philips et al. (2007). [100-105]

Switchgrass feedstock pretreatment

Finally, a number of emerging biological, thermal and chemical pretreatment technologies to extract polymeric sugars from lignocellulosic biomass are considered in this analysis, including dilute acid, ammonia fiber explosion (AFEX), aqueous ammonia, hot water, dilute

alkali and steam explosion. The achievable yields of cellulose and hemicellulose from switchgrass were estimated from Kumar & Murthy (2011), Tao et al. (2011), and Wyman et al. (2005) [106-108], and utility requirements were estimated from Aden et al. (2001), Humbird et al. (2011) and Kumar & Murthy (2011) [106,109,110]. It is assumed that the biomass remaining after sugar extraction and fermentation is co-fired to meet the utility requirements of the bio-refinery, with a LHV of 10.50 MJ/kg (50% moisture content) [98,111,112].

Simultaneous saccharification and fermentation

Following extraction from sugarcane, corn grain and switchgrass, respectively, sugars in the form of sucrose, starch and 5-carbon and 6-carbon sugar oligomers must be broken down to monomeric sugars via the process of saccharification. Conversion of sugars to glucose and fructose (from sucrose, starch and 6-carbon oligomers), and xylose (from 5-carbon oligomers) is achieved using enzymatic hydrolysis, with assumed efficiencies approaching the theoretical maximum.

Conversion of glucose, fructose and xylose to drop-in MD fuel is possible via a number of fermentation technologies, and we consider metabolism to five distinct platform molecules: triacylglycerides (TAGs), fatty acids, alkanes, iso-butanol (iBuOH) and ethanol (EtOH). The microorganism used for metabolism defines both the species of platform molecule and the mass conversion efficiency of monomeric sugar to that molecule. A range of monomer sugar-to-platform molecule mass conversion efficiencies, as a percentage of theoretical maximum mass yield, is considered here. The theoretical maximum mass conversion efficiencies of monomer sugars to TAGs, fatty acids and alkanes are estimated to be 31%, 42% and 34%, respectively, based on stoichiometry, and patent applications for microorganisms engineered for this purpose [113-116]. The theoretical maximum mass conversion efficiencies of monomer sugars to iso-butanol and ethanol are derived from the stoichiometry to be 41% and 51%, respectively, assuming the products of metabolism are alcohols, carbon dioxide and water. A review of the metabolic conversion of monomer

sugars to these and other platform molecules is given by Dugar & Stephanopoulos (2011) [116].

This analysis assumes simultaneous saccharification and fermentation, meaning that enzymatic hydrolysis and micro-organic metabolism occur simultaneously in the same bio-reactor. The utility requirements of pumping and continuous aeration and agitation required during these process operations are calculated from Najafpour (2007) and Couper et al. (2012), under an assumption of a batch fed bio-reactor with a total residence time of 96 hours [117-118].

Platform molecule extraction and purification

Upon completion of the saccharification and fermentation processes, the target platform molecule species must be separated and purified from the fermentation beer. This analysis considers three technologies for the separation and purification of TAGs, fatty acids and alkanes. Centrifugation may be employed to take advantage of the difference in the density of the platform molecule and the other components of the fermentation beer, and the utility requirements for the operation of centrifugal pumps are estimated from Vasudevan et al (2012) [119]. The utility requirements of hexane solvent extraction, which is used for extraction of vegetable oils from seed feedstocks in the production of biodiesel, are estimated based on data from Sheehan et al. (1998) [120]. Potassium hydroxide (KOH) steam lysing, followed by centrifugation, may be required if the platform molecule is not directly secreted, but is produced intra-cellularly, and the utility requirements for KOH steam lysing and centrifugation are estimated from Vaswani (2009) [121].

This analysis assumes that ethanol and iso-butanol separation and purification is achieved via distillation, taking advantage of the lower boiling point of alcohols compared to the other components of the fermentation beer. The utility requirements of distillation are estimated from Mei and ethanol industry data [101,122].

Upgrading to drop-in fuel

Finally, the separated and purified platform molecules are upgraded to a drop-in MD fuel product slate. For TAGs, fatty acids and alkanes, the mass conversion efficiency and utility requirements of upgrading platform molecules to MD fuel are based on the hydroprocessed esters and fatty acids (HEFA) process from Pearlson et al. (2013) [65]. The authors describe three steps by which soybean oil (composed primarily of TAGs) is upgraded to drop-in MD fuel: de-propenation to cleave the glycerin backbone from the TAG molecule; de-oxygenation to remove oxygen and saturate double bonds; and isomerization and catalytic cracking to refine straight chain alkanes to the desired carbon chain length distribution. It is assumed that the TAG product of micro-organic metabolism has a chemical composition similar to soybean oil (primarily carbon chain lengths of C18) [123], and that the HEFA process described in Pearlson et al. (2013) is an appropriate estimate of the energy and utility requirements of upgrading. Furthermore, because fatty acids do not contain a glycerin backbone, and alkanes do not contain a glycerin backbone, oxygen or double bonds, it is assumed that the utility requirements for upgrading of those platform molecules are approximately 66% and 33% of the Pearlson et al. (2013) estimates for the HEFA process, respectively. Note that micro-organic metabolism resulting in a carbon chain length distribution closer to MD fuel (for example, via algae or cyanobacteria synthesis to C10-C14) could increase fuel yield and reduce the upgrading effort required [115].

In order to upgrade ethanol and iso-butanol platform molecules to drop-in MD, it is assumed that three unit processes are required: dehydration to remove the hydroxyl functional group; oligomerization to produce longer chain alkanes; and hydroprocessing to the desired carbon chain length distribution. The mass conversion efficiencies and utility requirements of these processes are estimated based on a range of estimates provided by Byogy and Gevo, two companies working to commercialize this technology [124,125].

Minimum selling price

The MSP of MD fuels produced using AF technology is calculated by adapting the DCFROR model from Pearlson et al. (2013) [65]. The baseline facility size is 4000 barrels per day (bpd), and it is assumed that the 20-year plant is built using 20% equity financing and a 10-year loan with 5.5% interest. MSP is calculated assuming an internal rate of return of 15%, income taxes of 40% and 2% inflation per year. The DCFROR model is solved under these assumptions to find the MSP of all fuel products, such that the AF facility has a net present value (NPV) of zero. All prices are expressed in USD_{2012}.

Capital cost estimation

Ethanol facility capital costs from the literature are normalized to a dollars-per-unit-mass-feedstock-processed basis, in order to estimate pre-processing and fermenter capital costs for AF facilities. For sugarcane AF, a range of 20 to 30 USD_{2012}/kg of raw sugarcane milling and fermenter capacity is calculated from APEC-WG (2010) and Goldemberg (2008), respectively [126,127]. A range of 55 to 95 USD_{2012}/kg of corn grain dry milling and fermenter capacity is estimated from Urbanchuk (2010) and Wallace et al. (2005), respectively, for corn grain AF [128,129]. Finally, for switchgrass AF, a range of 115 to 215 USD_{2012}/kg of switchgrass pretreatment and fermenter capacity is estimated from Bain (2007) and Wallace et al. (2005) [129,130].

The additional capital costs for upgrading of TAGs, fatty acids or alkanes to drop-in MD are calculated from equipment cost estimates by Pearlson et al. (2013) [65]. The additional capital costs of the dehydration, oligomerization and hydroprocessing equipment, required to upgrade iso-butanol and ethanol to drop-in MD, is determined based on input from commercial operators Byogy and Gevo [124,125].

Operating cost and commodity price estimation

Fixed operating costs, including insurance, local taxes, maintenance, miscellaneous material and labor are estimated as a function of capital cost using heuristics from the petroleum refining industry from Handwerk & Gary [131].

Variable operating costs are based on utility, processing chemical and feedstock prices. Low, baseline and high natural gas prices are estimated using a 5-year average from 2008 to 2012, ± 2 standard deviations, as 1.20, 5.84 and 10.49 USD_{2012}/GJ, from EIA historical data [132]. It is assumed that electric power and water prices are 0.07 USD_{2012}/kWh and 0.09 USD_{2012}/m^3, respectively. Enzyme, yeast and processing chemical costs are estimated for sugarcane [133], corn grain [133], and switchgrass [105] on a per kilogram feedstock basis.

Sugarcane prices are based on a 5-year average of historic sugar commodity prices ± 2 standard deviations [134], and an assumed yield of 1 kg of sugar from 10 kg of raw sugarcane [135], as 20.74, 45.67 and 70.59 USD_{2012}/t of sugarcane. Corn grain prices are estimated using a 5-year average of historic commodity prices, ± 2 standard deviations, as 3.16, 6.17 and 9.18 USD_{2012}/ bushel [136]. Switchgrass prices, based on 50 USD_{2012} per short ton, ±50% to mirror variation in the other feedstock types, are estimated as 28.67, 57.33 and 86.00 USD_{2012}/t [137]. Finally, the relative values of the fuel products were estimated from 5-year averages of spot prices [138], where gasoline prices are used as a surrogate for naphtha. Note that this is a simplifying assumption, and that naphtha can be directly blended with gasoline only in limited volumes due to its low octane.

Results and discussion

The data sources described above are used to model the mass and energy balances for the AF MD fuel production process. This data is shown in Table 11, and is used in conjunction with GREET (.NET v1.0.0.8377) and the DCFROR model described above to calculate the lifecycle GHG emissions and MSP of AF MD fuels.

Table 11: Mass and energy balances for the low, baseline and high AF MD production processes considered in this analysis.

		Process inputs					Products							
		Make-up water	Electric power	Natural gas	Feedstock	Enzyme, yeast and preprocessing chemical costs	DDGS co-production	Electric power co-production	Heavy oil	Light ends	Naphtha	Jet	Diesel	Total fuel production
		[10^3 m^3/yr]	[GWh/yr]	[TJ/yr]	[kt/yr]	[1000 $/yr]	[kt/yr]	[GWh/yr]	[10^3 m^3/yr]					
Sugarcane AF	Low	2641	0	443	4379	3028	0	644	0	0	0	378	0	378
	Base	2275	0	673	3979	2751	0	205	0	23	5	33	171	233
	High	1619	0	632	2264	1566	0	99	0	19	10	60	28	116
Corn grain AF	Low	643	189	2254	1603	15202	519	0	0	0	0	378	0	378
	Base	941	137	2529	1074	10185	348	0	0	23	5	33	171	233
	High	966	139	2666	789	7484	256	0	5	0	21	73	18	116
Switchgrass AF	Low	1679	0	774	1538	74570	0	111	0	0	0	378	0	378
	Base	1051	125	673	1455	70535	0	0	0	23	5	33	171	233
	High	1067	233	253	1662	80587	0	0	5	0	21	73	18	116

Lifecycle GHG emissions

The range of results for the lifecycle GHG emissions of sugarcane, corn grain and switchgrass AF MD are shown in Figure 7a, broken out by two different methods of dealing with non-fuel co-products of the AF fuel production process: market based allocation and displacement. Figure 1a demonstrates that, although these renewable MD production pathways have the potential to reduce attributional lifecycle GHG emissions from the conventional MD baseline of 90 gCO_2e/MJ_{MD} (low and high estimates of 82.8 and 112.5 gCO_2e/MJ_{MD}, respectively) [9], there is significant variability in the calculated results. Variability in AF technology performance, which is determined in part by design decisions regarding the fuel production technology, affects the feedstock-to-fuel conversion efficiency and utility requirements. Furthermore, the co-product allocation methodology employed contributes to a range of results between -27.0 and 19.7, 47.5 and 117.5, and 11.7 and 89.8 gCO_2e/MJ_{MD} for sugarcane, corn grain and switchgrass AF, respectively. Note here that all results in this Chapter are expressed per unit of MD fuel, which includes both the diesel and jet fuel fractions of the total fuel product slate.

Figure 7b and shows baseline results for each pathway and emissions allocation method, disaggregated by the feedstock cultivation, feedstock transportation, fuel production, and fuel transportation and distribution steps. The fuel combustion CO_2 emissions are offset by a biomass credit, due to the biogenic nature of the feedstock. Under the assumption of the displacement method, co-product credits also act to offset emissions in other steps of the fuel production lifecycle. These co-products are excess electricity generation in the case of sugarcane and switchgrass AF, and DDGS used for animal feed in the case of corn grain AF. The data for the low, baseline and high scenarios under an assumption of market-based allocation is also given in Table 12.

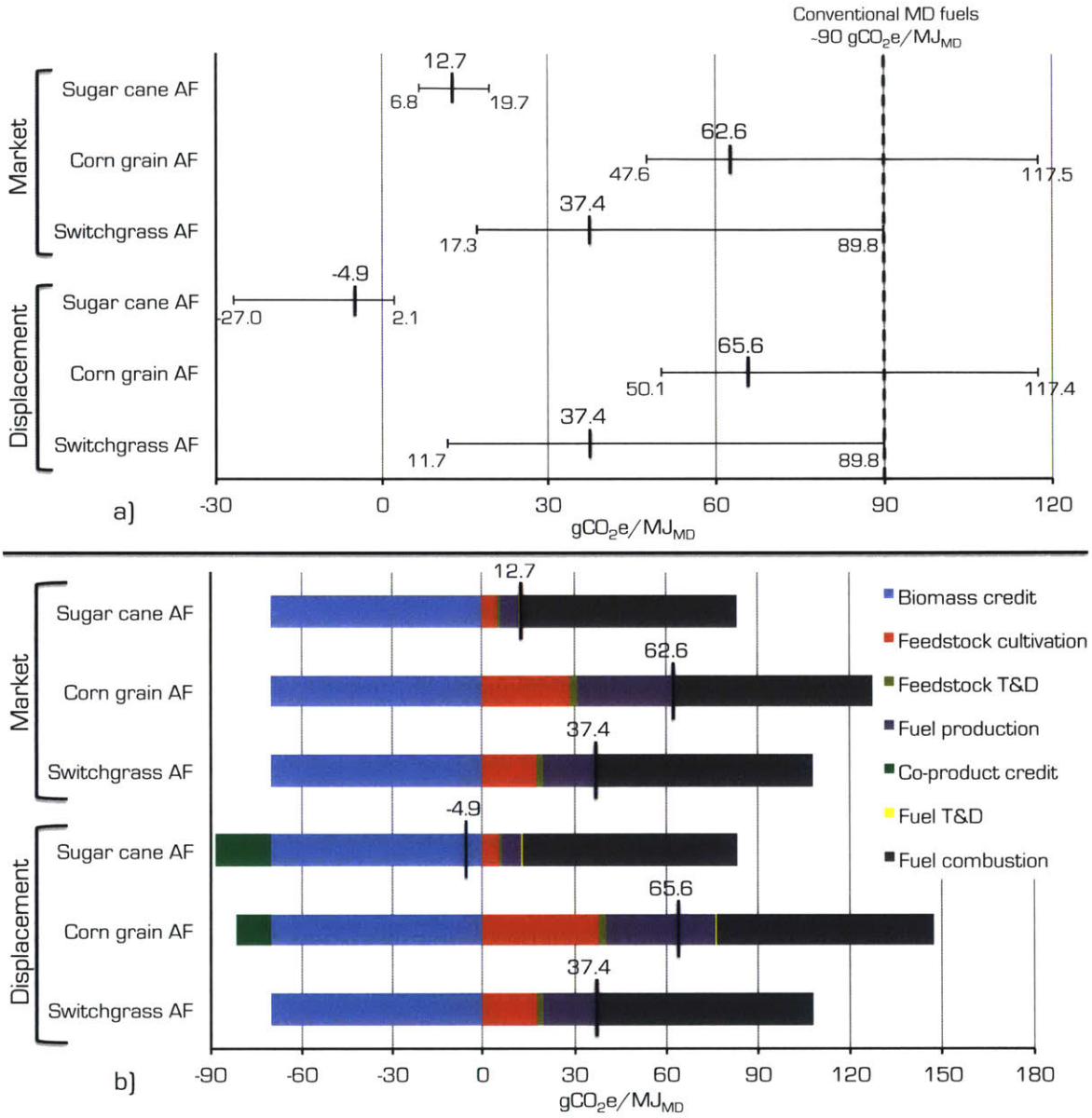

Figure 7: a) Range of lifecycle GHG emissions results under market-based allocation and displacement methods for dealing with emissions burdens to non-fuel co-products. Note that the whisker reflect variability, not probabilistic uncertainty, in the results. b) Baseline lifecycle GHG emissions, broken out by lifecycle step under market-based allocation and displacement methods for dealing with emissions burdens to non-fuel co-products.

Table 12: Low, baseline and high scenario results, broken out by lifecycle step assuming market-based allocation. Offsetting biomass carbon credits and CO_2 combustion emissions, as shown in Figure 7, are not shown here.

		Feedstock cultivation	Feedstock T&D	Feedstock to platform chemical conversion	Platform chemical to drop-in fuel upgrading	Fuel T&D	Total
Sugarcane AF	Low	3.1	0.6	0.0	2.5	0.5	**6.8**
	Base	4.9	1.0	0.0	6.2	0.5	**12.7**
	High	5.9	1.1	0.0	12.1	0.5	**19.7**
Corn grain AF	Low	26.2	1.9	13.3	5.6	0.5	**47.6**
	Base	28.9	2.1	15.6	15.4	0.5	**62.6**
	High	45.0	3.3	26.9	41.7	0.5	**117.5**
Switchgrass AF	Low	11.1	1.3	1.8	2.6	0.5	**17.3**
	Base	17.6	2.1	10.9	6.2	0.5	**37.4**
	High	39.7	4.7	40.2	4.6	0.5	**89.8**

The results in Figure 7b and Table 12 show that, compared to feedstock and fuel transportation and distribution, the feedstock cultivation, feedstock conversion to platform chemical, and platform chemical upgrading steps of the lifecycle are the major contributors to overall lifecycle GHG emissions of AF MD fuels These steps account for at least 83% of total lifecycle GHG emissions in all of the scenarios considered.

The difference in feedstock cultivation emissions between the pathways is largely due to N_2O emissions from fertilizer application. For example, under the baseline market-based allocation case, 1.3 (27%), 15.5 (54%) and 9.8 (56%) gCO_2e/MJ_{MD} of feedstock cultivation emissions are attributable to nitrogen fertilizer application for sugarcane, corn grain and switchgrass cultivation, respectively. This analysis assumes the default N_2O emissions factors associated with sugarcane, corn grain and switchgrass cultivation from GREET (.NET v1.0.0.8377).

In contrast, the difference in fuel production emissions between pathways is largely due to their requirements for external utilities for production processes. For example, no external utilities are required for sugarcane AF fuel production, whereas 0.020 kWh_{elec} and 0.27 MJ_{NG}, and 0.018 kWh_{elec} are required per MJ of corn grain and switchgrass AF fuel production, respectively, to meet the calculated process power and heat requirements. The difference in utility requirements between pathways is due to the co-generation of heat and power from

excess biomass in the sugarcane and switchgrass AF pathways. For example, power and heat co-generation from sugarcane bagasse combustion following sucrose extraction provides enough fuel for co-generation, such that the process power and heat requirements of sugarcane AF fuel production are satisfied and 0.029 kWh_{elec} of excess electricity is exported to the grid per MJ of MD production. Similarly, the combustion of lignin and other biomass residues from switchgrass following sugar extraction provides process heat and power that partially offsets the utility requirements calculated for AF fuel production, however some additional external electricity must be imported to satisfy process requirements. Note here that the values discussed above do not include natural gas for steam-methane reforming to meet the hydrogen requirements of hydroprocessing, although these additional requirements are included in the final GHG results.

In order to further understand the drivers of variability within and between the feedstock-to-fuel production pathways shown in Figure 7, a sensitivity analysis is carried out. The results of this sensitivity analysis are shown in Figure 8, highlighting the five parameters for each pathway that yield the largest change in results when varied in isolation.

For sugarcane AF, use of the displacement method instead of market-based allocation results in a negative lifecycle GHG footprint because the excess electricity exported to the grid generates a carbon credit, assumed to be equivalent to US grid-average transported electricity with a GHG intensity of 670.0 gCO_2e/kWh from GREET.

In comparison to the other feedstock types, the corn grain AF results are more sensitive to the type of platform molecule that is a product of fermentation. This is because all of the utilities required for corn grain AF fuel production must be imported from the grid, while the utility requirements of the sugarcane and switchgrass pathways are at least partially offset by heat and power co-generation. The overall feedstock-to-fuel conversion efficiency of MD fuel production via an iso-butanol platform molecule is lower than via fatty acid, which results in feedstock requirements that are 12% greater than in the baseline case. This additional feedstock quantity results in greater GHG emissions at each of the upstream feedstock and fuel production steps of the lifecycle.

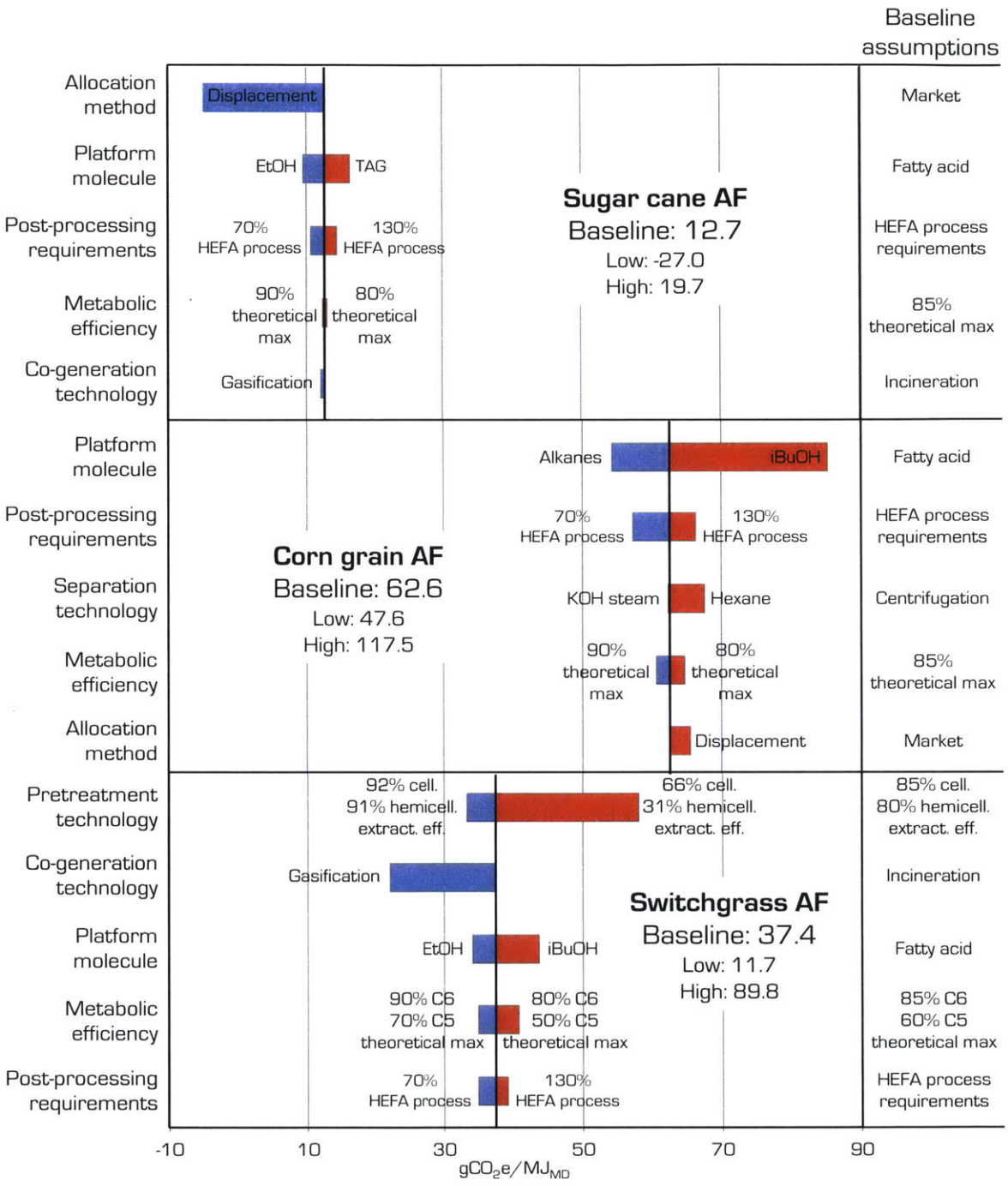

Figure 8: Sensitivity analysis of assumptions driving the lifecycle GHG emissions results for AF production technologies. The five assumptions leading to the largest change in results for each pathway are displayed, including both the methodological decision of market-based emissions allocation versus displacement, and parameters that define the mass and energy balances associated with AF MD fuel production.

The switchgrass AF pathway is most sensitive to the efficiency of monomer C5 and C6 sugar extraction from switchgrass. This is a reflection of the large range of values that are explored for this parameter, because this facet of lignocellulosic biofuel production technology that is still uncertain and has not yet been proven at commercial scale [88,90]. In addition, assuming gasification technology for excess biomass combustion reduces the lifecycle GHG footprint of switchgrass AF because the increased efficiency of electricity generation is enough to shift switchgrass AF fuel production from an electricity importing, to an electricity exporting process.

Land use change emissions

The potential contribution of land use change (LUC) emissions to lifecycle GHG emission is also quantified here for AF MD fuels. Direct LUC occurs when land is converted from its original use to cultivation of biomass feedstock, causing a one-time change in the soil and biomass carbon stock of the land. Indirect LUC occurs when biomass feedstock cultivation in one location changes land use patterns in some other location as a results of a change in market conditions, such as commodity prices. This analysis does not attempt to quantify the emissions associated with indirect LUC, however a number of peer-reviewed studies have quantified the size of this environmental impact on the lifecycle GHG emissions of ethanol and biodiesel, including Searchinger et al. (2008), Hertel et al. (2010), Plevin et al. (2010) and Lapola et al. (2010) [15-17,139].

This analysis calculates the potential lifecycle GHG emissions impact of direct LUC attributable to AF MD fuel production on previously uncultivated land using the carbon debt scenarios described in Fargione et al. (2008) [18]. Biomass yields for sugarcane and corn grain are estimated from the US National Agricultural Statistics Service (NASS), and for switchgrass from Wullschleger et al. (2010) [140,141]. The scenario results for all three AF feedstocks are shown in Table 13, assuming market-based allocation. The values are calculated based on the assumption that direct LUC emissions are amortized evenly over a 30-year period, in line with the US Environmental Protection Agency's method for dealing with emissions from LUC [46].

Table 13: Potential contribution of direct LUC to lifecycle GHG emission of AF MD production pathways.

		Original land use	LUC carbon debt [$MgCO_2/ha$]	Biomass yield [Mg/ha]	Biomass to AF MD (alloc. factors incl) [$kg_{rawfeed}/MJ_{MD}$]	30-year amortized LUC carbon debt [gCO_2/MJ_{fuel}]	Lifecycle GHG emissions including direct LUC [gCO_2/MJ_{MD}]
Sugarcane AF	Low	Cerrado wooded	165	83.3	0.31	20.2	27.0
	Base			75.7	0.49	35.4	48.1
	High			68.0	0.58	46.7	66.4
Corn grain AF	Low	Central grassland	134	11.3	0.10	38.4	86.0
	Base			9.4	0.11	51.2	113.8
	High			7.4	0.17	100.7	218.2
Switchgrass AF	Low	Abandoned cropland	6	18.8	0.12	1.3	18.6
	Base			12.9	0.19	2.9	40.3
	High			7	0.43	12.2	102.0

The results shown in Table 13 indicate that direct LUC emissions could significantly increase the lifecycle GHG emissions of AF MD fuels. For example, the baseline lifecycle GHG emissions of sugarcane, corn grain and switchgrass AF increase by 278%, 82%, and 8%, respectively, from their baseline no-LUC results when direct LUC is included. In the case of corn grain AF, the additional GHG emissions from direct LUC are sufficient to push the lifecycle GHG emissions of this fuel pathway above the conventional MD baseline of 90.0 gCO_2e/MJ_{MD}.

Although the land use conversions assumed in this calculation are possible for each of the individual feedstock-to-fuel pathways considered, direct LUC emissions burdens are highly dependent upon the specific scenario in which the feedstock is grown, and should be evaluated as such.

Minimum selling price

The MSP results for AF MD are shown in Figure 9, broken out by the contributions of capital, feedstock operating, and non-feedstock operating production costs. Low, baseline and high results range from 0.61 to 2.63, 0.84 to 3.65, and 1.09 to 6.30 $USD_{2012}/liter_{MD}$ for sugarcane, corn grain and switchgrass AF, respectively. Tabular data is also available in

Appendix B. Only the low scenario for sugarcane AF MSP is below the 2013 US gate price for conventional fuels of \$0.80/liter$_{MD}$.

For reference, Figure 9 shows the US gate price of MD fuels of approximately 0.80 USD$_{2012}$/liter$_{MD}$, from October 2013 when this analysis was originally carried out [142]. Note that, as of the writing of this thesis in November 2016, US gate prices for MD fuel have fallen to approximately \$0.38 USD$_{2012}$/liter$_{MD}$. However, because the electricity, natural gas, and other liquid fuel prices used in the calculation of MSP were based on historical averages up to 2013, the 2013 MD fuel price is retained in the figures presented here for the sake of internal consistency. Furthermore, there is substantial uncertainty around the drivers of conventional MD fuel price, even in the short term. For example, the US EIA projects that the price of crude oil will be between 57 and 146 USD$_{2012}$/bbl in 2020 [143].

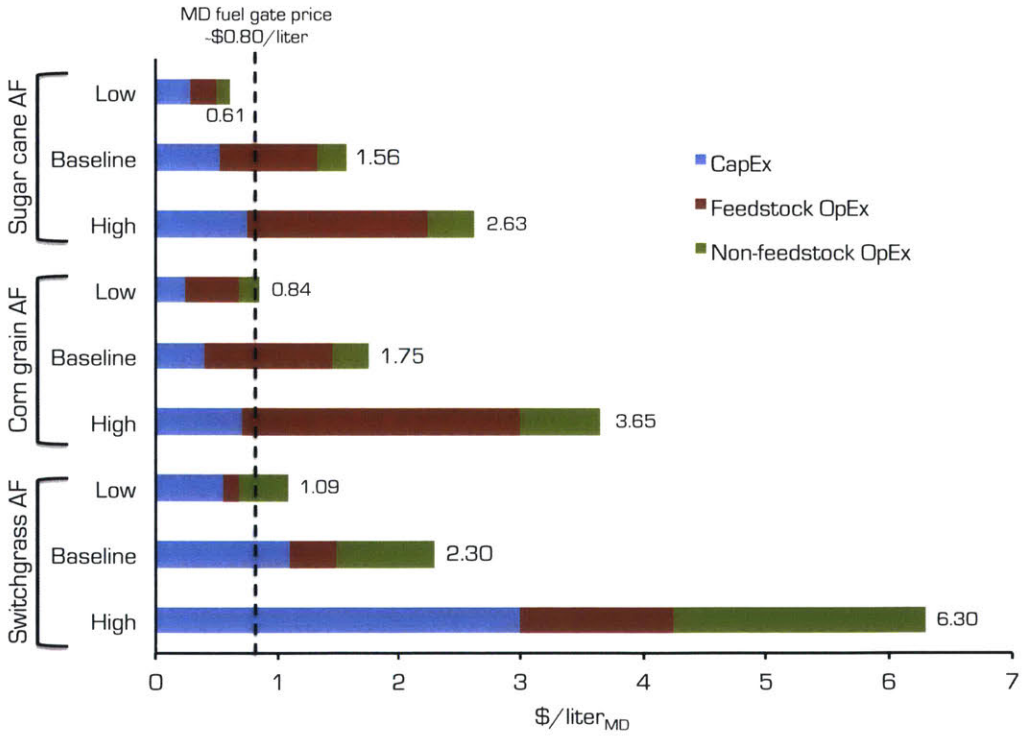

Figure 9: Low, baseline and high MSP of sugarcane, corn grain and switchgrass AF, broken out by the contributions of capital cost (CapEx), feedstock operating costs (feedstock OpEx), and non-feedstock operating costs (non-feedstock OpEx). These results are compared to a conventional MD fuel gate price of \$0.80 USD$_{2012}$/liter$_{MD}$ from late 2013 when this analysis was originally carried out. MD fuel gate prices at the time of writing this thesis are approximately \$0.38 USD$_{2012}$/liter$_{MD}$.

Figure 9 demonstrates that there is significant variability in the MSP of each of the AF fuel pathways, and that feedstock costs are the greatest contributor to variability in the MSP of sugarcane and corn grain AF. In contrast, capital costs are the largest contributor to variability in the MSP of switchgrass AF, which reflects the high capital costs of equipment for cleaning and size reduction, and pretreatment reactors, for lignocellulosic biomass [106].

In order to explore the drivers of variability within AF pathways, a sensitivity analysis of MSP to feedstock-to-fuel conversion efficiency, feedstock costs, capital costs and facility size is carried out. The results are shown in Figure 10.

The results in Figure 10 are consistent with the observation from Figure 9, that feedstock costs contribute to greater variability in MSP for the sugarcane and corn grain AF pathways, and that capital costs contribute to greater variability in MSP for the switchgrass AF pathway. In addition, the findings indicate that MSP of AF MD derived from all three feedstocks is particularly sensitive to feedstock-to-fuel conversion efficiency, and especially in the case of switchgrass. Similar to the results for lifecycle GHG emissions, this is in part because lignocellulosic pretreatment and co-fermentation of glucose, fructose and xylose has not yet been proven at the commercial scale. The wide range of parameters considered here is intended to capture variability in the way in which AF fuel production technology could be implemented at commercial scale.

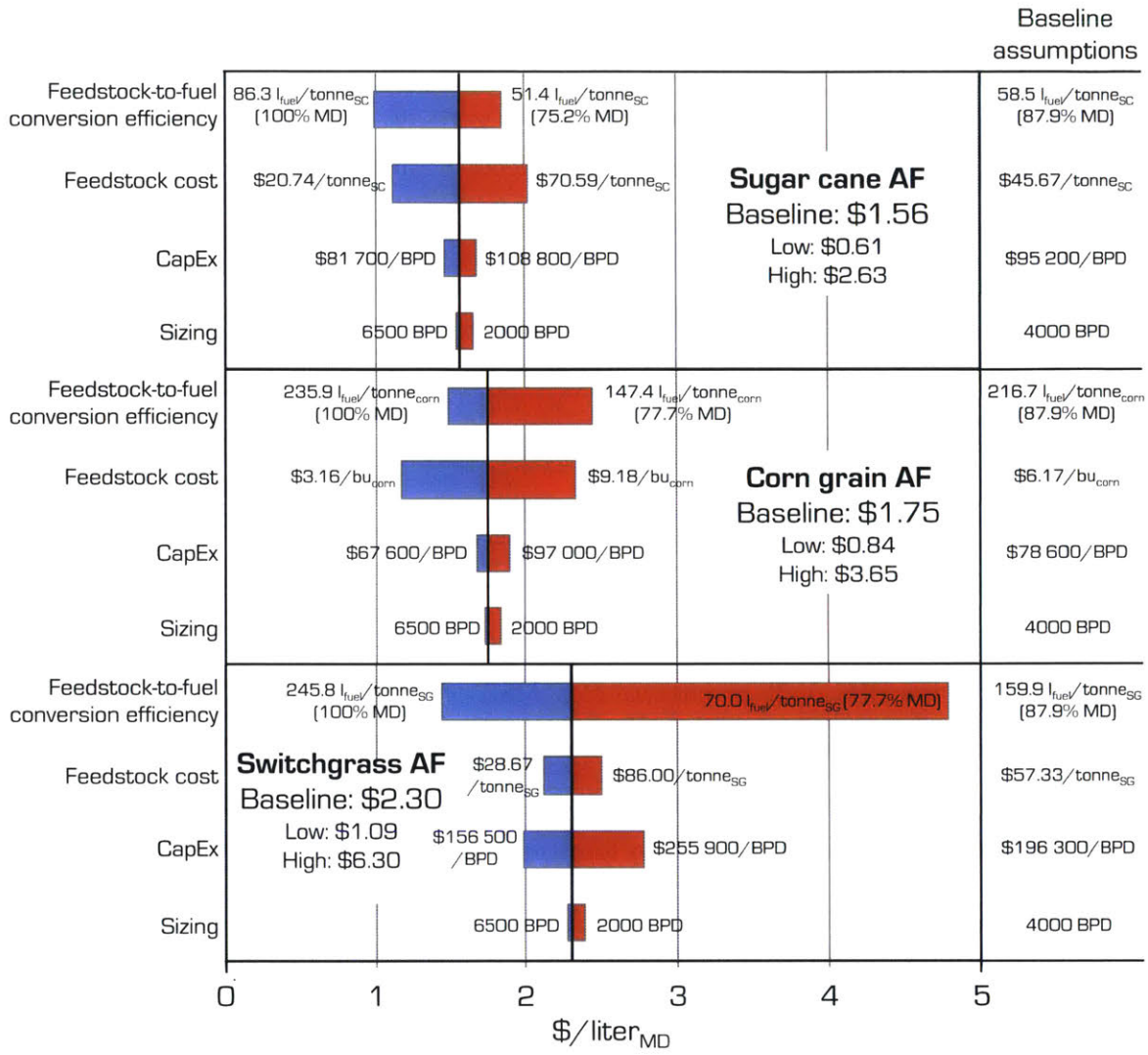

Figure 10: MSP sensitivity analysis. The variability due to feedstock-to-fuel conversion efficiency, capital costs and facility size is quantified for each pathway.

Limitations and areas for future work

Future work in this area could build on the analysis presented in this Chapter in a number of ways. First, the scope of technologies defined as fermentation and advanced fermentation (AF) considered in this analysis is broad, encompassing sugars derived from three disparate feedstock types and micro-organic metabolism to five different target platform molecules. This is a methodological choice made at the outset in order to characterize the environmental and economic performance of an entire class of MD fuel production

technologies, and to quantify the differences between various technology choices within that technology class. However, future research could involve higher-resolution assessment of more specifically defined fuel production processes within the AF class of technologies. For example, synthesized iso-paraffinic (SIP) fuels (via farnesene) and alcohol-to-jet (ATJ) fuels (via C2 to C5 alcohols) are the only pathways that fit the AF definition and are certified under D7566 for use in aircraft turbine engines [87]. More detailed chemical process modeling of these specific conversion pathways, and the feedstocks actually used for fuel production, would provide a more precise estimate of lifecycle GHG emissions and MSP of the fuels likely to be used, and therefore better inform policy regarding these fuels. Furthermore, as these technologies advance towards commercial-scale production, empirical data should be used to verify the mass and energy balances calculated here and in subsequent work.

In order to deal with variability and uncertainty in key assumptions and input parameters a scenario-based approach is used here to establish upper- and lower-bounds on lifecycle GHG emissions and MSP. However, this makes it difficult to draw conclusions about the relative likelihood of different outcomes within the range of results. Therefore, this work could be built upon by quantifying uncertainty associated with the results. Stochastic Monte Carlo analysis has been used to quantify uncertainty in LCA and TEA studies of ethanol and biodiesel [144-147], as well as in research that has leveraged components of the work presented here for assessment of drop-in MD fuel technologies [148,149]. Uncertainty quantification is especially informative when using TEA to assess the impact of policies on economic viability, as there is a financial value associated with risk that is not captured when using a deterministic approach.

This analysis also demonstrates that lifecycle GHG emissions of AF MD fuels are sensitive to the potential contribution of LUC emissions, and that direct LUC could negate the GHG benefit of AF fuels relative to petroleum-derived MD. The LUC emissions factors used here are illustrative only, however the quantification of direct and indirect LUC emissions attributable to biomass-derived fuels is an active area of research in the field of economic modeling. A holistic evaluation of the environmental feasibility of AF production technologies should include these additional climate impacts, as well as non-climate impacts

such as: water use and availability for feedstock and biofuel production [150]; the impacts of feedstock cultivation on soil nutrient removal and contaminated water runoff [151]; and non-GHG climate impacts [152].

Summary

The work presented in this Chapter is the first peer-reviewed study of the environmental and economic feasibility of AF technologies for producing renewable drop-in MD fuels, including jet and diesel fuel. The results show that, although the LCA results are highly variable, AF MD production technologies offer the potential for a reduction in GHG emissions compared to conventional MD fuels. Under the baseline assumptions sugarcane, corn grain and switchgrass AF provide attributional lifecycle GHG emissions reductions of 86%, 30% and 58% from conventional MD, respectively. Furthermore, lifecycle GHG emissions can be minimized by feedstock and technology decisions. For example, sugarcane and switchgrass AF have relatively lower lifecycle GHG emissions than corn grain AF, and the emissions for both pathways may be further reduced via the co-generation of process heat and power from excess biomass, especially using more efficient technologies such as gasification instead of incineration. Lifecycle GHG emissions may also be reduced for all of the pathways by increasing overall feedstock-to-fuel conversion efficiency. This can be achieved by increasing monomer sugar yields from the feedstock, increasing efficiency of platform molecule separation processes, and by increasing the efficiency of micro-organic metabolism of sugars to the target platform molecule.

This analysis also demonstrates that LUC emissions are a key determinant of the lifecycle GHG emissions of AF technologies, however these results are highly dependent upon the situation in which the feedstock is cultivated. For example, if AF MD feedstock is grown on land that had not previously been cultivated, this analysis finds that inclusion of direct LUC emissions could increase the lifecycle GHG footprint of sugarcane, corn grain and switchgrass AF by 279%, 82% and 8%, respectively, under baseline assumptions. Conversely, if the feedstock is grown on land that was already being used for cultivation of that crop, there are no direct LUC emissions attributable to the fuel. Therefore, direct LUC

emissions should be evaluated specific to the situation in which the feedstock is being produced. Indirect LUC emissions should be evaluated in the context of larger-scale biofuel production goals or policies, and are beyond the scope of this work.

The MSP of AF MD fuels is also found to be highly variable, however only the low scenario for sugarcane AF has an MSP below the 2013 baseline price for petroleum-derived MD fuels of 0.80 $USD_{2012}/liter_{MD}$. This indicates that commercial-scale AF MD production is likely to come at a cost premium to petroleum-derived fuels. The MSP results are most sensitive to assumptions regarding the overall feedstock-to-fuel conversion efficiency, feedstock costs, and capital costs of AF production technologies. One interesting opportunity for reducing the capital costs of AF MD fuels is to retrofit existing ethanol production facilities instead of constructing new greenfield facilities. For example, if feedstock pre-processing and fermenter capital costs could be reduced by 50% by retro-fitting existing facilities, the baseline MSP for sugarcane, corn grain and switchgrass AF would go down to 1.30, 1.55 and 1.64 $USD_{2012}/liter_{MD}$, respectively. As mentioned above, feedstock-to-fuel conversion efficiency could be improved by increasing sugar extraction and metabolic yields, and this is especially intriguing because if feedstock-to-fuel conversion efficiency is maximized, both lifecycle GHG emissions and MSP would be reduced.

In addition to the technical and commodity price aspects captured in the sensitivity analysis, the feasibility of AF technologies is subject to the prevailing economic and policy conditions and should be considered with regard to these factors. For example, under US RFS2 advanced biofuel producers generate renewable identification numbers (RINs) that would be worth approximately 0.27 $ per $liter_{MD}$ [153], which could significantly improve the economic viability of AF MD fuels. Alternatively, a policy that monetizes the potential reduction in lifecycle GHG emissions that AF fuels provide compared to petroleum-derived fuels, such as a carbon tax or cap-and-trade scheme, would also positively affect these technologies' economic viability.

In summary, this Chapter demonstrates that jet and diesel fuels produced from sugarcane, corn grain and switchgrass using AF technologies have the potential to reduce lifecycle GHG emissions compared to petroleum-derived fuels, but that this environmental benefit

likely comes at a production cost premium. In addition, this analysis finds that the environmental and economic performance of AF MD fuels depends upon decisions regarding technology selection, as well as the successful technical and commercial development of these technologies. A number of challenges remain on this front including: variability in feedstock composition and quality; sugar extraction from recalcitrant lignocellulosic materials; hydrolysis efficiency; enzyme separation and re-use; feedstock pre-processing costs; metabolic efficiencies of fermenting microorganisms, especially of 5-carbon sugars; and facility integration [85,88,151]. This analysis quantifies the impact of these aspects using sensitivity analysis, and indicates that addressing these challenges will be critical for the environmental and economic feasibility of AF jet and diesel fuels.

The work contained in this Chapter is published in *Energy & Environmental Science* with co-authors Robert Malina, Hakan Olcay, Matthew Pearlson, James Hileman, Adam Boies and Steven Barrett.

Staples, M.D., Malina, R., Olcay, H., Pearlson, M.N., Hileman, J.I., Boies, A. & Barrett, S.R.H. (2014). Lifecycle greenhouse gas footprint and minimum selling price of renewable diesel and jet fuel from fermentation and advanced fermentation production technologies. *Energy & Environmental Science, 7,* 1545-1554. DOI: 10.1039/c3ee43655A

4. Dynamic cost-benefit assessment of alternative jet fuels

Motivation and context

In Chapter 3, lifecycle analysis (LCA) and techno-economic analysis (TEA) methods are used to quantify the environmental and economic performance of drop-in middle distillate (MD) fuels, including jet fuel, from fermentation and advanced fermentation (AF) production technologies. The analysis finds that, under baseline assumptions, AF MD fuels offer potential reductions in attributional lifecycle greenhouse gas (GHG) emissions of 30% to 86% compared to conventional petroleum-derived fuels, but that the cost of producing AF fuel is approximately 2-5 times the gate price of conventional MD. These results highlight a trade-off between the potential climate benefit, and fuel cost premium, of using AF jet fuel for aviation. This Chapter quantifies the potential time-evolution of this trade-off, expanded to a scope of diverse alternative jet (AJ) feedstock-to-fuel pathways.

Anticipated growth in crude oil and conventional jet (CJ) fuel prices could decrease the relative cost premium of AJ [153], and the societal benefits of GHG emissions mitigation are expected to grow in future years as physical and economic systems become more stressed by climate change [155]. In addition learning-by-doing, also referred to as learning curve effects, could contribute to a reduction in the production costs of AJ as experience with the technologies accumulates, as has been empirically observed in the analogous corn ethanol [156,157], sugarcane ethanol [158,159] and vegetable oil biodiesel industries [160,161]. Insofar as learning-by-doing contributes to improvements in efficiency and a reduction in process input requirements, the lifecycle environmental impact of AJ fuel production may also improve over time. All of these time-dependent factors indicate that the climate damages mitigated by replacing CJ with AJ may exceed the additional cost premium of producing AJ at some point in the future, even if that is not the case today.

Therefore, the aim of this Chapter is to test the hypothesis that the societal benefits of a policy of large-scale AJ adoption outweigh the societal costs, in terms of the climate damages

and fuel production costs attributable to aviation, when changes over time are taken into account. A system dynamics approach is used to capture the time- and path-dependence of the societal climate and fuel production costs of AJ and CJ outlined above, as well as potential non-linearities and feedbacks associated with large-scale adoption of AJ fuels. These include the impacts of AJ feedstock demand on agricultural commodity prices and ultimately AJ production costs, the potential for CO_2 emissions from land use change (LUC), and the impact of fuel price on commercial aviation demand. The results of this cost-benefit assessment (CBA) identify the AJ production pathway characteristics that drive the balance of costs and benefits to society, in terms of climate damages and fuel production costs, attributable to aviation.

Methods and materials

The work presented in Chapter 3 represents just one contribution to a large engineering literature that uses LCA and TEA methods to characterize the performance of specific AJ technologies. Therefore, the first step in this analysis is to augment previous LCA and TEA work in order to consistently compare between disparate feedstock-to-fuel production pathways.

Bann et al. (2017) is used as the starting point for the TEA side of the analysis [148]. The authors use a stochastic discounted cash flow rate of return (DCFROR) model to compare the minimum selling price (MSP) of ten feedstock-to-fuel pathways under consistent financial assumptions. These pathways include eight feedstocks (soybean oil, tallow, yellow grease, corn grain, sugarcane, herbaceous biomass, woody biomass and municipal solid waste (MSW)) and six fuel production technologies (hydroprocessed esters & fatty acids (HEFA), advanced fermentation (AF), hydrothermal liquefaction (HTL), aqueous phase processing (APP), Fischer-Tropsch (FT) and fast pyrolysis (FP)).

Next, the lifecycle GHG emissions associated with these production pathways are assessed by drawing on the existing literature: Stratton et al. (2011, 2010) for vegetable oil HEFA and lignocellulosic FT [9,162]; Seber et al. (2013) for tallow and yellow grease HEFA [63]; Staples

et al. (2014) and Trivedi et al. (2015) for sugarcane, corn grain and lignocellulosic AF [11,50]; Olcay et al. (2013) for lignocellulosic APP [163]; Suresh (2016) for MSW FT [149], and; GREET1 2015 for lignocellulosic pyrolysis [44]. The LCA results for these pathways are re-calculated using energy allocation at all stages of the lifecycle, and 100-year global warming potential CO_2 equivalents, including climate carbon feedbacks, from the Intergovernmental Panel on Climate Change Fifth Assessment Report (IPCC AR5) (34 gCO_2e/gCH_4 and 298 gCO_2e/gN_2O) to enable comparison across studies [1]. Energy-based emissions allocation is selected to distribute emissions burdens amongst fuel and non-fuel products by a meaningful measure of their usefulness (in contrast to mass-based allocation), while remaining robust to temporal and spatial variation in commodity prices and emissions factors (in contrast to market-based allocation and the displacement method, respectively).

A comparison of the pathways represented by Bann et al. (2017) and the identified LCA studies reveals an imperfect matching of the harmonized TEA and LCA data [148]. However, for the purposes of this analysis, a number of simplifying assumptions are made in order to maximize the scope of technologies that are characterized in terms of lifecycle GHG emissions and MSP. These assumptions and the pathways covered are summarized in Table 14.

Table 14: Feedstock-to-fuel pathway scope, data sources, and simplifying assumptions.

Fuel production technology	Feedstock	TEA data source	LCA data source
HEFA	Soybean oil	Bann et al. (2017)	Stratton et al. (2011) GREET1 2015
	Rapeseed oil Palm oil Jatropha oil	Assumed equivalent to soybean oil HEFA pathway from Bann et al. (2017)*	
	Tallow Yellow grease	Bann et al. (2017)	Seber et al. (2014)
AF	Sugarcane Corn grain Herbaceous lignocellulosic crop	Bann et al. (2017)	Staples et al. (2014) Trivedi et al. (2015)
	Agricultural residue	Assumed equivalent to herbaceous lignocellulosic crop AF pathway from Bann et al. (2017)*	
FT	Herbaceous lignocellulosic crop Agricultural residue Woody lignocellulosic crop Forestry residue	Assumed equivalent to MSW FT pathway, plus additional feedstock cost and minus revenue from scrap, from Bann et al. (2017)*	Stratton et al. (2011) GREET1 2015
	MSW	Bann et al. (2017)	Suresh (2016)
FP	Agricultural residue	Bann et al. (2017)	Assumed equivalent to renewable diesel pyrolysis pathway in GREET1 2015†
	Forestry residue	Assumed equivalent to agricultural residue FP pathway from Bann et al. (2017)*	
APP	Woody lignocellulosic crop Forestry residue	Bann et al. (2017)	Olcay et al. (2013)
HTL	Woody lignocellulosic crop Forestry residue	Bann et al. (2017)	Assumed equivalent to analogous FT pathways in GREET1 2015†

*Denotes simplfying assumption for TEA data coverage
†Denotes simplifying assumption for LCA data coverage

The TEA and LCA data for these pathways, calculated using consistent financial, emissions allocation and climate metric assumptions for the purposes of cross-comparison, are summarized in Figure 11. The nominal lifecycle GHG emissions value in each study of interest (the mid or mean value for LCA data from the literature, and the default value for LCA data from GREET1 2015 [44]) for each AJ pathway is normalized against lifecycle GHG emissions from conventional petroleum-derived jet (CJ) fuel of 88.3 gCO_2e/MJ on the x-axis [162]. Note that this value differs from the result reported by Stratton et al. (2010) due to the use of updated values for GWP_{100} including climate-carbon feedbacks. The y-axis shows the cost premium of AJ over CJ, calculated from the mean MSP of AJ minus the 3-year average of CJ, 0.56 USD_{2015}/liter [142].

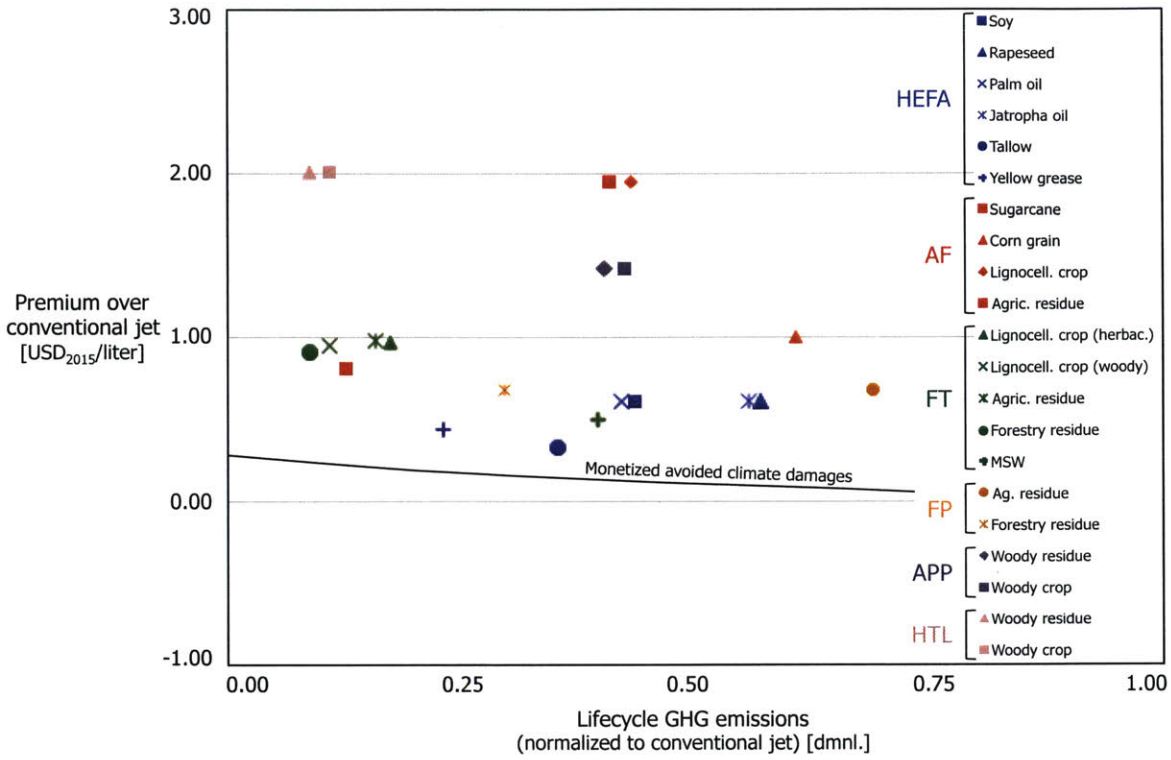

Figure 11: TEA and LCA data for AJ production technologies, using consistent assumptions. Monetized avoided climate damages are plotted as a function of the reduction in lifecycle emissions compared to CJ, a mean value from APMT-Impacts Climate for an emissions year of 2020, shown in black.

In order to compare between the disparate metrics of cost and environmental performance shown in Figure 11, the monetized avoided climate damages of a reduction in lifecycle GHG emissions is plotted. This curve is generated using the Aviation environmental Portfolio Management Tool v23 (APMT)-Impacts Climate [164]. APMT probabilistically quantifies the net present value (NPV) of changes in global societal welfare, calculated on the basis of the change in mean surface temperature of the Earth as a result of net radiative forcing of GHG emissions attributable to aviation [165-168]. The curve in Figure 11 depicts the change in mean NPV, divided by total fuel burn volume for an emissions year of 2020, as a function of percentage reduction in lifecycle emissions from CJ including well-to-pump (WTP) CO_2, CH_4 and N_2O, and combustion CO_2 emissions. The curve is calculated assuming a societal discount rate of 2%, Representative Concentration Pathway (RCP) 4.5, and Shared Socio-economic Pathway (SSP) 1.

The TEA and LCA data presented in Figure 11 indicate that, across all of the AJ production pathways considered, there is potential for a reduction in lifecycle GHG emissions. However, this climate benefit comes at a fuel cost premium compared to CJ, demonstrating that the climate-cost trade-off identified in Chapter 3 is not unique to AF technologies. Furthermore, all of the examined AJ pathways lie above and to the right of the curve from APMT, which indicates that the cost premium of AJ compared to recent CJ market prices is greater than the monetized NPV of the climate benefit for an emissions year of 2020.

Figure 11 is useful for a static assessment of the climate benefit and production cost trade-off associated with AJ technologies, however it fails to capture how this trade-off may evolve over time, as well as how the private costs of fuel production presented here can be used in a CBA regarding costs to society. Therefore, the next step in this analysis is to quantify the potential impact of learning-by-doing on the lifecycle GHG emission and production costs of AJ technologies.

Private and societal costs of AJ production

The stochastic DCFROR model developed by Bann et al. (2017) is used to calculate the MSP of AJ fuel for the pathway scope outlined in Table 14 [148]. MSP is broken out for each feedstock-to-fuel pathway by the mean contributions of capital cost, fixed operating cost, feedstock and non-feedstock variable operating costs, income tax, and revenue from non-MD fuel and co-products. Mean annual feedstock input and fuel yield quantities are also calculated.

These parameters are generated for two cases for each pathway: capital and fixed operating costs and fuel yield deterministically set to the mode value of the parameter distributions; and capital and fixed operating costs deterministically set to the minimum value, and fuel yield set to the maximum value in their distributions [148]. The first case is calculated to represent the n^{th} plant MSP of commercial scale fuel production, and the second case is calculated to represent the minimum achievable MSP of commercial scale fuel production, taking into account the potential for learning-by-doing, or learning curve effects, as

discussed above. The mean feedstock requirements, capital and non-feedstock operating costs, non-MD fuel revenue, and proportion of total fuel yield (on an energy basis) that is MD, are reported in

Table 15. Private MSP can be calculated from these parameters as a function of feedstock price, as shown in Equation 4.

Table 15: n^{th} plant and minimum mean contributions to AJ private MSP, adapted from Bann et al. (2017) [148]. Feedstock requirements are reported in the following units for each of the feedstocks: oil or waste grease for HEFA pathways; 15.5% moisture content corn grain; 50% moisture content sugarcane stalk; dry biomass for lignocellulosic pathways; and preprocessed and dried MSW.

Fuel production technology	Feedstock		Feedstock requirement, f [t_{feed}/t_{MD}]	Capital costs, $CapEx$ [USD_{2015}/t_{MD}]	Non-feedstock operating costs, $OpEx$ [USD_{2015}/t_{MD}]	Non-MD fuel revenue, R [USD_{2015}/t_{MD}]	MD proportion of total fuel yield [%]
HEFA	Soybean, rapeseed, palm & jatropha oil	n^{th}	1.31	244	277	84	91.5%
		minimum	1.25	232	249	84	
	Tallow	n^{th}	1.31	244	277	84	91.5%
		minimum	1.25	232	249	84	
	Yellow grease	n^{th}	1.31	244	277	84	91.5%
		minimum	1.25	232	249	84	
AF	Corn grain	n^{th}	4.99	706	454	424	90.8%
		minimum	3.82	671	408	408	
	Sugarcane	n^{th}	2.64	805	311	199	90.8%
		minimum	1.89	765	268	193	
	Herbaceous biomass & agricultural residue	n^{th}	10.29	1638	1145	90	90.8%
		minimum	6.63	1462	970	90	
FT	Herbaceous lignocellulosic crop	n^{th}	7.74	1155	564	180	89.1%
		minimum	6.99	1113	488	177	
	Woody lignocellulosic crop	n^{th}	7.36	1155	564	180	89.1%
		minimum	6.65	1113	488	177	
	Agricultural residue	n^{th}	7.83	1155	564	180	89.1%
		minimum	7.08	1113	488	177	
	Forestry residue	n^{th}	6.67	1155	564	180	89.1%
		minimum	6.03	1113	488	177	
	MSW	n^{th}	3.80	1155	564	311	89.1%
		minimum	3.54	1113	488	306	
FP	Herbaceous biomass	n^{th}	9.33	1479	1388	1967	48.4%
		minimum	8.29	1314	1201	1941	
APP	Woody biomass	n^{th}	7.36	1691	1209	869	80.2%
		minimum	6.99	1606	1121	845	
HTL	Woody biomass	n^{th}	13.46	2958	1684	2317	38.8%
		minimum	13.13	2886	1560	2299	

Equation 4: Private MSP.

$$MSP_{priv} = f \cdot p_{feed} + CapEx + OpEx - R$$

where

MSP_{priv}	= private minimum selling price [USD_{2015}/t_{MD}]
f	= feedstock requirement [t_{feed}/t_{MD}]
p_{feed}	= feedstock price [USD_{2015}/t_{MD}]
CapEx	= capital costs [USD_{2015}/t_{MD}]
OpEx	= non-feedstock operating costs [USD_{2015}/t_{MD}]
R	= non-MD fuel revenue [USD_{2015}/t_{MD}]

The private MSP for a feedstock-to-fuel pathway, calculated using Equation 4, represents the price that a private fuel producer would need to receive in order to break even on its MD fuel products, including AJ. However, the cost-benefit approach of this analysis is ultimately concerned with AJ fuel production costs to society (as opposed to the costs to the fuel purchaser) in terms of scarce resources such as land, labor and capital. Therefore, in order to better reflect societal costs, MSP is also calculated by removing the components of production cost that reflect monetary transfers (between producers, consumers, or the government), with no corresponding use of scarce resources. Specifically, the 15% private profit margin assumed for the calculation of private MSP is reduced to 3.2%, an estimate of the societal opportunity cost of capital based on long-term treasury bond rates from the US Office of Management and Budget [169], and the income tax rate is reduced from 16.9% to 0%. The market prices of other resources associated with fuel production are assumed to reflect their shadow prices - the societal opportunity costs (in the case of inputs, such as feedstock and utilities) and the utility derived from consumption (in the case of outputs, such as non-MD fuel products and non-fuel co-products) [170].

Mean societal MSP is calculated using the stochastic DCFROR model for the n^{th} plant and minimum cases. These results are compared to the analogous data points for private MSP in order to estimate a linear relationship between private and societal AJ production costs, as shown in Table 16.

Table 16: Estimated linear relationship between private and societal MSP.

Fuel production technology	Feedstock	Societal minimum selling price, MSP_{soc}, as a function of MSP_{priv} [USD_{2015}/t_{MD}]
HEFA	Soybean, rapeseed, palm & jatropha oil	$0.943(MSP_{priv}) - 69.84$
	Tallow	$0.924(MSP_{priv}) - 54.27$
	Yellow grease	$0.897(MSP_{priv}) - 38.12$
AF	Corn grain	$0.805(MSP_{priv}) - 53.30$
	Sugarcane	$0.814(MSP_{priv}) - 190.48$
	Herbaceous biomass & agricultural residue	$0.723(MSP_{priv}) - 154.41$
FT	Lignocellulosic	$0.723(MSP_{priv}) - 154.41$
	MSW	$0.754(MSP_{priv}) - 415.12$
FP	Herbaceous biomass	$0.730(MSP_{priv}) - 524.10$
APP	Woody biomass	$0.676(MSP_{priv}) - 297.37$
HTL	Woody biomass	$0.732(MSP_{priv}) - 1103.66$

Societal costs of CJ production

The societal costs of CJ production are calculated using the method presented in Withers et al. (2014) [171]. Crude oil producers' and refiners' profit margins are estimated, as a function of retail fuel prices, to be between 26-33% and 7-11%, respectively [172], and the corporate tax rate on these profits is assumed to be 16.9% [173]. The societal cost of crude oil is calculated by subtracting the estimated profit margin, and income tax on that profit, from the market price of crude oil. The societal cost of refining is calculated by subtracting refinery profits and taxes from the differential between crude oil and distillate fuel prices. 3.2% is added back on top of both components to capture the societal opportunity cost of capital, and the sum of the two reflects an estimate of societal CJ production cost [169].

Lifecycle emissions of AJ and CJ

The lifecycle emissions of the AJ production technologies of interest are characterized based on existing studies, as outlined in Table 14, updated to use energy allocation at all stages of

the lifecycle, and 100-year GWP CO_2e values from IPCC AR5. The nominal value in each study of interest (the mid or mean value in the case of values from the literature, and the default value in the case of GREET1 2015) is assumed to represent the lifecycle emissions of n^{th} plant commercial AJ production.

The LCA results for these pathways are augmented to quantify the potential for reductions in lifecycle emissions from learning-by-doing, as discussed above, by accounting for the potential impact of improvements in agricultural productivity and process efficiencies.

Improvements in agricultural productivity

Lifecycle emissions from feedstock production are modeled as a function of input quantity, such as nutrient application or diesel fuel, per unit of feedstock product. Therefore, in order to assess changes in lifecycle emissions from this step both agricultural yields and agricultural inputs per unit area must be considered.

The potential for increases in the agricultural yields of soybean, rapeseed, palm oil, corn grain and sugarcane are modeled in the same manner as described in the Energy crops section of Chapter 2. FAOSTAT historical yield data are collected for the crops and applicable world regions of the existing LCA studies. The upper-bound potential for yield improvement is defined by a linear increase of 1.5% of 2013 yields out to 2050, where yields are limited to agro-climatically attainable rainfed yields under advanced input levels from the GAEZ model [28,29]. Historical yields are not available for jatropha and switchgrass, so the potential yield improvements for these crops are estimated from Jongschaap et al. (2007) and English et al. (2010), respectively [174,175].

Areal nutrient application rates and farming energy inputs corresponding to improved yields in future years are estimated from a number of sources for soybean [176-181], rapeseed [44,176,177,179,182], oil palm [176,177,179,183-185], jatropha [9,176,177,185-187], corn grain [44,176-179], sugarcane [176,177,188], switchgrass [176,177,189-191], agricultural residues [44,176,177,191] and forestry residues [176,177,192].

The potential yield and areal agricultural input data are combined, and the resultant minimum estimates of agricultural inputs per unit of feedstock production, as well as values that define the n^{th} plant cases, are shown in Table 17.

Improvements in fuel production process efficiency

Lifecycle emissions of AJ production may also come down over time as fuel production processes become more efficient and require fewer feedstock and utility inputs. Therefore, the potential for improvements in total fuel yield per unit of feedstock input are estimated based on the highest yield reported in the LCA literature for each pathway, corresponding to the minimum MSP case reported in

Table 15. In addition, potential improvements in vegetable oil extraction rates specific to the HEFA pathways are estimated from the literature for soybean (10%) [193], rapeseed (15%) [194], oil palm (15%) [195], and jatropha (15%) [195]. The resulting conversion efficiencies of raw feedstock to total liquid fuel, in terms of LHV, are reported in Table 18.

Table 17: Agricultural inputs considered in the n^{th} plant and minimum cases for calculating lifecycle emissions.

Feedstock	Input	Unit	n^{th}	minimum
Soybean	N	g/bu	49.9	17.5
	P	g/bu	207	64
	K	g/bu	344	119
	Diesel	btu/bu	10683	3092
	Natural gas	btu/bu	1354	557
	Liquefied petroleum gas	btu/bu	418	131
	Gasoline	btu/bu	3711	1343
	Electricity	btu/bu	552	200
Rapeseed	N	kg/tonne	54.7	40.7
	P	kg/tonne	15.3	5.3
	K	kg/tonne	2.9	5.0
	Diesel	mmbtu/tonne	0.5	0.6
Palm	N	kg/short ton	9.5	3.7
	P	kg/short ton	0.0	2.2
	K	kg/short ton	0.0	6.7
	Diesel	btu/short ton	207692	207692
Jatropha	N	g/kg	36.6	31.8
	P	g/kg	14.0	12.6
	K	g/kg	40.2	31.3
	Diesel	btu/kg	1420	1420
Corn grain	N	g/bu	423	276
	P	g/bu	146	95.2
	K	g/bu	151	98.8
	Diesel	btu/bu	4727	2649
	Natural gas	btu/bu	1297	1041
	Liquefied petroleum gas	btu/bu	1720	1034
	Gasoline	btu/bu	1412	989
	Electricity	btu/bu	451	309
Sugarcane	N	g/tonne	800	541
	P	g/tonne	300	203
	K	g/tonne	1000	676
	Diesel	btu/tonne	36385	37840
	Natural gas	btu/tonne	20425	16340
	Liquefied petroleum gas	btu/tonne	17860	10716
	Gasoline	btu/tonne	11685	8180
	Electricity	btu/tonne	8550	5985
Switchgrass	N	g/short ton	8298	4220
	P	g/short ton	114	69.5
	K	g/short ton	227	139
	Diesel	btu/short ton	187451	65360
	Electricity	btu/short ton	14544	10180
Corn stover	N	kg/short ton	8.0	6.6
	P	kg/short ton	2.3	2.4
	K	kg/short ton	13.6	12.3
	Diesel	btu/short ton	285604	150800
Forest residue	Diesel	btu/short ton	132180	109158

Table 18: Overall efficiency (LHV) of feedstock to total liquid fuel conversion in the n^{th} plant and minimum cases. Feedstock LHV is calculated on the basis of raw feedstock, before feedstock extraction in the case of vegetable oils.

Fuel production technology	Feedstock	n^{th}	minimum
HEFA	Soybean	40.1%	46.5%
	Rapeseed	66.2%	80.1%
	Palm	60.3%	73.0%
	Jatropha	62.6%	75.7%
	Tallow	93.4%	98.3%
	Yellow grease		
AF	Sugarcane	10.2%	14.3%
	Corn grain	40.4%	52.7%
	Herbaceous lignocellulosic crop	25.7%	40.0%
	Agricultural residue		
FT	Herbaceous lignocellulosic crop	48.0%	52.0%
	Agricultural residue		
	Woody lignocellulosic crop		
	Forestry residue		
	MSW	59.0%	63.2%
FP	Agricultural residue	54.1%	60.9%
	Forestry residue		
APP	Woody lignocellulosic crop	38.8%	40.9%
	Forestry residue		
HTL	Woody lignocellulosic crop	43.8%	44.7%
	Forestry residue		

The resultant lifecycle GHG emissions for the n^{th} plant and minimum cases, taking into account reductions in agricultural inputs and improvements in fuel production efficiencies, are presented in Table 19. Petroleum-derived CJ fuel is also reported for comparison.

Table 19: Resultant lifecycle GHG emissions for n^{th} plant and minimum cases in [gCO_2e/MJ].

Fuel production technology	Feedstock	n^{th}	minimum	Note
HEFA	Soybean	38.8	30.7	
	Rapeseed	50.5	37.5	
	Palm	37.5	23.6	
	Jatropha	49.3	40.3	
	Tallow	31.5	27.4	
	Yellow grease	20.5	17.9	
AF	Sugarcane	11.2	3.7	
	Corn grain	53.9	31.0	
	Herbaceous lignocellulosic crop	38.4	13.2	
	Agricultural residue	36.4	18.2	
FT	Herbaceous lignocellulosic crop	15.5	7.9	
	Agricultural residue	14.0	11.0	
	Woody lignocellulosic crop	9.6	4.9	
	Forestry residue	7.8	7.0	
	MSW	35.3	26.4	Potential reduction in lifecycle emissions is partially due to a 25% greater credit for the replaced waste management strategy. This could be achieved by strategically deploying FT MSW technologies where no landfill gas recovery is taking place.
FP	Agricultural residue	61.1	51.6	Calculated based on pyrolysis diesel pathways in GREET1 2015
	Forestry residue	26.5	22.1	
APP	Woody lignocellulosic crop	35.8	29.2	In absence of access to the LCA model for this pathway, the minimum reported lifecycle emissions value from Olcay et al. (2013) defines the 'minimum' case.
	Forestry residue	37.7	27.1	
HTL	Woody lignocellulosic crop	9.6	4.9	In the absence of LCA data for these pathways, they are assumed equivalent to the analagous FT pathways in terms of lifecycle GHG emissions.
	Forestry residue	7.8	7.0	
Petroleum-derived CJ fuel		88.3		

Time-evolution of AJ lifecycle GHG emissions and societal production costs

Figure 12 provides a summary of the potential change in AJ technologies' lifecycle GHG emissions and societal production costs over time, relative to CJ, accounting for: potential reductions from learning-by-doing; the increased societal benefit of CO_2 mitigation in an emissions year of 2050 from APMT; and a 140% increase in CJ prices by 2050 based on the reference case of the 2015 Annual Energy Outlook [154]. These intermediate results provide support for the hypothesis that the societal benefits of GHG mitigation from AJ could outweigh the fuel cost premium compared to CJ in the future, as many of the AJ feedstock-to-fuel pathways fall below and to the left of the monetized climate benefit from APMT.

Furthermore, the societal costs of producing AJ could potentially drop below those of CJ (resulting in a negative premium on the y-axis) for a number of pathways by 2050. A comparison of the results shown in Figure 11 and Figure 12 highlight the time-dependent nature of AJ technologies' environmental and economic characteristics, relative to CJ. This comparison also implies path-dependence, because the improvements in AJ characteristics from learning-by-doing, represented in Figure 12, are a function of accumulated experience with the specific technology. If no fuel is produced, there is no mechanism to move down the learning curve and towards the minimum case lifecycle GHG emissions and societal production costs that are represented here.

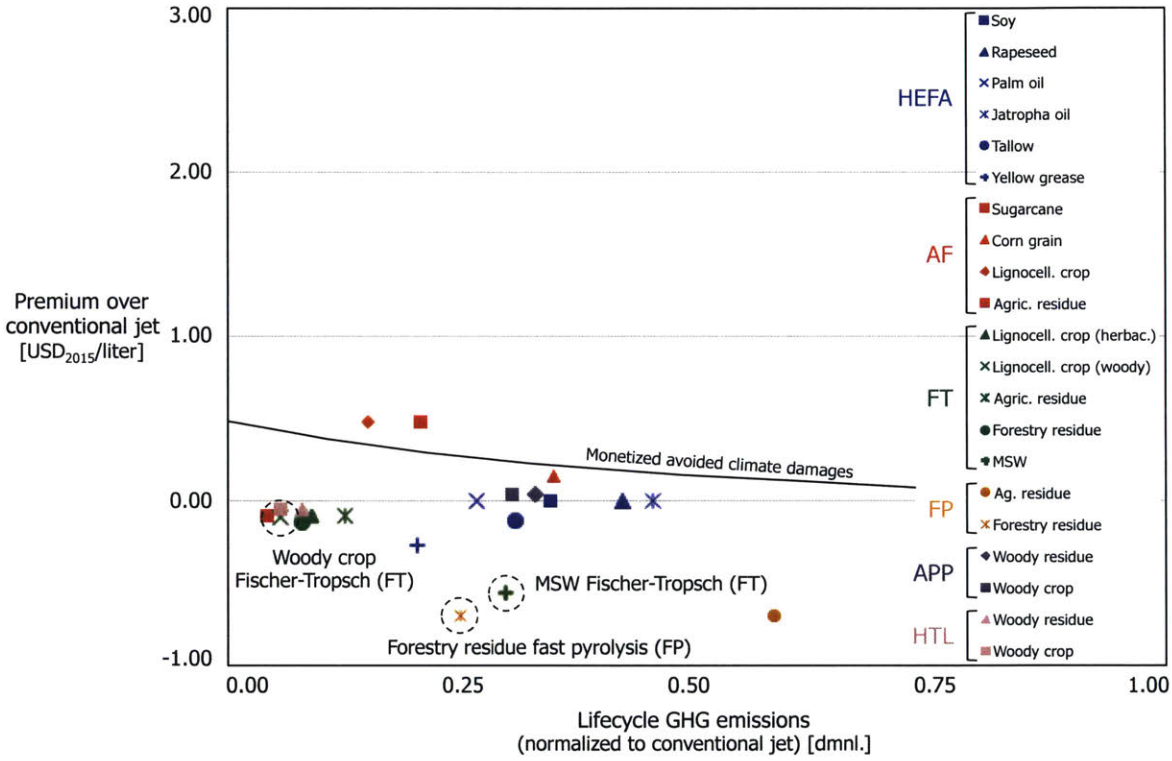

Figure 12: TEA and LCA results using consistent assumptions, including the potential for reductions in the production cost and lifecycle GHG emissions of AJ production from learning-by-doing. In addition, the y-axis represents the difference in the societal cost of fuel AJ production in the minimum case, and the societal cost of CJ projected to 2050. The monetized avoided climate damages are plotted as a function of the reduction in lifecycle emissions compared to conventional jet fuel, a mean value from APMT-Impacts Climate for an emissions year of 2050.

The results in Figure 12 are used to identify three pathways for further investigation: short-rotation woody crop FT, MSW FT, and forestry residue FP. These pathways are selected because all three lie on or near the Pareto frontier of maximum reduction in lifecycle GHG emissions and minimum production cost premium compared to CJ, meaning it is more likely for these pathways that the societal benefits of AJ adoption outweigh the costs. In addition, the three feedstock types associated with the selected pathways have distinct characteristics: short-rotation woody crops are produced via commercial or industrial agriculture, forestry residues are the byproducts of the existing forestry industry, and MSW is a waste product that, in many cases, is currently disposed of in landfills.

System dynamics model

The adoption of AJ derived from woody crop FT, MSW FT and forestry residue FP is modeled using a system dynamics approach. System dynamics is the technique of modeling systems *"characterized by interdependence, mutual interaction, information feedback, and circular causality"* including *"complex social, managerial, economic or ecological"* structures as *"a system of coupled, nonlinear, first-order differential (or integral) equations"* [196]. This method has been used to provide insight in applications as diverse as developing strategies to combat the spread of diabetes, to the dynamics of the cold war arms race [197], and has been particularly useful to assess the dynamics of adoption of new energy technologies [198-200], including advanced biofuels [201,202].

System dynamics is employed here in order to capture the time- and path-dependence, and non-linearities and feedbacks, of large-scale AJ adoption, and the resulting impacts on the societal climate change and fuel production costs of commercial aviation. The following sections describe key elements of the model.

Learning-by-doing

The formulation developed by Vimmerstedt et al. (2015) and Newes et al. (2011) for learning curves of advanced biofuels technologies is adopted here [202,203], as shown in Equation 5.

Equation 5: Learning-by-doing for advanced biofuels.

$$M = \begin{cases} 1 - (1 - M_0)\left(\frac{L^*}{E}\right)^{\left(\frac{1-PR}{ln2}\right)} & \text{for } E \geq L^* \\ M_0 & \text{otherwise} \end{cases}$$

$$L^* = \max\{L, E_0\}$$

$$m = m_{\text{early}} \cdot (1 - M) + m_{\text{minimum}} \cdot M$$

where

M	= degree of maturity, ϵ (0,1)
M_0	= initial maturity, ϵ (0,1)
L	= min. experience required for learning, units of cumulative production
L^*	= effective min. experience required for learning, units of cumulative production
E	= cumulative experience, units of cumulative production
E_0	= initial cumulative experience, units of production
PR	= progress ratio, percentage of maturity gap, (1-M), remaining after each doubling of cumulative production
m_{early}	= MSP or LCA characteristic of interest, n^{th} plant
m_{minimum}	= MSP or LCA characteristic of interest, minimum
m	= MSP or LCA characteristic of interest

This formulation is more meaningful than the single factor learning curve, traditionally used to model learning-by-doing of energy technologies [204,205], because a single factor learning curve implicitly has an asymptote of zero. By using Equation 5, however, the parameter m asymptotically approaches the minimum case value, which is defined by physical or practical limits on the degree to which that characteristic may improve over time.

The degree of maturity of feedstock requirements *(f)*, non-feedstock operating costs (OpEx), non-MD fuel revenue *(R)*, and lifecycle GHG emissions, are modeled as a function of cumulative production of MD fuels. In contrast, the maturity of the capital cost characteristic (CapEx) is modeled as a function of the cumulative number of facilities constructed, meaning that there are two parallel learning processes modeled. The n^{th} plant value of each MSP or LCA characteristic is assumed to correspond to initial maturity, M_0, of

50%, which is then used to calculate m_{early}. Initial cumulative experience, E_0, is assumed to be zero. A progress ratio *(PR)* of 90% is assumed based on a review of empirical studies of learning-by-doing for biofuel production, meaning that 90% of the gap between m and $m_{minimum}$ remains after each doubling of cumulative production [156-161].

The minimum cumulative volume of MD fuel production required for learning-by-doing to take place is assumed to be 6.4 million metric tonnes of MD, equivalent to the annual production of approximately 30 medium-sized (5000 bpd) bio-refineries. Similarly, the minimum cumulative number of MD fuel production facilities required for learning-by-doing to begin taking place for CapEx is assumed to be 30. These values of L were selected for the two learning processes to reflect an established commercial drop-in MD fuel production industry, where the next unit of production (in terms of fuel volume or production facility) could be considered *"n^{th}"*. As a point of comparison, approximately 30 ethanol production facilities were in operation in the US by the mid-1980s, at which point reductions in industrial processing costs had been empirically observed [157].

Recall that the assumed initial maturity of these technologies is 50%, corresponding to the n^{th} plant cases for both lifecycle GHG emission and production costs. This means that AJ production technologies are assumed to have the characteristics of n^{th} plant facilities until learning curve effects begin to accumulate, and that the lifecycle GHG emissions and production costs of these technologies leading up to n^{th} plant or commercial-scale production are not fully captured here.

Demand elasticity of price of agricultural commodities

An increase in feedstock demand for policy-mandated biofuel production (such as the scenarios investigated here) may lead to increases in feedstock price and, *ceteris paribus,* an increase in biofuel production costs. For example, Roberts & Schlenker (2013) estimate that a 5% increase in demand for agricultural production (in terms of caloric value) for biofuel feedstock under the US Renewable Fuels Standard 2 (RFS2) resulted in a 20% increase in commodity prices [206]. This feedback mechanism on the production costs of AJ is modeled

as a function of global projected agricultural production [39], and the demand elasticity of price of agricultural commodities [206].

LUC emissions

Increased demand for feedstock may also lead to changes in agricultural land use patterns. A number of studies have demonstrated that the resulting changes in the carbon stock of the soil and biomass on that land may negate the lifecycle benefit of biofuels relative to petroleum derived fuels [15-18,139].

This analysis draws on a review of partial- and general-equilibrium modeling studies to capture the potential impact of LUC emissions attributable to increased demand for lignocellulosic feedstock [207]. The results from Ahlgren & Di Lucia (2014) are used to calculate that between 0.7 and 19.5 t_{CO2} LUC emissions occur per tonne of incremental annual demand for cultivated lignocellulosic feedstock ($t_{inc.\ feed}$). Calculation of this value assumes an ethanol yield of 90 gal/short $tonne_{feed}$, and an allocation ratio of 9% of LUC emissions to non-fuel products, as per GREET1 2015 [44].

Price elasticity of demand for aviation

Winchester et al. (2015) indicates that the mandated use of high-cost AJ may result in a reduction in demand for aviation services, and a corresponding emissions benefit that exceeds the lifecycle emissions benefit of AJ compared to CJ [208]. Therefore, this analysis accounts for the relationship between fuel prices and demand for aviation services as a function of two economic variables from the literature. The elasticity of the price of aviation with respect to fuel price is estimated to range between 0.105 and 0.46 [209,210], and the elasticity of air transport demand with respect to the price of aviation is estimated to range between -0.9 and -0.4 [209,211]. The product of the two provides an estimate of the elasticity of air transport demand with respect to fuel price, ranging from -0.042 to -0.414.

Simplified causal loop diagram of system dynamics model

The feedback structure of the resulting system dynamics model is depicted in Figure 13, consisting of two reinforcing loops and two balancing loops. The two reinforcing loops operate through the private cost of AJ, *"AJ private cost"*, which is decomposed into capital cost, feedstock operating costs and non-feedstock operating costs of aviation biofuel production *("AJ CapEx", "AJ feedstock OpEx"*, and *"AJ non-feedstock OpEx"*, respectively).

As more aviation biofuel production facilities come into production, there is an accumulation of experience with facility construction *("Maturity of AJ facility construction")*. This decreases capital expenses and thereby decreases private costs of AJ *("AJ private cost")*. *Ceteris paribus*, a decrease in the costs of AJ relative to CJ would increase demand for jet fuel and AJ specifically *("Total jet fuel demand", "Target AJ production volume")*, which would increase the *"AJ production volume shortfall"* (defined as the discrepancy between the desired and actual availability of AJ. In response to a larger value of *"AJ production volume shortfall"*, more AJ facilities will be constructed and brought into production, with a delay for construction time. This reinforcing loop is represented as R1 in Figure 13.

More AJ production facilities *("AJ production facilities")* lead to an increase in the annual production volumes of AJ *("Annual AJ production")*. Production of AJ results in an accumulation of experience and an increasing maturity of commercial AJ production technology *("Maturity of AJ production process")*. Greater maturity leads to more efficient production, resulting in decreased feedstock requirements *("Specific feedstock requirements")* and therefore feedstock operating costs *("AJ feedstock OpEx")*, as well as decreased non-feedstock operating costs *("AJ non-feedstock OpEx")*. This leads to lower *"AJ private costs"*, and the remainder of this second reinforcing loop (R2) is completed along the same path as R1, as shown in Figure 13.

A higher quantity of *"AJ production facilities"* leads to an increase in *"Annual feedstock demand"*, which increases *"Feedstock cost"*. This increases *"AJ feedstock OpEx"* and *"AJ private cost"*. An increase in the costs of AJ relative to CJ fuel would decrease demand for AJ *("Target AJ production volume")*. This would decrease *"AJ production volume shortfall"* and decrease the number of new AJ production facilities *("AJ production facilities")*. This first balancing loop is

labeled as B1 in Figure 13. The second balancing loop (B2) reflects that as more *"AJ production facilities"* increase annual production *("Annual AJ production")* and decreases the discrepancy between desired and actual availability of aviation biofuel *("AJ production volume shortfall")*.

In addition to the feedback loops described above, the system dynamics model captures non-linearities associated with GHG emissions from LUC (as a function of incremental changes in *"Annual feedstock demand"*) and changes in *"Total jet fuel demand"* (as a function of *"AJ private cost"*, *"CJ private cost"*, and *"Elasticity of aviation demand WRT fuel price"*).

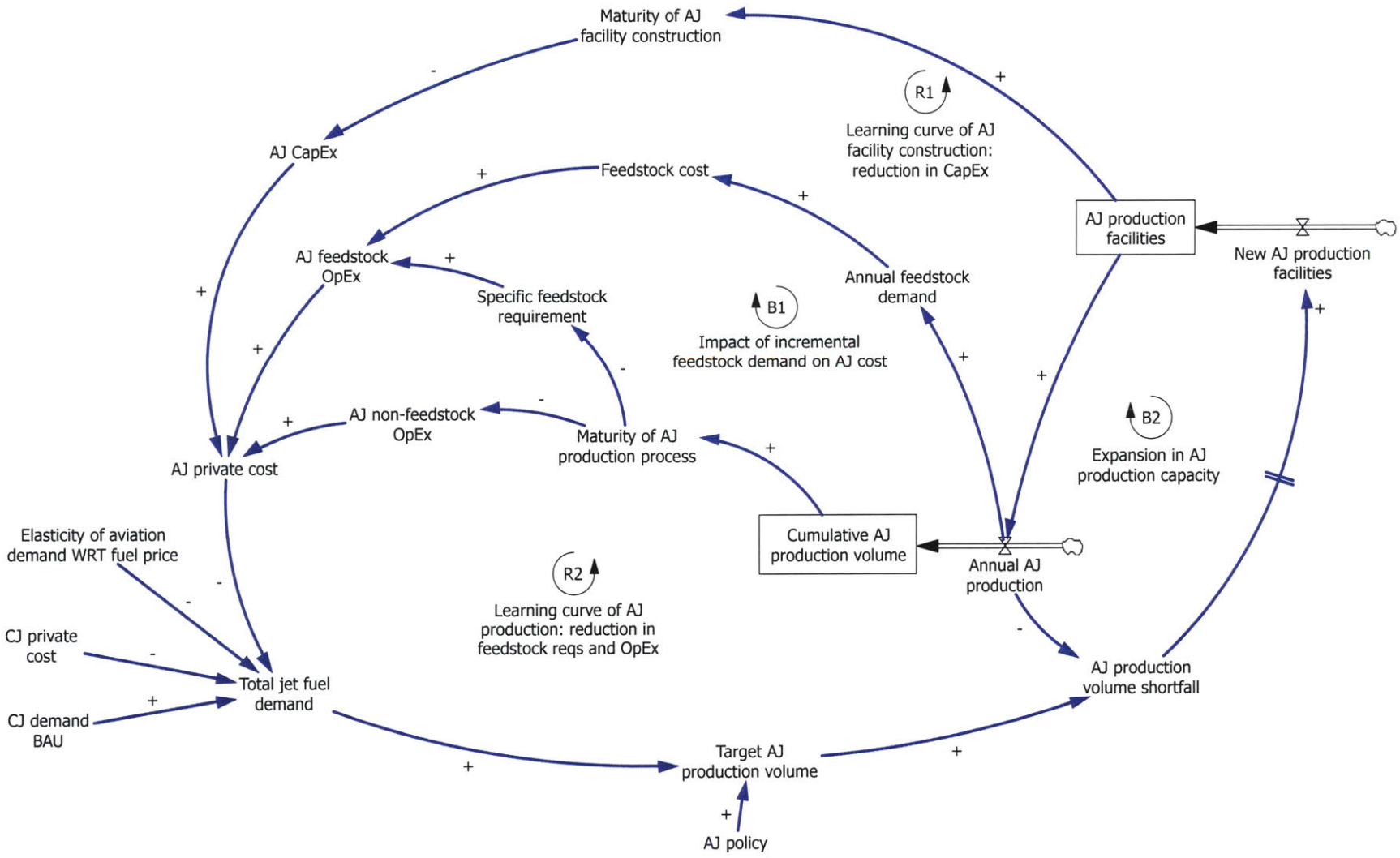

Figure 13: Simplified causal loop diagram of the system dynamics model.

Monetized climate impacts

The probability distribution functions (PDFs) of societal NPV of climate damages from CO_2, CH_4 and N_2O WTP and combustion CO_2 emissions are estimated as a function of societal discount rate and emissions year from APMT, assuming RCP4.5 and SSP1 in all cases. The PDFs of societal NPV of climate damages from non-CO_2 combustion impacts of CJ and AJ are calculated from APMT as well, also as a function of societal discount rate and emissions year. These distributions are used to monetize the climate damages from aviation for use in the CBA.

Commodity prices and conventional jet fuel demand

The annual prices of CJ and AJ feedstock, and global demand for conventional jet fuel, are each modeled here as a stochastic differential process in time, S_t, known as Geometric Brownian Motion, of the general form shown in Equation 6 [212].

Equation 6: Geometric Brownian Motion.

$$dS_t = \mu \cdot S_t dt + \sigma \cdot S_t dW_t$$

where

μ	= percentage drift
σ	= percentage volatility
W_t	= standard normal random variable

The starting point for commodity prices, annual percentage volatility, and annual percentage drift parameters are estimated for business-as-usual (BAU) CJ demand [76,213] and CJ market price [142,143] from historical data. The starting point commodity prices for delivered lignocellulosic and MSW feedstocks are derived from the literature [214,149], and historical market prices for first generation biofuel feedstocks are used to estimate their annual percentage price drift and volatility [215-220].

Simulation setup and parameter definition

The system dynamics model defined by the relationships described above is built using Vensim DSSP software, v6.4b. Commercial aviation fuel burn is simulated from 2015 to 2050, and the model returns the difference in annual climate damages and fuel production costs between the policy case and the BAU, no policy case.

For each feedstock-to-fuel pathway of interest, this analysis considers a policy where AJ replacement of CJ begins at 0% in 2020, and ramps up to 10% replacement by 2035. AJ production continues to grow from 2035 to 2050 to maintain 10% of total jet fuel demand. 2020 was selected as the policy start year because AJ currently makes up a negligibly small fraction of total commercial aviation fuel burn, and commercial scale AJ production facilities require a design, permitting and construction lead-time of approximately three years [65]. Therefore very little replacement of CJ with AJ will occur before this time. In addition, 2020 coincides with the starting point of ICAO's aspirational goal of carbon-neutral growth, facilitated by a global market-based measure under which alternative jet fuels will be eligible to count towards airlines' emissions reduction obligations [81].

10% replacement by 2035 would require 55 million tonnes of AJ production annually, or approximately 450 medium-sized (5000 bpd) AJ production facilities worldwide if 50% of total fuel production is drop-in jet fuel. This number drops to approximately 270 facilities if it is assumed that 85% of total fuel products are either drop-in jet or diesel to be blended with CJ up to 10% [221]. In contrast, annual production of first-generation biofuels (ethanol and biodiesel) is approximately 100 million tonnes [74]. This means that, without taking production capacity away from its current uses, 10% replacement of CJ would require approximately doubling global biofuel production capacity by 2035. Therefore, this level of replacement was selected because it is large enough to have an appreciable impact on the climate damages of aviation without exceeding the order of magnitude of historical precedent.

A paired Monte Carlo approach, using 10000 runs, quantifies uncertainty in the resulting annual climate damages and fuel production cost estimates. The definition of key parameters, and their probability distributions, is contained in Table 20.

Table 20: Parameter and probability distribution function definition for system dynamics simulation.

Parameter		Value	Units	Distribution	Source	Note
CJ demand	Initial, 2015	274	[10^6 t_{jet}/yr]	Uniform (min, max) (270,279)	ICAO (2013)	
	Volatility	2.55%	[%/yr]	Point value	US EIA (2016a)	Std. dev. of annual percentage change in jet fuel demand, 1991-2012
	Drift	3.50%	[%/yr]	Point value	ICAO (2013)	
CJ price	Initial, 2015	574.94	[USD_{2015}/t_{jet}]	Point value	US EIA (2016b)	
	Volatility	27.10%	[%/yr]	Point value	US EIA (2016b)	Std. dev. of annual percentage change in jet fuel demand, 1991-2012
	Drift	3.14%	[%/yr]	Triangular (min, max) (0.83%, 4.65%)	US EIA (2015)	
Feedstock price	Initial, 2020 woody crop	80.00	[USD_{2015}/t_{feed}]	Uniform (min, max) (60, 100)	US DOE (2016)	Delivered feedstock costs
	Initial, 2020 forestry residue					
	Initial, 2020 MSW	0.00	[USD_{2015}/t_{feed}]	Point value	Suresh (2016)	
	Volatility	21.90%	[%/yr]	Point value	Index Mundi (2016a-f)	Std. dev. of annual percentage change in first generation biofuel feedstock prices (palm, rapeseed, soybean, corn grain, sorghum, sugarcane), 1991-2015
	Drift	1.73%	[%/yr]	Uniform (min, max) (1.04%, 2.53%)		Annual percentage change in first generation biofuel feedstock prices (palm, rapeseed, soybean, corn grain, sorghum, sugarcane), 1991-2015
Specific LUC emissions factor		7	[t_{CO2}/t_{feed}]	Uniform (min, max) (0.7, 19.5)	Ahlgren & Di Lucia (2014)	
Demand elasticity of feedstock price		4	dmnl.	Uniform (min, max) (2, 5)	Roberts & Schlenker (2013)	
Fuel price elasticity of aviation demand		-0.62	dmnl.	Triangular (min, max) (-0.042,-0.414)	Wadud (2015), IATA (2008), Koopmans & Lieshout (2016)	
Progress ratio	Fuel production	90%	[%]	Triangular (80%, 95%)	Chen & Khanna (2012), Hettinga et al. (2009), van den Wall Bake (2009), Goldemberg et al. (2004), Berghout (2008), Nogueira et al. (2016)	
	Facility construction	90%				

The result of the model runs is the 2020 NPV of the difference between the policy and no policy cases, in terms of climate damages and fuel production costs to society, discounted according to the selected societal discount rate.

Results and discussion

The results for the three AJ production pathways are shown in Figure 14. These are broken out in a stepwise manner to illustrate the contribution of different impacts on the change in NPV of societal climate damages and fuel production costs of aviation, over the modeled assessment period of 2015-2050. First, starting from the left of each panel in Figure 14, there is a reduction in the climate damages of aviation from WTP GHG and combustion CO_2

emissions (first column, labeled as lifecycle CJ emissions), and non-CO_2 combustion emissions (second column) from petroleum-derived conventional jet (CJ) fuel. This is due to the replacement of CJ with alternative jet (AJ) fuel. This reduction in climate damages is partially offset by the WTP GHG, combustion CO_2, and non-CO_2e emissions from AJ (third and fourth columns). For the woody crop FT pathway, LUC CO_2 emissions attributable to AJ further offset the reduction in climate damages from replacing CJ with AJ (fifth column). The first blue column shows the mean value of Monte Carlo results for the net change in climate damages. The second and third columns from the right show the change in the societal fuel production costs, broken out by the reduction in the costs for CJ production that is offset, and increase in costs for AJ production. The rightmost column shows the mean change in the total NPV of societal climate damages and fuel production costs, as well as the 95% confidence interval (CI).

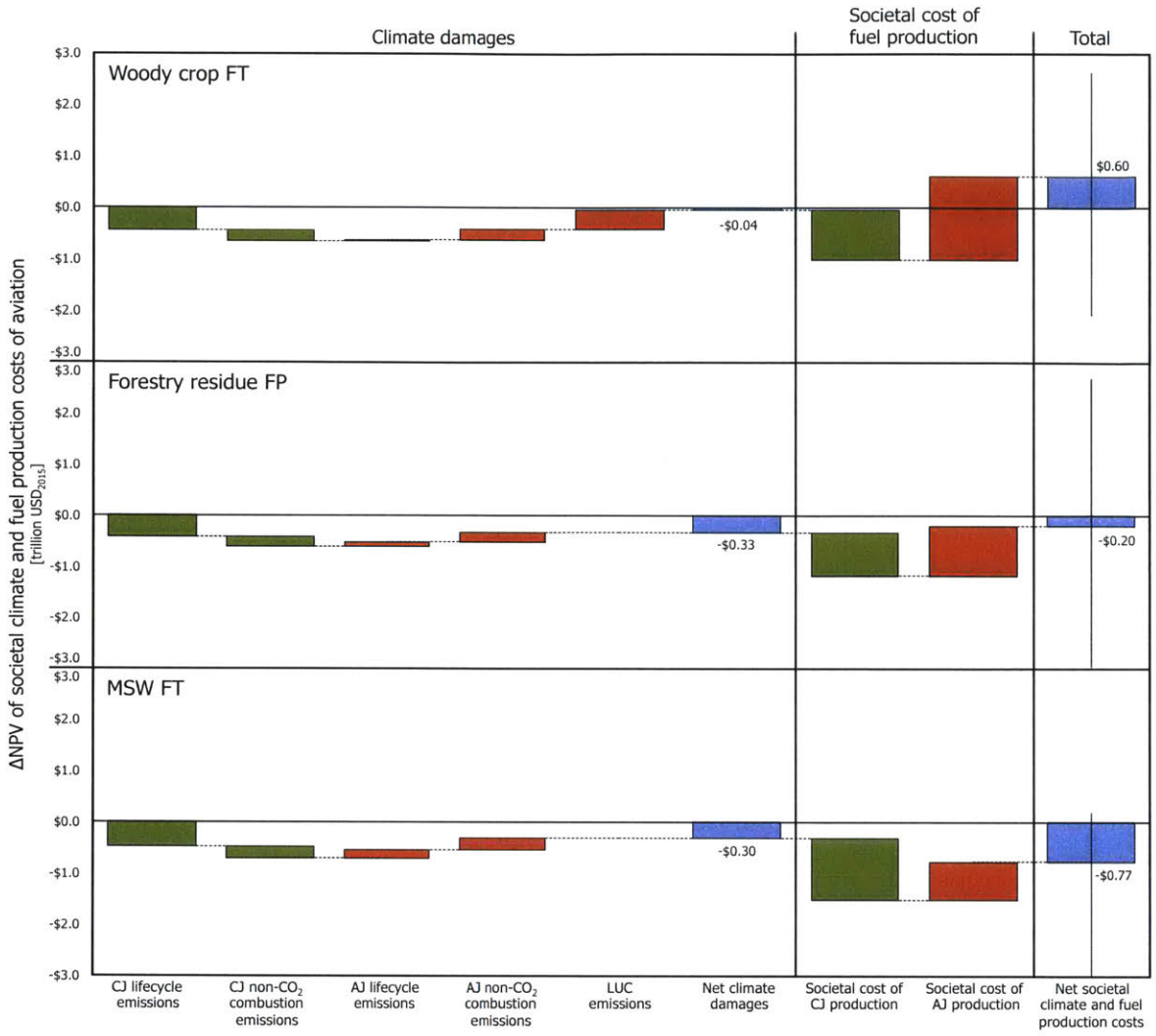

Figure 14: Change in NPV of societal climate and fuel production costs of aviation, 2015-2050. The 95% CI is shown only for net results. Forestry residue FP and MSW FT 2.5th percentiles are at -3.2 and -5.6 trillion USD_{2015}, respectively, but are not shown for practical representation of the results.

A comparison of the results shown in Figure 14 illustrates the unique characteristics of the three AJ production pathways examined. For the woody crop FT pathway, emissions from LUC offset 90% of the lifecycle and non-CO_2 combustion emissions benefit of replacing CJ with AJ. In addition, the NPV of societal fuel production costs of woody crop FT AJ is calculated to be 66% greater than the CJ that it is replacing. The net result is a mean increase in NPV of 0.60 trillion USD_{2015}, which is equivalent to a 4.2% increase in the NPV of societal climate damages and fuel production costs under the no policy, no AJ adoption case.

In contrast, because the FP pathway is assumed to use forestry residue feedstocks that do not carry the risk of changes in land use patterns attributable to AJ production, the reduction in climate damages from replacing CJ with AJ is not undermined by LUC emissions. In addition, the societal resource costs of forestry residue FP AJ is calculated to be only 15% greater than the CJ that it is replacing. This is in part because, although the FT and FP pathways have similar characteristics in terms of the capital and operating expenses of fuel production, the FP process is estimated to have potential for greater total fuel yield than lignocellulosic FT (60.9% compared to 52.0% feedstock-to-fuel LHV efficiency, respectively, as shown in Table 18), and therefore requires less feedstock per unit of AJ production. The combination of these two factors results in a net decrease of 0.20 trillion USD_{2015} of the mean NPV of societal climate damages and fuel production costs of aviation, equivalent to a 1.4% decrease compared to the no AJ policy case.

Similar to the forestry residue FP pathway, MSW FT makes use of a feedstock for which there is assumed to be no risk of emissions from LUC.[1] In addition, because the baseline assumption is that MSW is a no-cost waste feedstock, the societal cost of CJ production eventually exceeds that of MSW FT. As a result, the societal NPV of the fuel production cost of MSW FT is 38% less than the CJ that it is replacing. In net, the MSW FT pathway results in a decrease of 0.77 trillion USD_{2015} of the mean NPV of societal climate damages and fuel production costs, equivalent to a 5.4% decrease from the no AJ policy case.

Sensitivity analysis

A sensitivity analysis is carried out in order to quantify the impact of key parameters on the results, as shown in Figure 15. The findings are reported as the probability of a net reduction in the NPV of societal climate damages and fuel production costs, compared to the no AJ

[1] The LCA study used to characterize emissions for the MSW FT pathway does account for changes in GHG emissions due to a change in the waste management strategy of an MSW feedstock, such as landfill gas emissions [149]. However, in this thesis LUC emissions refers to CO_2 emissions resulting from a change in the soil and biomass carbon stock of land used for feedstock cultivation and recovery, and therefore does not apply to the changes in landfill gas emissions that are otherwise captured in the LCA of the MSW FT pathway.

policy case, calculated on the basis of 10000 Monte Carlo runs. For all three of the pathways the societal discount rate, annual average growth rate of CJ price, fuel price elasticity of aviation demand, and initial feedstock price, were varied in isolation. In addition, the demand elasticity of feedstock price, annual average growth rate of feedstock price, and LUC emissions factor, were varied in isolation for the woody crop FT and forestry residue FP pathways. The grey dashed line indicates a 50% probability that there is a net reduction in the NPV of societal climate damages and fuel production costs for a given scenario.

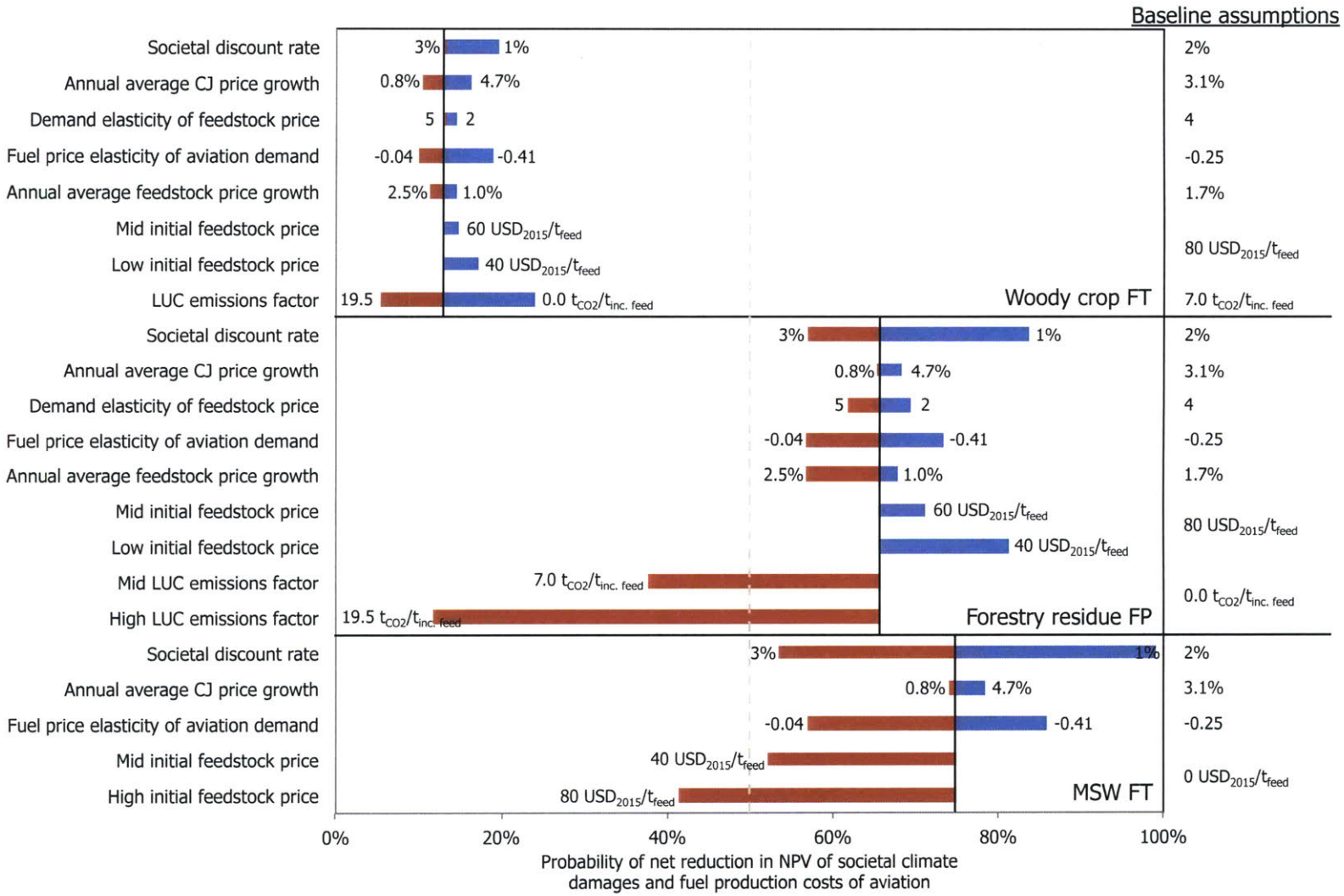

Figure 15: Sensitivity of change in NPV of societal climate damages and fuel production costs of aviation to individual parameters, 2015-2050. The results shown correspond to the proportion of total Monte Carlo runs that result in a decrease in the NPV of aviation.

Figure 15 indicates that the results across the three pathways are particularly sensitive to assumptions regarding the societal discount rate, fuel price elasticity of aviation demand, feedstock price (in terms of both initial price and annual average growth rate), and LUC emissions factor. In general, a lower societal discount rate results in a higher probability of a reduction in NPV, and vice versa. This is because, with a decreasing discount rate, the present value of avoided climate damages increases more quickly than the present value of the societal costs of fuel production.

In addition, the probability of a reduction in NPV increases with a higher assumed fuel price elasticity of aviation demand. This is because the societal cost of fuel production is positively correlated with the private costs of AJ and CJ. As the fuel price elasticity of demand increases, there is less jet fuel demand in Monte Carlo runs where fuel price (the weighted average of the private costs of AJ and CJ) is high and more jet fuel demand in runs where fuel price is low, which results in a decrease in the mean societal cost of fuel production across all 10000 iterations.

The probability of a reduction in NPV also increases if the societal cost of AJ production decreases relative to CJ (due to lower annual average feedstock price growth, initial feedstock price, or demand elasticity of feedstock price; or higher annual average CJ price growth), and vice versa. Finally, the probability of a reduction in NPV also has an inverse relationship with the LUC emissions factor associated with incremental feedstock demand.

Tradespace analysis

In order to further illustrate the interdependence and influence of the key parameters identified in Figure 15 on the probability of a reduction in NPV, a tradespace analysis is carried out. The parameters selected for this analysis are the societal discount rate, initial feedstock price, and the LUC emissions factor. The societal discount rate is of particular interest, and is included in both tradespace analyses of the other variables, because it represents a subjective analytical choice rather than a measurable parameter. The initial feedstock price and LUC emission factor parameters are included because they represent

characteristics that differentiate the findings between the three pathways considered: Figure 14 shows a mean reduction in NPV for the forestry residue FP and MSW FT pathways in part because it is assumed there is no risk of LUC emissions; and MSW FT has the greatest mean reduction in NPV in part because of the assumption of a no-cost feedstock.

The results in Figure 16 show the tradespace of societal discount rate, initial feedstock cost and the probability of a reduction in NPV. The dashed line indicates the contour of a 50% probability, and the assumptions corresponding to the baseline case shown in Figure 1 are highlighted on the figure. In all three cases a net reduction in NPV is more likely than not to the left of the contour line.

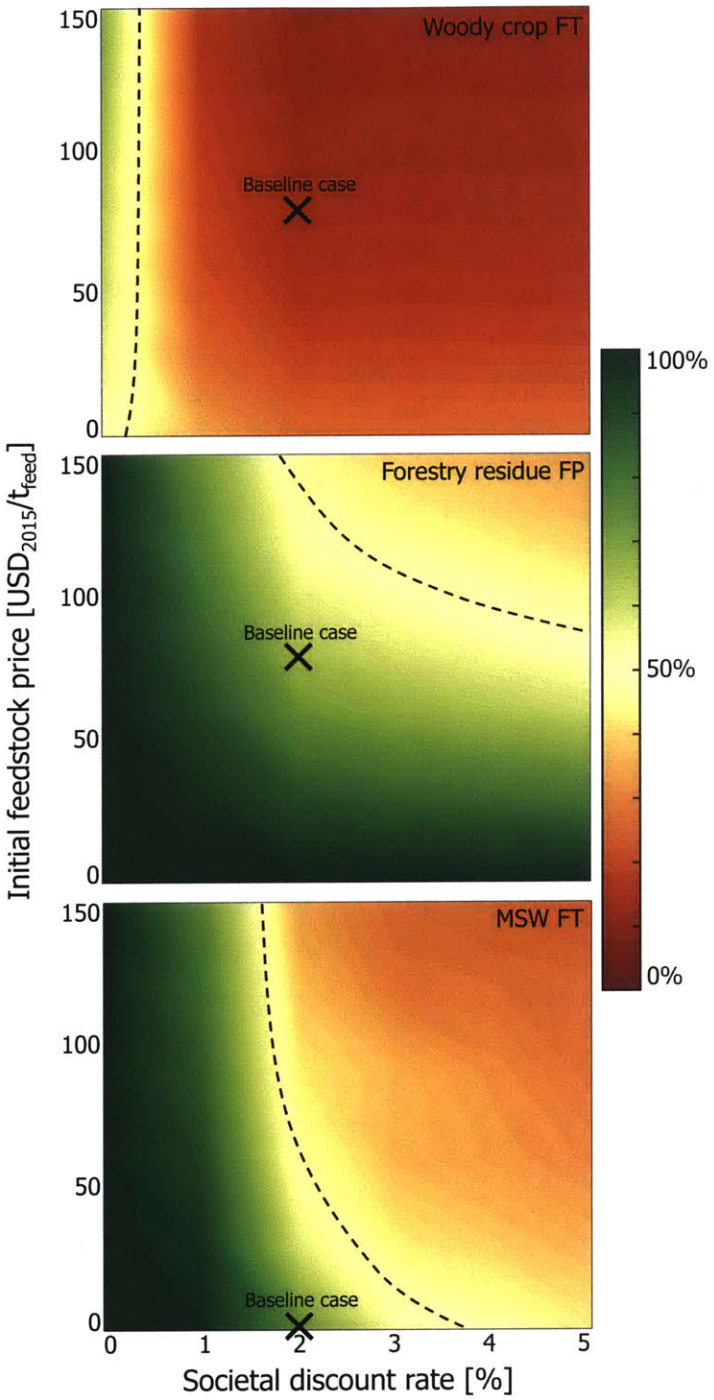

Figure 16: Probability of a reduction in the NPV of societal climate and fuel production cost of aviation, 2015-2050. Results are generated using the baseline assumptions outlined above, and varying the assumed societal discount rate and initial feedstock cost. The dashed contour indicates a 50% probability of a reduction in NPV, and the × indicates the baseline assumptions from the results shown in Figure 14.

In the woody crop FT case, a probability greater than 50% only occurs when the societal discount rate is less than 1%. The contour moves to the right as the initial feedstock cost increases because, at very low discount rates, the increased societal value of mitigated GHG emissions, combined with the reduction in total jet fuel demand due to the high cost of AJ fuel (and corresponding reduction in climate damages, fuel production costs, and proportional share of LUC emissions) outweighs the increased societal unit cost of AJ production.

For forestry residue FP and MSW FT, there is a large parameter space to the bottom left where the probability of a reduction in NPV is greater than 50%. In both cases, the sensitivity of the probability of a reduction in NPV to changes in the initial feedstock price increases with the societal discount rate. At discount rates greater than approximately 3.7%, the probability of the MSW FT pathway resulting in a net reduction in NPV drops below 50% regardless of the initial feedstock price. This is because, at higher discount rates, the additional societal cost of producing AJ in the first few years outweighs the present value of the avoided climate damages. At equivalent initial feedstock prices, for example 50 USD_{2015}/t_{feed}, the probability of a net reduction in NPV is greater for forestry residue FP than the MSW FT pathway. This is because the FP pathway is characterized by higher total fuel yield per unit feedstock, and higher non-MD fuel revenue per unit of fuel production, which partially offsets the societal production cost premium of AJ fuel produced using FP technology.

The results in Figure 17 show the tradespace of the societal discount rate, LUC emissions factor and the probability of a reduction in NPV. Results are shown for the forestry residue FP pathway because it is possible that this pathway could make use of a short rotation woody crop or some other lignocellulosic feedstock that could result in LUC emissions. Results are not shown for the MSW FT pathway because the use of an MSW feedstock is unlikely to result in a change in soil and biomass carbon stocks.

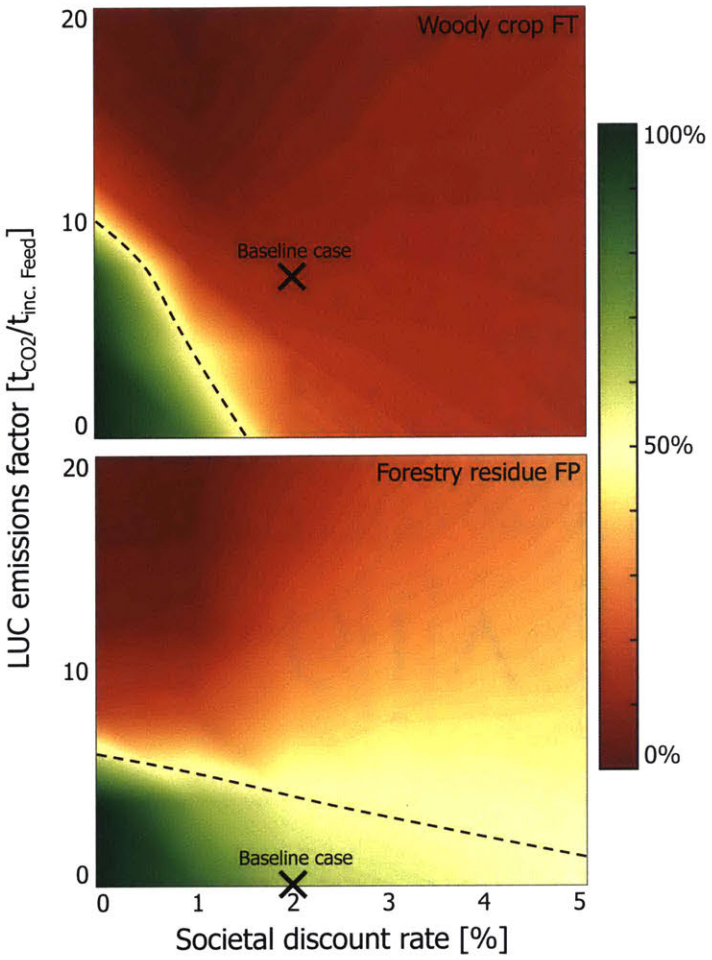

Figure 17: Probability of reduction in the NPV of societal climate and fuel production costs of aviation, 2015-2050. Results are generated using the baseline assumptions outlined above, and varying the assumed societal discount rate and assumed LUC emissions factor. The dashed contour indicates a 50% probability of a reduction in NPV, and the × indicates the baseline assumptions from the results shown in Figure 14.

As indicated in Figure 17, the probability of a net reduction in NPV is greater than 50% only in the bottom left corner of the parameter space for both fuel pathways. If the LUC emissions factor is greater than 10 or 6.2 $t_{CO2}/t_{inc.\ feed}$ in the woody crop FT and forestry residue FP cases, respectively, there is no discount rate at which the probability of a reduction in NPV is greater than 50%. For the woody crop FT pathway, the probability of a reduction in NPV does not exceed 50% independent of the LUC emissions factor at a societal discount rate above 1.5%.

Limitations and areas for future work

The analysis presented in this Chapter could potentially be expanded upon in a number ways, as discussed below.

Additional environmental and economic costs and benefits to society

The scope of the analysis presented here is limited to lifecycle GHG emissions, LUC emissions and the production costs of AJ relative to CJ because these are the characteristics that have both motivated and inhibited interest in the use of AJ production technologies for aviation. However, a more comprehensive CBA of AJ adoption would include additional environmental, economic, and societal impacts.

For example, this analysis does not consider the air quality impacts of low-sulfur and – aromatic content AJ [223,224], the lifecycle water footprint of fuel production [150], or the climate impacts of surface albedo change due to LUC [225]. In addition, the current work does not account for the impacts of economic diversification and development from the establishment of a new AJ production industry, particularly in rural and feedstock-growing regions [226,227], or the country-specific energy security benefits of reducing reliance on fossil fuels [228]. Future work in this area could quantify the societal costs and benefits from these and other environmental and economic impacts of AJ, as they are identified, in order to compare them to results in this thesis.

Societal opportunity cost of scarce resources and system boundary expansion

In order to capture the societal cost of scarce resource inputs required for AJ production, such as biomass feedstock, this analysis assumes that the market price of a commodity is representative of its societal opportunity cost, or shadow price [170]. In effect, this assumption implies that the market price of a commodity is a valuation of the best, foregone

alternative use of that scarce resource outside of the system boundary of interest, which in this case is the global commercial aviation sector.

If the system boundary of interest is expanded beyond aviation, however, the societal opportunity cost should also include the foregone societal benefit of using scarce resources to mitigate environmental externalities. For example, the market price of biomass does not reflect the potential to mitigate climate damages from electricity generation by co-firing of biomass with coal, but if the system boundary of interest includes sectors beyond aviation this foregone environmental benefit should be added to the market price of biomass to better reflect its societal opportunity cost. Assuming a thermal boiler efficiency of 38%, and specific GHG emissions of 248 gCO_2/MJ and 0 gCO_2/MJ from coal and biomass-fired electricity generation, respectively, 1 $t_{\text{forestry residue}}$ could offset 1.89 t_{CO2} [44]. At a societal discount rate of 2% and an emissions year of 2020 in APMT, the avoided monetized climate damages have a mean NPV of 131.38 $USD_{2015}/t_{\text{forestry residue}}$. If this foregone environmental benefit were added to the initial feedstock costs considered for the results shown in Figure 16, there would be a significant decrease in the probability of a net reduction in NPV.

Similarly, if the system boundary is expanded beyond the aviation sector, the societal opportunity cost of capital resources should also include the foregone societal benefit of their use to mitigate environmental externalities in other sectors. One measure of this environmental opportunity cost is the price of CO_2 emissions offsets. Assuming an offset price of 10 USD_{2015}/t_{CO2} [229], a societal discount rate of 2% and an emissions year of 2020 in APMT, each dollar used to produce AJ has an environmental opportunity cost with mean NPV of 6.94 USD_{2015}. In effect, if the societal opportunity cost of using scarce capital resources to produce AJ includes the foregone climate benefit of purchasing CO_2 offsets, the total societal opportunity cost of capital is approximately 8 times the currency value.

It should be noted that these examples are selected for illustrative purposes only, and that the societal opportunity cost of scarce resource inputs is contingent upon both the system boundary of interest, and the alternative uses of those resources that are actually available. For instance, the foregone environmental benefits calculated above are dependent on the possibility of using that biomass to offset coal-fired electricity generation, and the availability

and effectiveness of CO_2 offsets. In any case, these system boundary issues, and accurate evaluation of societal shadow prices for scarce resources, is an area for future research that is applicable to environmental CBA beyond the context of aviation, or large-scale AJ adoption.

Summary

This Chapter presents a dynamic CBA that quantifies the societal costs and benefits of aviation, in terms of climate damages and fuel production costs, under a policy of large-scale AJ adoption. This is achieved by parameterizing the performance of a diversity of AJ feedstock-to-fuel production pathways on the basis of their lifecycle GHG emissions, production costs and feedstock requirements, quantifying the potential for time- and path-dependent improvement in these technologies relative to CJ, and accounting for the feedbacks and non-linearities of large-scale adoption using a system dynamics approach. The results quantify the degree to which the different attributes of AJ production technologies drive the balance of the climate change benefits and fuel production costs of large-scale adoption, from a societal perspective. In particular, the findings highlight the importance of two specific characteristics of AJ production technologies.

First, this analysis finds that the probability of a reduction in NPV of the societal costs of aviation is sensitive to the societal opportunity cost of AJ feedstock. This is shown in Figure 16, where market price is used as a proxy for societal opportunity cost. If the societal opportunity cost of feedstock is lower because the societal benefits of using it for some other purpose are lower, *ceteris paribus*, the probability of net reduction in NPV will be greater. This points toward the potential importance of residue and waste feedstocks for minimizing the societal production costs of AJ. Unlike agricultural commodities that are already traded and provide a clear benefit to society in the form of food and animal feed (such as cereal, sugar or vegetable oil crops), uncollected residues and wastes do not currently provide a traded societal benefit. This implies that the societal opportunity cost of using these feedstocks for AJ production is potentially lower than agricultural commodities. In some cases, there may even be a negative societal opportunity cost associated with the use of residue and waste feedstocks. For example, the use of MSW for AJ production could

reduce the costs incurred for landfilling that would otherwise have to take place to dispose of the waste [222]. Therefore, in order to maximize reductions in the societal climate and fuel production costs of aviation, large-scale AJ adoption should make use of feedstocks with lower societal opportunity costs, including wastes and residues.

Second, this Chapter illustrates that LUC emissions can negate the lifecycle emissions benefit of AJ relative to CJ. This is exacerbated by the fact that LUC emissions are more likely to occur at the beginning of a policy of AJ adoption, as fuel production is ramping up and incremental increases in feedstock demand are the largest. As a result, the climate damages from LUC emissions are subject to less discounting than the potential reductions in climate damages from lifecycle emissions in later years. This is the case even for the FP pathway (assuming the use of a land-based lignocellulosic crop feedstock), which is the most promising pathway considered in this analysis based on the results shown in Figure 12: a LUC emissions factor of 6.2 $t_{CO2}/t_{inc.\ feed}$ or greater pushes the probability of a net reduction in NPV below 50% at any societal discount rate. This sensitivity to LUC emissions is only further heightened for the other AJ pathways characterized in this Chapter, due to smaller lifecycle GHG emissions benefits, or larger societal production cost premiums compared to CJ. Furthermore, LUC emissions factors may be even greater for AJ pathways that rely on non-lignocellulosic feedstocks, such as sugarcane, wheat, or vegetable oil crops [207]. These findings suggests that, if even a modest risk of LUC emissions is present for a particular feedstock-to-fuel pathway, a reduction in net NPV is only likely if the AJ pathway has characteristics similar to, or better than, the forestry residue FP pathway assessed here, and the societal discount rate is sufficiently low. This is a very limited target design space for AJ technologies. Therefore, large-scale AJ adoption should make use of feedstocks that do not carry a risk of either direct or market-mediated indirect LUC emissions in order to maximize the probability of reductions in the societal climate and fuel production costs of aviation. Residue and waste feedstocks also represent an opportunity on this front, as their production does not require arable land area to the same degree as cultivated energy crops.

In addition to the societal opportunity costs and potential LUC emissions of AJ feedstocks, the importance of which are demonstrated by the analysis here, further environmental and economic aspects of large-scale AJ production need to be considered for a holistic

assessment of these technologies. Many of these potential impacts are a function of the scale of production that would be required to significantly reduce the climate impact of commercial aviation.

For example, ramping up global AJ production to offset 10% of CJ demand by 2035 (assuming green diesel can be blended with CJ up to 10%), with a corresponding reduction of 5-9% in the lifecycle CO_2 emissions of aviation, would require the commissioning of approximately 18 new AJ production facilities each and every year from 2020 to 2035. Assuming that the feedstock used to produce this fuel was a lignocellulosic energy crop with yields of 10 t/ha, it would require ~40 Mha of arable land area for cultivation, or ~3% of current global arable land area [28]. Reallocating the use of existing croplands, expanding cropland area into uncultivated areas, intensifying production on existing croplands, or even the harvesting of agricultural residues to satisfy this additional biomass demand, could have significant implications for matters of societal importance, such as biodiversity [230], soil quality and nutrient retention [34,35,231], water quality [151] and food prices [232,233]. These impacts are not considered in this CBA, although they represent additional limitations on the design space of an AJ feedstock-to-fuel pathway for which the societal benefits outweigh the costs.

Finally, the results shown in Figure 15, Figure 16 and Figure 17 indicate that the societal climate and fuel production costs of aviation are dependent on the societal discount rate. At low discount rates, the economic damages from climate change experienced by future generations are more highly valued. Therefore, even modest reductions in the GHG emissions have a societal value that outweighs the additional costs of fuel AJ production. On the other hand, at high discount rates the economic damages from climate change have a lower societal value. Therefore, the reduction in GHG emissions must be larger in magnitude, or the cost premium of AJ fuels must be smaller, for a net reduction in the societal NPV of climate and fuel production costs of aviation. In both cases the findings of this Chapter illustrate that the selection of discount rate, which reflects the value that society places on the economic welfare of future generations, is a key driver of the balance of societal climate and fuel production costs of a policy of large-scale AJ adoption.

5. Conclusions

The purpose of this thesis is to enhance the field of environmental and economic technology assessment for policy, with a focus on bioenergy as an alternative to fossil fuels and the use of alternative fuels for commercial aviation. This final chapter summarizes the contributions and findings of the work presented above, and briefly discusses areas for future research in this field.

Contributions and findings

The first part of this thesis quantifies the global potential for bioenergy resources to reduce anthropogenic greenhouse gas (GHG) emissions from fossil fuels. A maximum of 4.9-38.7 Gt_{CO2e}, or 9-68%, of annual global lifecycle GHG emissions from fossil fuel heat, electricity, and transportation fuels could be mitigated by the use of bioenergy by 2050. The range of results reported in this analysis reflects nine different scenarios, which define the potential availability of bioenergy resources and projected demand for fossil fuels that could be offset by bioenergy in 2050. The findings demonstrate that greater availability of bioenergy resources (due to greater availability of arable land and higher projected agricultural yields on those lands), and greater demand for fossil fuels, both lead to larger calculated potential for bioenergy to contribute to GHG emissions mitigation.

In addition to the constraints on biomass availability that have been well established in the literature, including arable land area and agricultural yields, this work demonstrates that the maximum mitigation potential is further limited by the lifecycle GHG and LUC emissions of bioenergy, and the lifecycle GHG emissions of the fossil fuels it could be used to offset. Maximizing reductions in lifecycle GHG emissions requires limiting deployment of global primary bioenergy resources to 29-91% of what is potentially available for use. In addition, going beyond the calculated point of bioenergy deployment that maximizes GHG emissions reductions could result in offsetting the next unit of fossil fuel energy with a unit of

bioenergy that has higher lifecycle GHG and LUC emissions, and therefore contributes to a net increase in anthropogenic GHG emissions.

Significantly, the results of this work show that offsetting demand for fossil fuel-fired heat and electricity is 1.6-3.9 times more effective for emissions mitigation than offsetting demand for fossil fuel-derived liquid fuels when considering the use of global bioenergy resources to maximize GHG emissions reductions. Despite this, liquid fuels make up between 18-49% of total final bioenergy in the nine scenarios considered. Therefore, maximizing lifecycle GHG emissions reductions from the use of bioenergy requires a mix of end-uses, including biomass-derived transportation fuels.

This finding is especially relevant for the aviation industry. By mid-century, aviation's contribution to annual anthropogenic CO_2 emissions is expected to grow to approximately 4% [77]. The long development and certification timelines for new aircraft and engine technologies, in addition to slow fleet turnover, mean that commercial aviation will remain dependent on energy-dense liquid fuels in the coming decades [55-57,80]. Drop-in AJ fuels derived from biomass, with chemical properties similar to petroleum-derived convention jet (CJ) fuels, are a promising near-term technology option to reduce the climate impact of aviation because of the biogenic nature of their combustion CO_2 emissions, and because they are compatible with the existing fleet of aircraft.

The second contribution of this thesis is to characterize a class of technologies used for AJ production, referred to as fermentation and advanced fermentation (AF), in terms of their lifecycle GHG emissions and costs of production. This is carried out using the methods of lifecycle and techno-economic analysis (LCA and TEA), and is the first assessment of this emerging class of technologies. Because AF fuel production does not yet exist at the commercial or industrial-scale, empirical data are unavailable for these processes. Therefore, this analysis draws upon data from chemical process models developed for ethanol and biodiesel production, petroleum refinery design literature, and primary science on engineered microorganisms for advanced biofuel production, in order to quantify the mass and energy balances associated with AF production. The results show that middle distillate (MD) fuels produced via AF, including jet and diesel, could reduce lifecycle GHG emissions by 30-86%,

but that the cost of producing AF fuels is approximately 2-5 times the price of conventional MD.

In addition to uncertainty about the how these technologies will develop and perform at commercial-scale, much of the variability in findings is driven by technology choices. For example, AF MD fuels derived from sugarcane, via an ethanol platform molecule, have lower lifecycle GHG emissions and minimum selling price (MSP) than the other feedstock-to-fuel pathways investigated. Therefore, the impact of key parameters on the environmental and economic performance of AF MD fuels is quantified in this thesis. The results identify metabolic efficiency (in part defined by the selection of platform molecule), the efficiency of platform molecule separation and upgrading processes, and the efficiency of process electricity and heat co-generation as key drivers of AF MD lifecycle GHG emissions and MSP. Higher overall feedstock-to-fuel conversion efficiency, as a function of each of the process steps described above, is shown to result in reductions in both lifecycle GHG emissions and MSP. Furthermore, the MSP of the sugarcane and corn grain AF MD pathways are shown to be particularly sensitive to feedstock cost, whereas the MSP of switchgrass AF MD is more sensitive to capital cost. The results of this analysis can be used to inform technology decisions and areas for future research that could improve the performance of AF MD fuels relative to conventional MD in the future.

The third contribution of this thesis is to quantify the societal costs and benefits of a policy of large-scale AJ adoption, in terms of the climate damages and fuel production costs attributable to aviation. A diversity of feedstock-to-fuel AJ production pathways are characterized in terms of their lifecycle GHG emissions and costs, both to the fuel purchaser, and to society in terms of scarce land, labor and capital resources required for production. The results show that, across all of the technologies considered, there is a tradeoff between the potential climate benefit and incremental production cost of AJ relative to CJ. In addition, this analysis quantifies the degree to which this climate-cost trade-off may evolve over time due to learning-by-doing of nascent AJ production technologies, increases in the costs of CJ fuels, and the increasing societal value of GHG emissions mitigation. In order to account for the time- and path-dependent characteristics of AJ technologies, as well as potential environmental and economic non-linearities and feedbacks associated with large-

scale deployment, a cost-benefit assessment (CBA) is carried out using a system dynamics approach.

This work demonstrates that the balance of societal costs and benefits of a policy of large-scale AJ adoption is sensitive to the characteristics of the feedstock-to-fuel pathway under consideration. In particular, the analysis highlights the potential importance of low societal opportunity cost and low LUC risk feedstocks for maximizing the probability of a net reduction in the NPV of societal climate and fuel production costs of aviation. For example, even when considering the Pareto frontier of AJ pathways that minimize lifecycle GHG emissions and production cost premium compared to CJ, high societal opportunity cost feedstocks (initial feedstock cost $\geq$ 140 $USD_{2015}/t_{feedstock}$), or high LUC emissions (LUC emissions $\geq$ 4.2 $t_{CO2}/t_{inc.\ feedstock}$), could reduce the probability of a reduction in the societal climate and fuel production costs of aviation to below 50%. Therefore, the findings emphasize the potential importance of AJ derived from low LUC risk and low societal opportunity cost feedstocks, specifically wastes and residues, as a means to minimize the costs of aviation to society.

In summary, this thesis finds that lifecycle GHG and LUC emissions are a binding constraint on the potential for bioenergy to contribute to global GHG emissions reductions. Furthermore, maximizing the anthropogenic climate change mitigation potential of bioenergy requires using these resources to offset demand for a mix of fossil fuel end-uses, including liquid transportation fuels. Next, this work demonstrates that biomass-derived AF MD fuels could reduce the lifecycle GHG emissions of fuel for road transportation and commercial aviation by 30-86%, but that this environmental benefit comes a production cost 2-5 times greater than petroleum-derived fuels. Finally, this thesis concludes with a CBA of large-scale AJ adoption for the commercial aviation industry. The results indicate that whether such a policy results in a net increase or decrease of costs to society depends on the subjective selection of a discount rate for the analysis, and the characteristics of the feedstock-to-fuel pathway of interest. In particular, AJ fuels derived from low LUC risk and low societal opportunity cost feedstocks, such as wastes and residues, are identified as the production pathways most likely to result in a reduction of the climate and fuel production costs of aviation to society.

Future work

This thesis points to a number of areas of interest for future research on the topics of bioenergy and AJ technologies, and also more generally for technology assessment with the goal of informing policy making.

The analysis presented here, as well as previous work to assess the environmental impacts of bioenergy including AJ production technologies [9,12], has used GWP_{100} as the climate metric of choice. This is a methodological decision made almost by default in many LCA studies, although its consequences for the conclusions may be significant when non-CO_2 GHG emissions are associated with the technology of interest [234]. In addition, LUC emissions are often dealt with by simply amortizing a pulse of emissions over the duration of a project or policy period, and CO_2 uptake from biomass growth is usually assumed to occur simultaneous to bioenergy combustion such that there is no net CO_2 climate impact. These simplifying assumptions associated with the timing of CO_2 fluxes in the atmosphere may misrepresent the physical reality and climate change impacts of interest, depending on the scope and purpose of the study [235]. Therefore, future assessment of bioenergy and AJ technologies should carefully consider the goals of the analysis, and select a climate metric and simplifying assumptions that capture the physical processes sufficiently to answer the research question at hand.

This work is focused on quantifying the climate and production cost characteristics of bioenergy and AJ production technologies. However, additional environmental, economic, and societal impacts of bioenergy technologies should be included in a holistic assessment of their feasibility from a societal perspective, including potential impacts on air, water, and soil quality, land use patterns, commodity prices, and energy security [34,35,151,230-233]. Future research should aim to better characterize the performance to bioenergy technologies with respect to these non-climate impacts at the scale of process engineering, but also at the scale of economy-wide impacts when assessing potential policy options.

In order to better inform policy making, the technology assessment techniques employed here would benefit from improved methods of quantifying societal value. For example,

discount rate is identified as a key determinant of the probability of a net reduction in the societal climate and fuel production costs of large-scale AJ adoption, however the selection of this value is a subjective choice that leads to ambiguity in the conclusions that can be drawn from the analysis. A stronger theoretical basis for evaluating societal costs and benefits in future years would help to resolve this issue. In addition, the analysis presented here relies on the use of market prices as a proxy for the societal opportunity costs, or shadow prices, of scarce commodities. An improved measure of the societal value of commodity resources would improve the accuracy of future research building on this thesis.

Pursuit of these future research directions is especially important for AJ technologies, because airlines will be able to use AJ to meet their emissions reduction obligations under ICAO's Global Market-based Measure [81]. This means there will additional financial incentive for deployment of AJ production. This thesis, and subsequent work to quantify the environmental and economic impacts of AJ use, will help to inform more societally beneficial development of these technologies.

Appendix A

Energy crops

Yield projection methods and data sources

The areal yield of cultivated energy crops depends upon plant characteristics, agricultural practices and the agro-climatic conditions where the cultivation is taking place. In order to take these aspects into account, this analysis draws upon data from the Global Agro-ecological Zones (GAEZ) model, and empirical yield data from the statistics division of FAO (FAOSTAT). 4 categories of cultivated energy crops are represented with 12 specific crop types:

Starchy crops: maize grain, sorghum grain and cassava

Sugary crops: sugarcane and sugar beet

Vegetable oil crops: soybean, rapeseed, jatropha and oil palm

Lignocellulosic crops: switchgrass, miscanthus and reed canary grass

Historical average yield data for 8 of these crops (soybean, rapeseed, oil palm, maize grain, sorghum grain, cassava, sugarcane and sugar beet) is collected from FAOSTAT data for 5 world regions: and is extrapolated to 2050 under three different assumptions as described in Chapter 2. The result is 3 projections of average areal yields in each of the world regions, for the 8 crops of interest.

The spatial heterogeneity of energy crop yields is captured by scaling regionally-averaged GAEZ data on maximum agro-climatically attainable yields, which is available globally at a 0.083° resolution, to match the estimates of 2050 yields extrapolated from historical FAOSTAT data. The GAEZ data is generated for "advanced" inputs levels, which reflects market-oriented farming that is fully mechanized, using high-yielding varieties and the optimum application of nutrients and pesticides [236]. This assumption is made because

economic development by 2050 could mean that advanced farming techniques are applied in all regions of the world. In addition, we assume rainfed cultivation so that potential yields are not over-estimated in the face of competition for scarce fresh water resources in the future. These data are generated for the 2050 Hadley climate projections, on all land that is assigned a suitability index of "good" or better for the crop of interest in the GAEZ model.

In order to reflect the concept of yield plateaus [237], we limit the extrapolated 2050 yields in each region by the maximum agro-climatically attainable average yields from the GAEZ model. In cases where the historical yields exceed the advanced-input rainfed agro-climatically attainable yields from GAEZ (e.g. in the case of sugar beet), the maximum historical yields are assumed to represent the maximum attainable average yield. In the case of oil palm cultivation in OECD and REF, and sugarcane and cassava cultivation in REF, there is no historical data, and therefore scaling factors are derived from those calculated for other world regions. The extrapolated 2050 yields for 8 crops, in the regions for which historical data exist, are shown in the Yield projection section below.

No historical yield data is available from FAOSTAT for the 4 remaining crops (jatropha, switchgrass, miscanthus and reed canary grass), as they have not been grown at commercial scale to date. In this case, GAEZ yield data for these crops is scaled such that average yields reflect the range of anticipated yields from these crops in the literature. In the case of jatropha that is 1.4-2.0 $tonnes_{oil}$/ha [183,238], and for herbaceous lignocellulosic crops that is 10.5-24.0 $tonnes_{dm}$/ha [36].

The scaling factors that are applied to the maximum agro-climatically attainable yields, obtained from GAEZ, to reflect the average yields in 2050 extrapolated from FAOSTAT historical data are shown in Table 21.

Table 21: Scaling factors, applied to GAEZ data, in order to reflect 2050 yield estimates.

		Soy oil	Rapeseed oil	Jatropha oil	Oil palm	Maize grain	Sorghum grain	Sugarcane	Sugarbeet	Cassava	Switchgrass	Miscanthus	Reed canarygrass
MAF	Low	0.31	0.59	0.41	0.17	0.25	0.12	0.63	2.58	0.35	0.45	0.44	0.92
	Mid	0.51	1.00	0.50	0.17	0.25	0.16	0.63	2.58	0.51	0.73	0.72	1.51
	High	0.71	1.00	0.59	0.26	0.48	0.42	0.94	2.66	0.96	1.02	1.00	2.11
LAM	Low	0.63	0.58	0.41	0.64	0.43	0.40	0.77	1.80	0.46	0.45	0.44	0.92
	Mid	0.87	0.58	0.50	0.74	0.66	0.54	1.00	1.80	0.54	0.73	0.72	1.51
	High	1.00	1.00	0.59	0.74	0.66	0.72	1.00	1.80	1.00	1.02	1.00	2.11
ASIA	Low	0.39	0.60	0.41	0.68	0.59	0.15	0.80	1.91	0.81	0.45	0.44	0.92
	Mid	0.39	0.87	0.50	0.72	0.78	0.16	0.92	2.00	1.00	0.73	0.72	1.51
	High	0.88	1.00	0.59	0.77	0.87	0.53	1.00	2.00	1.00	1.02	1.00	2.11
OECD	Low	0.68	0.76	0.41	0.66	1.00	0.51	0.74	1.90	0.24	0.45	0.44	0.92
	Mid	0.85	1.00	0.50	0.73	1.00	0.51	0.74	1.90	0.24	0.73	0.72	1.51
	High	1.00	1.00	0.59	0.76	1.00	0.89	1.00	1.90	0.88	1.02	1.00	2.11
REF	Low	0.47	0.65	0.41	0.66	0.75	0.36	0.74	1.59	0.46	0.45	0.44	0.92
	Mid	0.94	0.78	0.50	0.73	1.00	0.77	0.82	1.80	0.57	0.73	0.72	1.51
	High	0.94	1.00	0.59	0.76	1.00	0.77	0.99	1.80	0.96	1.02	1.00	2.11

Regions where historical yields are greater than agro-climatically attainable rainfed, advanced input yields predicted by GAEZ. In this case, historically obtained yields were assumed to remain constant until 2050.

Regions where insufficient historical data exist to calculate scaling factors, therefore they are estimated from values obtained for other regions.

Crops for which no historical data exist. Scaling factors are based on the yields predicted in the literature: Jongschaap et al. (2007) and Aachten (2008) for jatropha, Searle & Malins (2014) for lignocellulosic energy crops

World region country groupings

Table 22: World region country groupings.

MAF		LAM	ASIA	OECD	REF
Algeria	Madagascar	Argentina	Afghanistan	Australia	Albania
Angola	Malawi	Aruba	Bangladesh	Austria	Armenia
Bahrain	Mali	Bahamas	Bhutan	Belgium	Azerbaijan
Benin	Mauritania	Barbados	Brunei Darussalam	Canada	Belarus
Botswana	Mauritius	Belize	Cambodia	Cyprus	Bosnia and Herzegovina
Burkina Faso	Mayotte	Bolivia (Plurinational State of)	Hong Kong SAR	Denmark	Bulgaria
Burundi	Morocco	Brazil	China	Finland	Croatia
Cameroon	Mozambique	Chile	Macao SAR	France	Czech Republic
Cape Verde	Namibia	Colombia	Democratic People's Republic of Korea	Germany	Estonia
Central African Republic	Niger	Costa Rica	Fiji	Greece	Georgia
Chad	Nigeria	Cuba	French Polynesia	Greenland	Hungary
Comoros	Oman	Dominican Republic	India	Guam	Kazakhstan
Congo	Palestinian Territories	Ecuador	Indonesia	Iceland	Kyrgyzstan
Cote d`Ivoire	Qatar	El Salvador	Lao People's Democratic Republic	Ireland	Latvia
Democratic Republic of the Congo	Reunion	French Guiana	Malaysia	Italy	Lithuania
Djibouti	Rwanda	Grenada	Maldives	Japan	Montenegro
Egypt	Saudi Arabia	Guadeloupe	Micronesia (Fed. States of)	Luxembourg	Poland
Equatorial Guinea	Senegal	Guatemala	Mongolia	Malta	Republic of Moldova
Eritrea	Sierra Leone	Guyana	Myanmar	Netherlands	Romania
Ethiopia	Somalia	Haiti	Nepal	New Zealand	Russian Federation
Gabon	South Africa	Honduras	New Caledonia	Norway	Serbia
Gambia	South Sudan	Jamaica	Pakistan	Portugal	Slovakia
Ghana	Sudan	Martinique	Papua New Guinea	Puerto Rico	Slovenia
Guinea	Swaziland	Mexico	Philippines	Spain	Tajikistan
Guinea-Bissau	Syrian Arab Republic	Nicaragua	Republic of Korea	Svalbard and Jan Mayen Islands	The former Yugoslav Republic of Macedonia
Iran (Islamic Republic of)	Togo	Panama	Samoa	Sweden	Turkmenistan
Iraq	Tunisia	Paraguay	Singapore	Switzerland	Ukraine
Israel	Uganda	Peru	Solomon Islands	Turkey	Uzbekistan
Jordan	United Arab Emirates	Suriname	Sri Lanka	United Kingdom	
Kenya	United Republic of Tanzania	Trinidad and Tobago	Taiwan	United States of America	
Kuwait	Western Sahara	United States Virgin Islands	Thailand		
Lebanon	Yemen	Uruguay	Timor-Leste		
Lesotho	Zambia	Venezuela (Bolivarian Republic of)	Vanuatu		
Liberia	Zimbabwe		Viet Nam		
Libyan Arab Jamahiriya					

Yield projection data

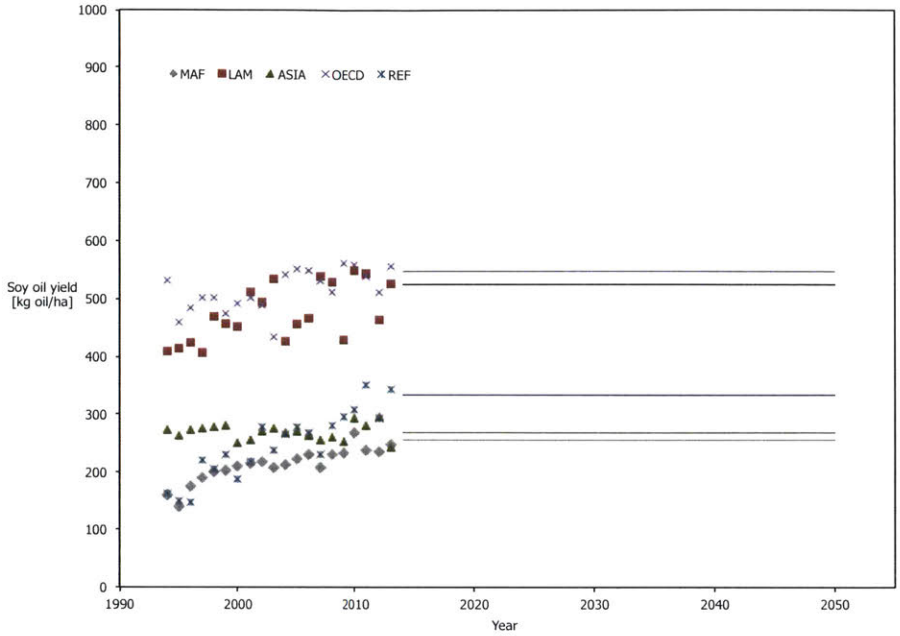

Figure 18: Low soybean oil yield extrapolation to 2050.

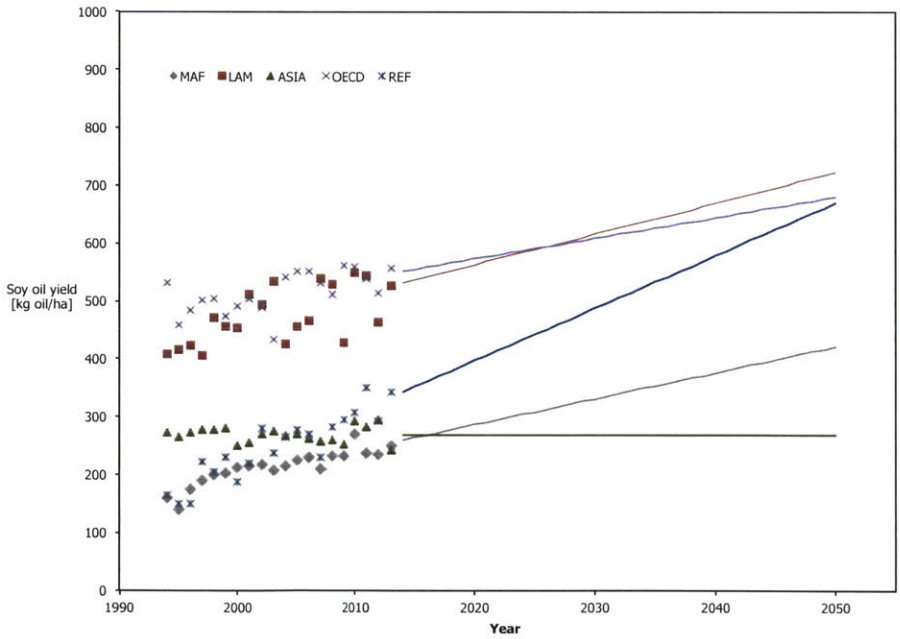

Figure 19: Mid soybean oil yield extrapolation to 2050.

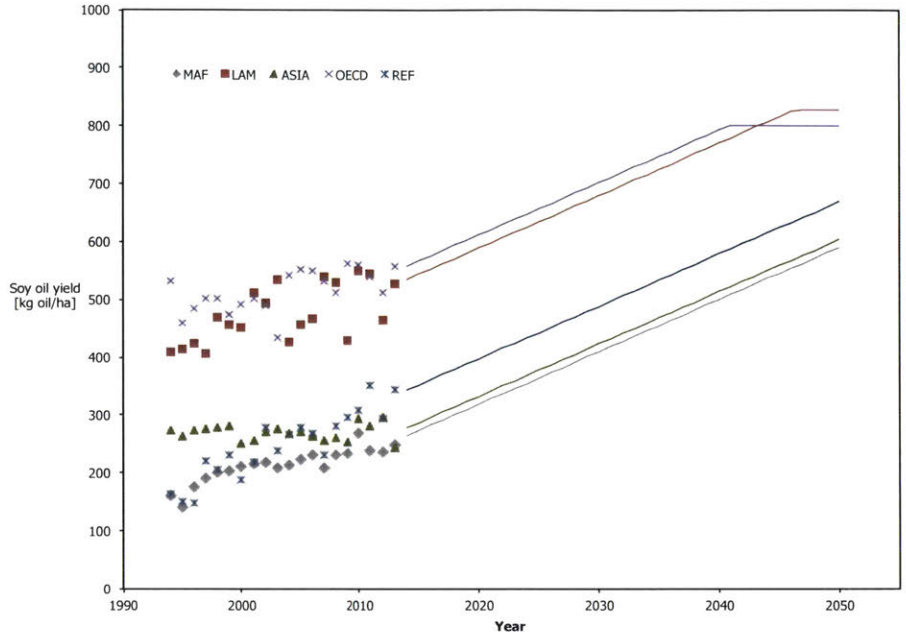

Figure 20: High soybean oil yield extrapolation to 2050.

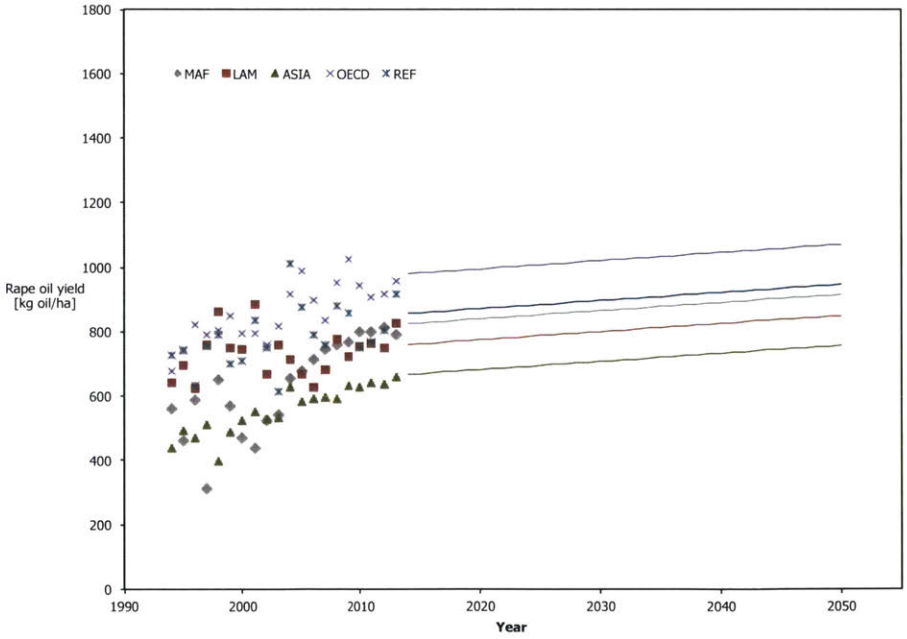

Figure 21: Low rapeseed oil yield extrapolation to 2050.

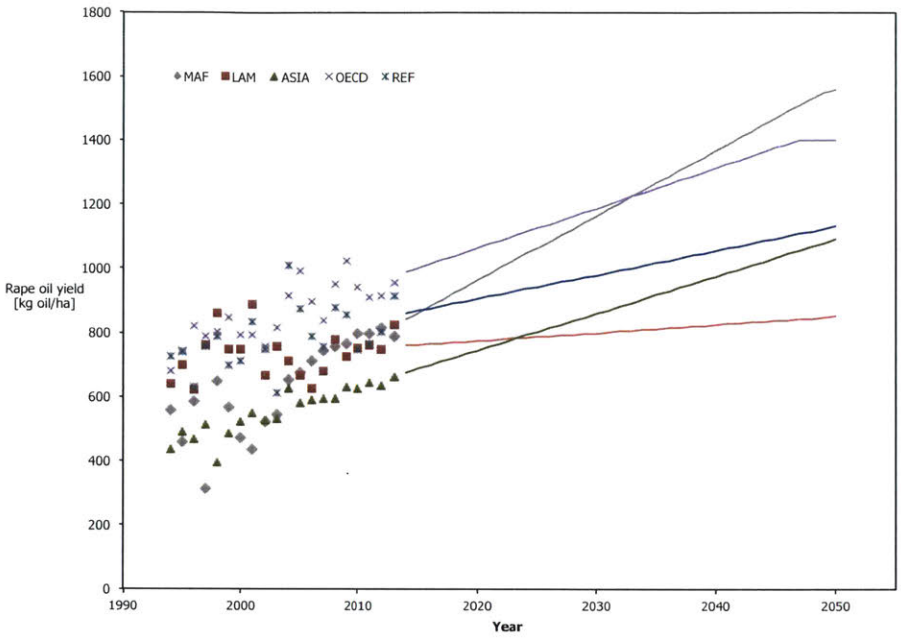

Figure 22: Mid rapeseed oil yield extrapolation to 2050.

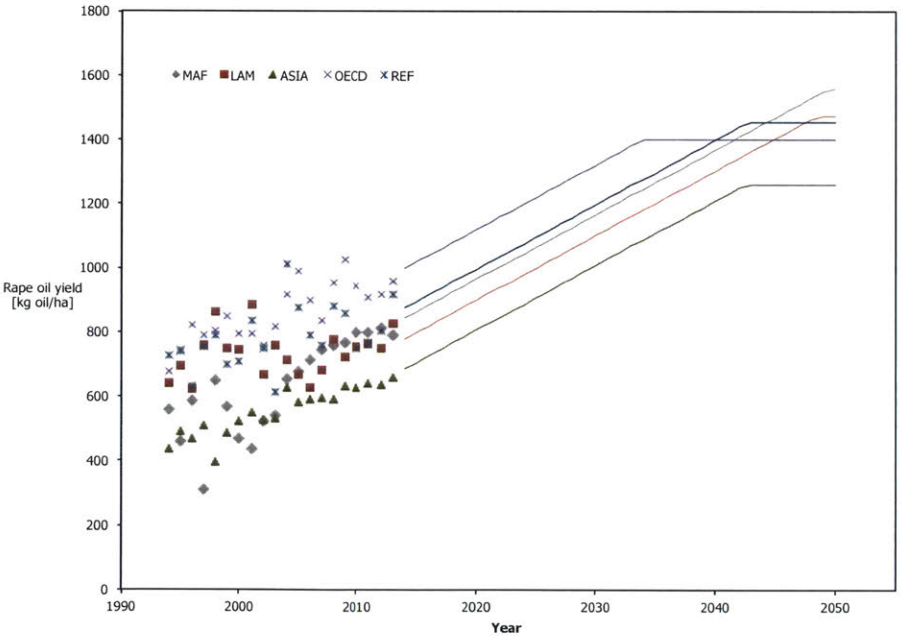

Figure 23: High rapeseed oil yield extrapolation to 2050.

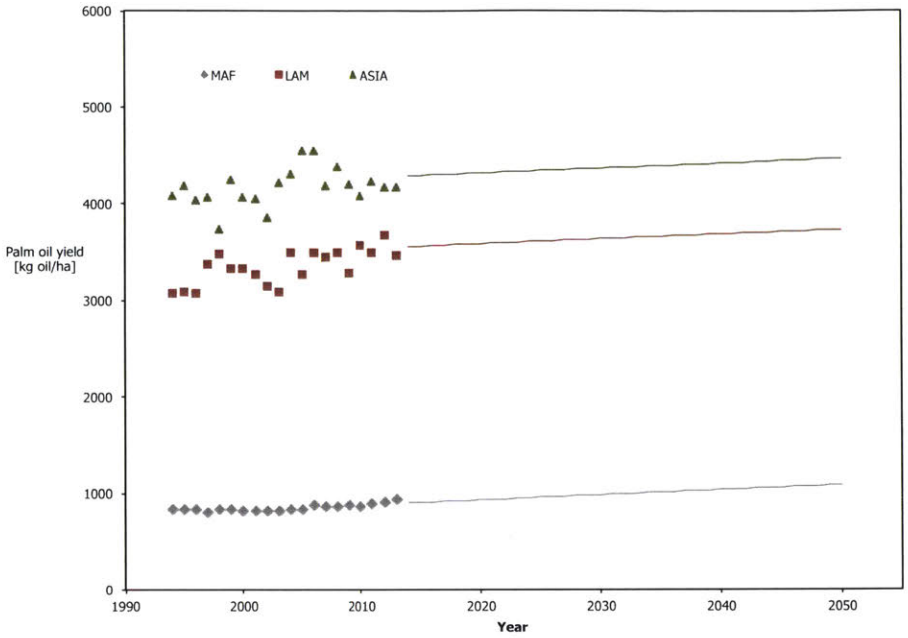

Figure 24: Low palm oil yield extrapolation to 2050.

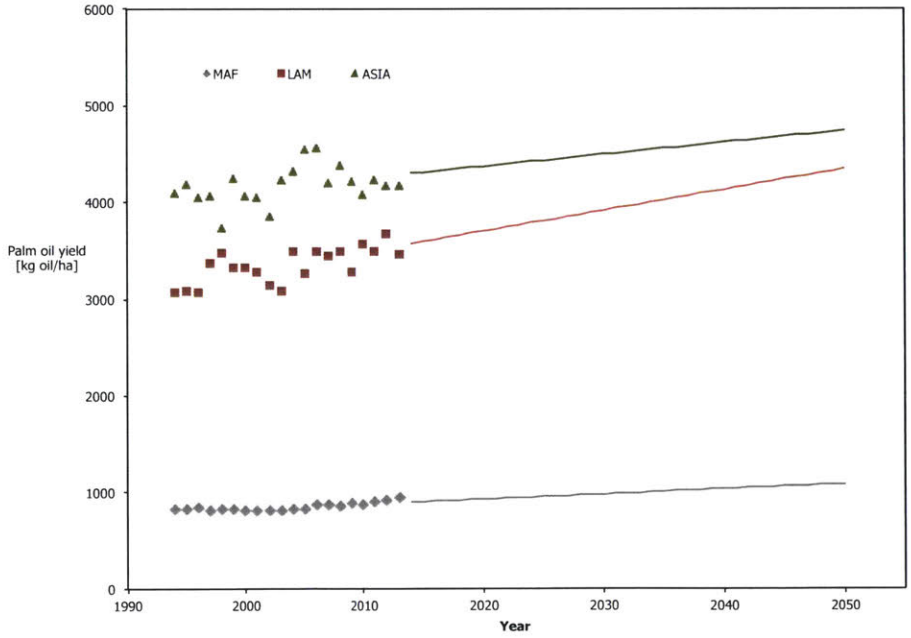

Figure 25: Mid palm oil yield extrapolation to 2050.

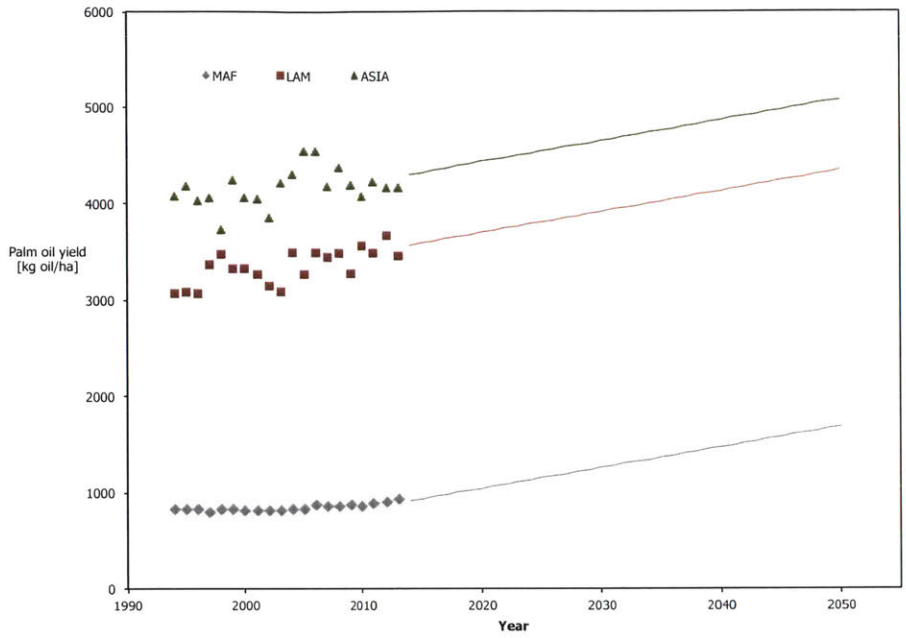

Figure 26: High palm oil yield extrapolation to 2050.

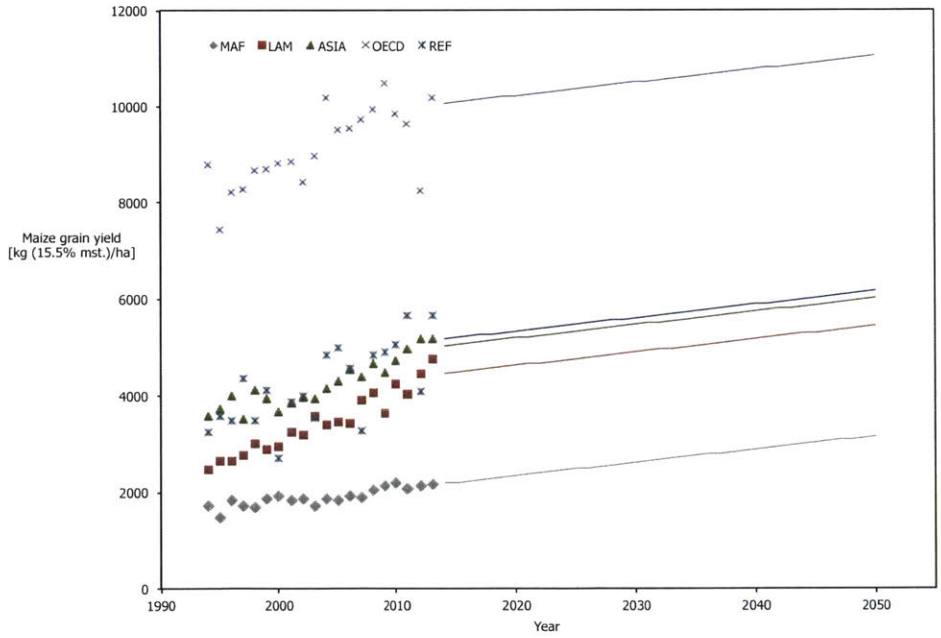

Figure 27: Low maize grain yield extrapolation to 2050.

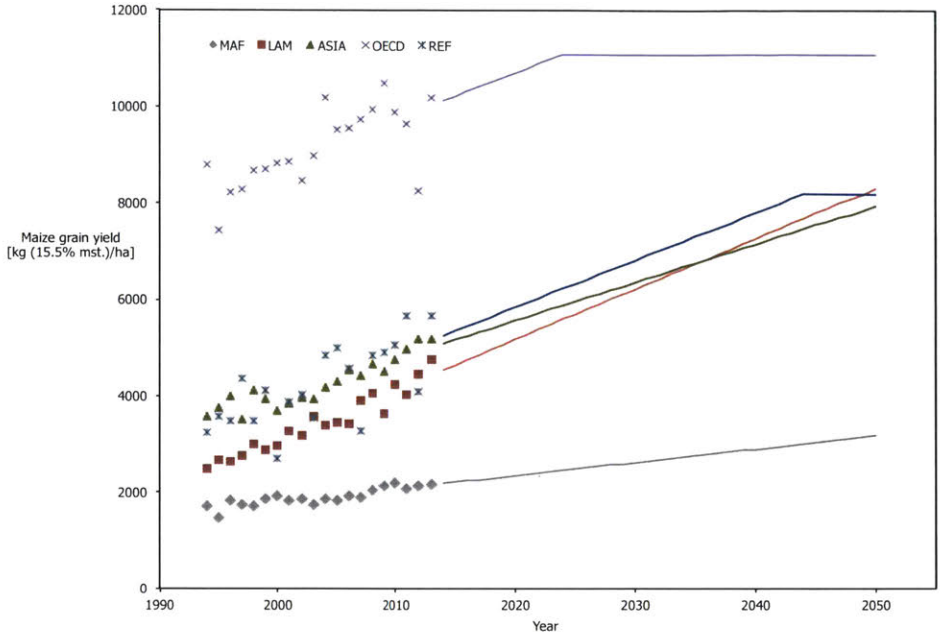

Figure 28: Mid maize grain yield extrapolation to 2050.

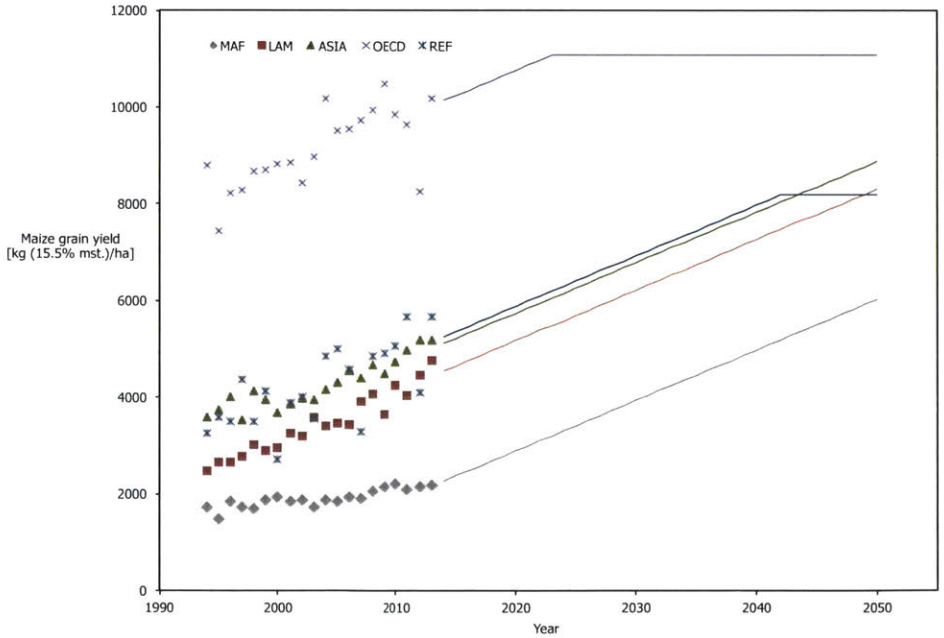

Figure 29: High maize grain yield extrapolation to 2050.

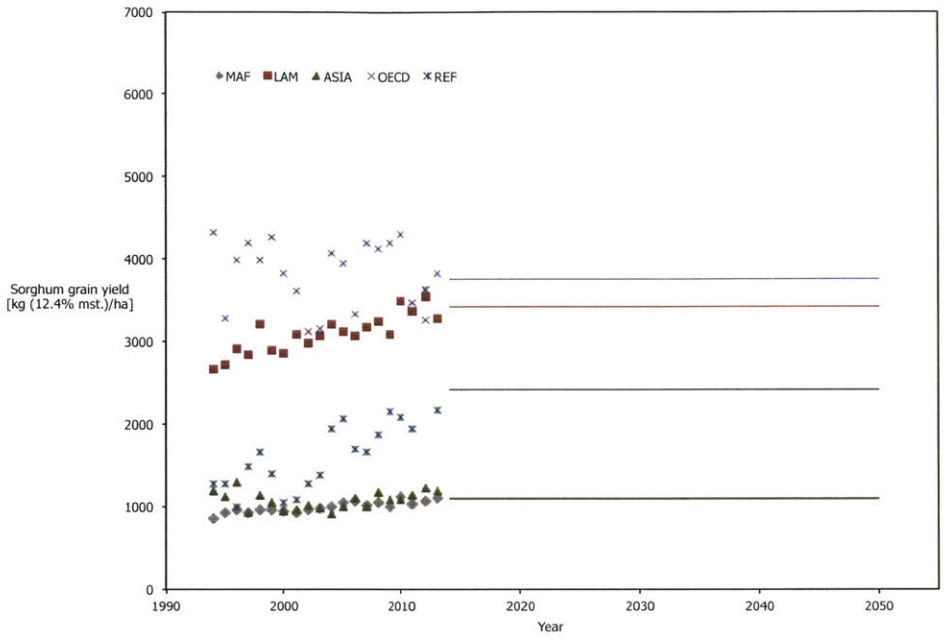

Figure 30: Low sorghum grain yield extrapolation to 2050.

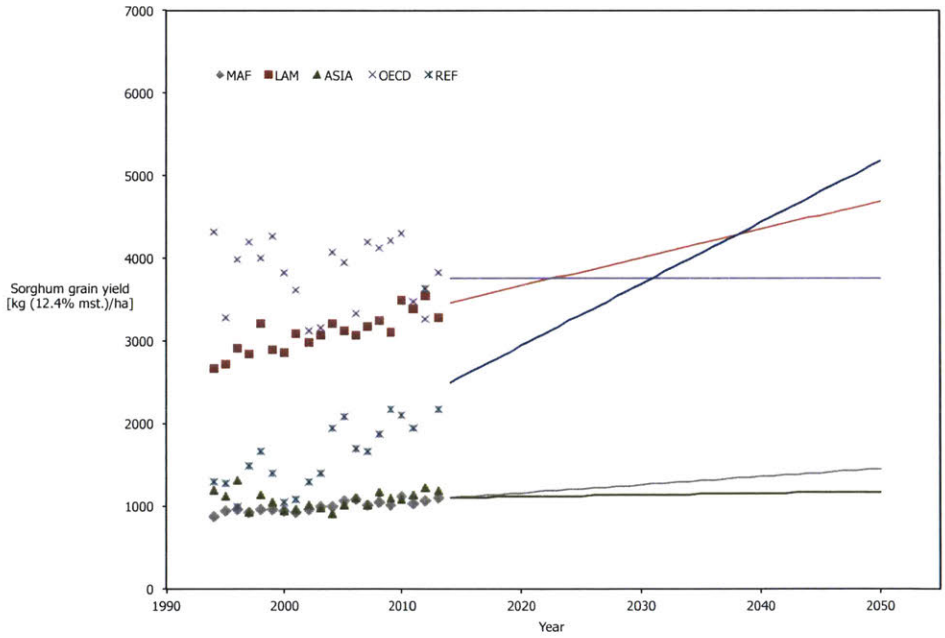

Figure 31: Mid sorghum grain yield extrapolation to 2050.

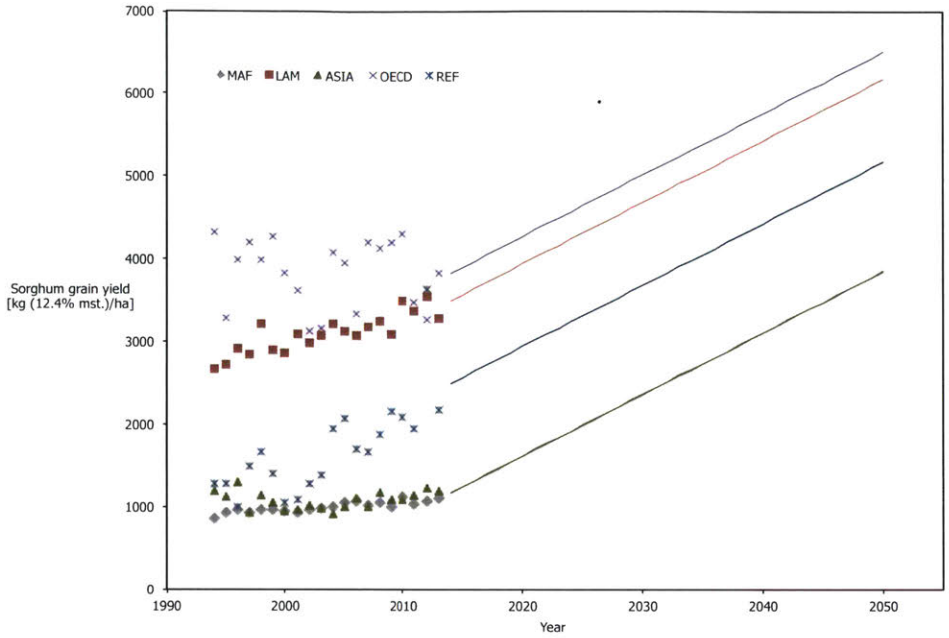

Figure 32: High sorghum grain yield extrapolation to 2050.

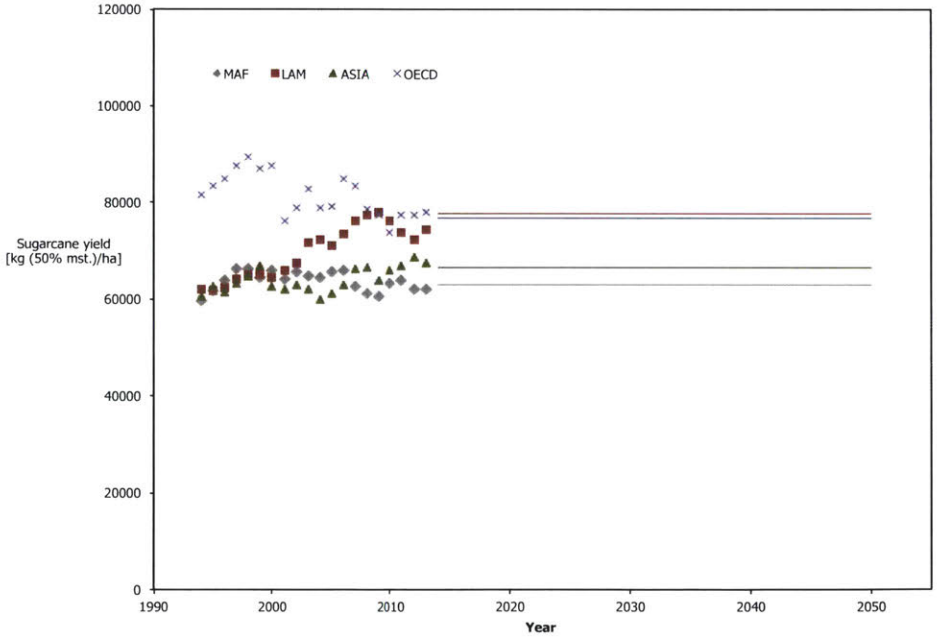

Figure 33: Low sugarcane yield extrapolation to 2050.

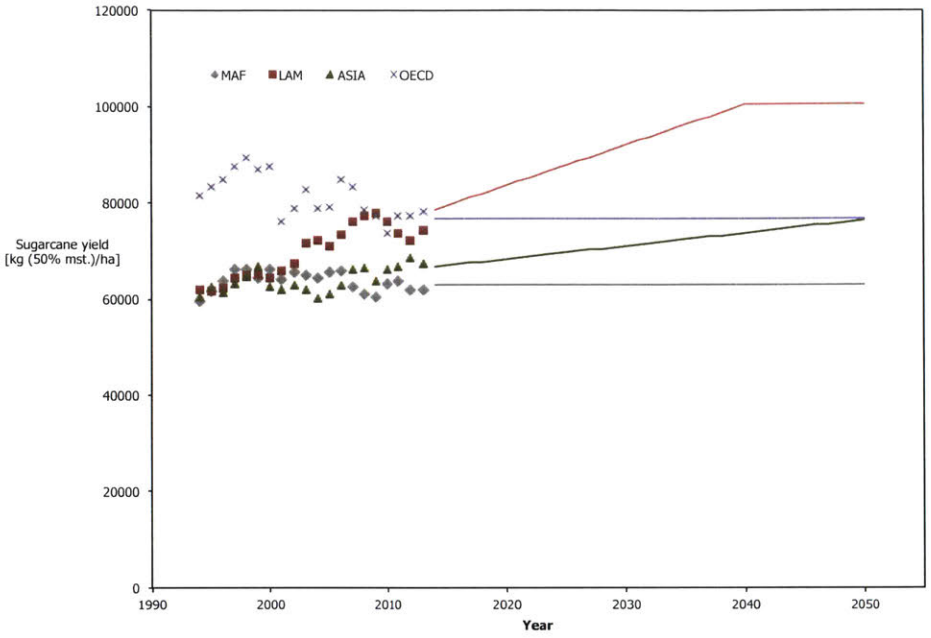

Figure 34: Mid sugarcane yield extrapolation to 2050.

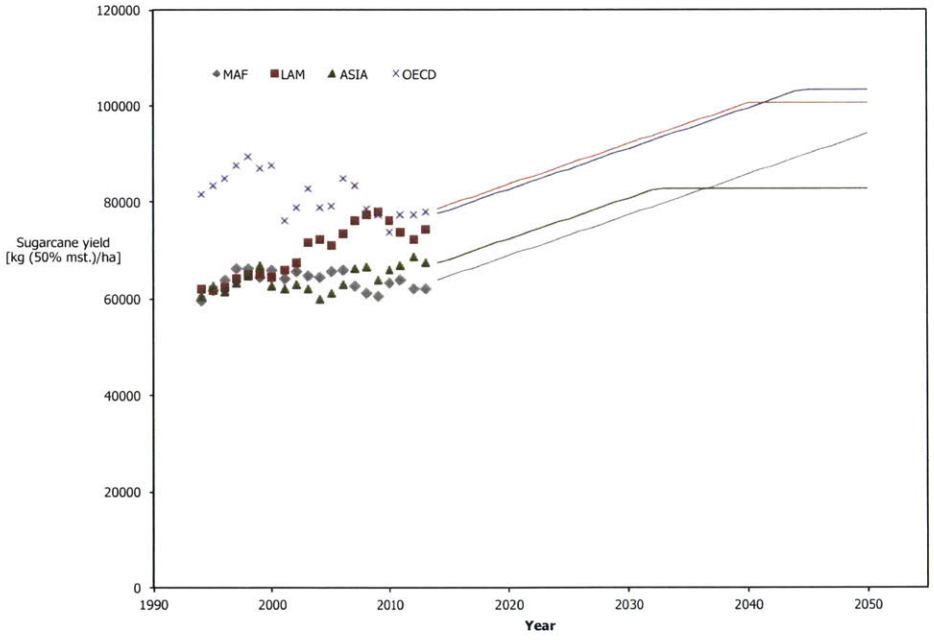

Figure 35: High sugarcane yield extrapolation to 2050.

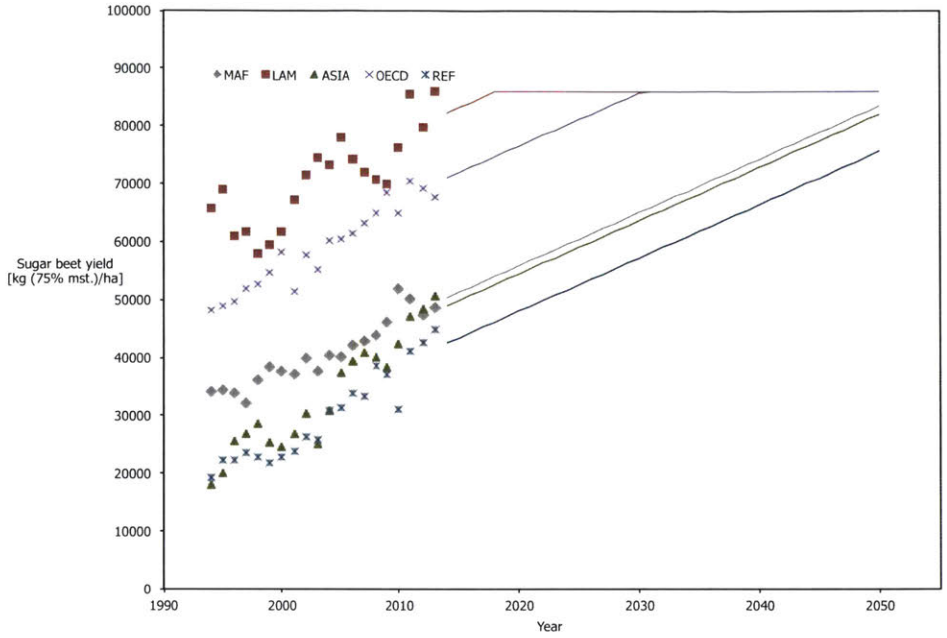

Figure 36: Low sugar beet yield extrapolation to 2050.

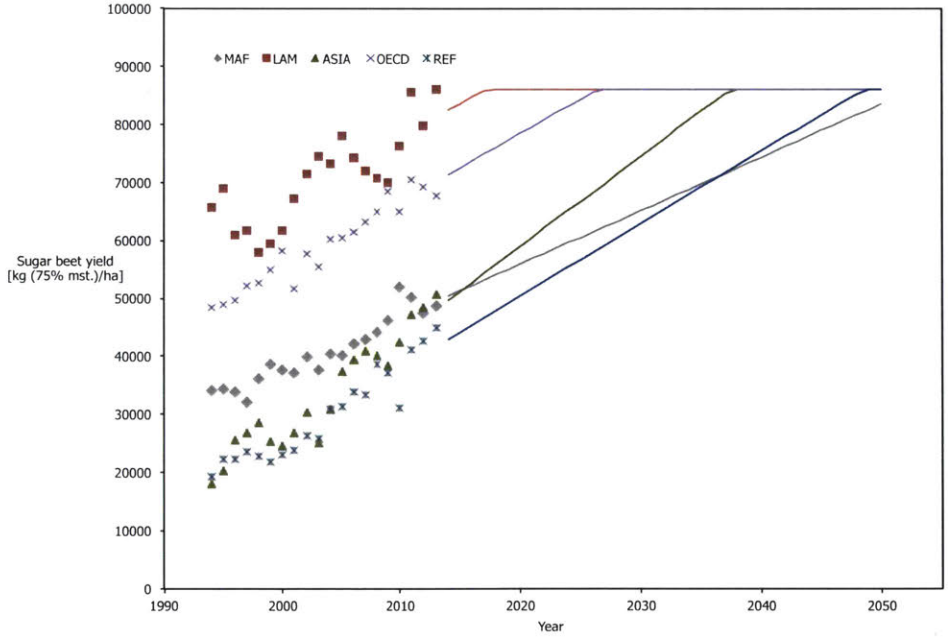

Figure 37: Mid sugar beet yield extrapolation to 2050.

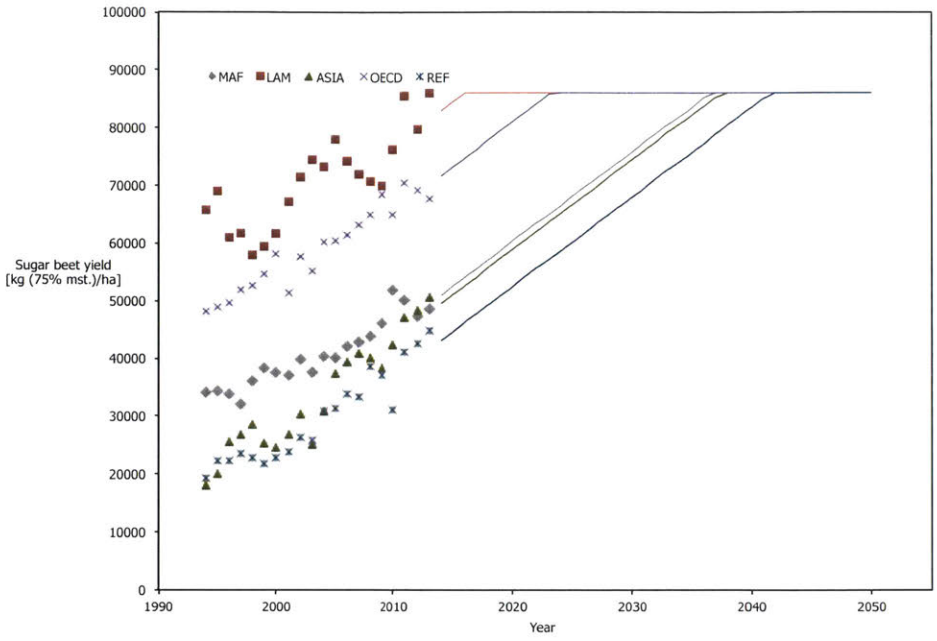

Figure 38: High sugar beet yield extrapolation to 2050.

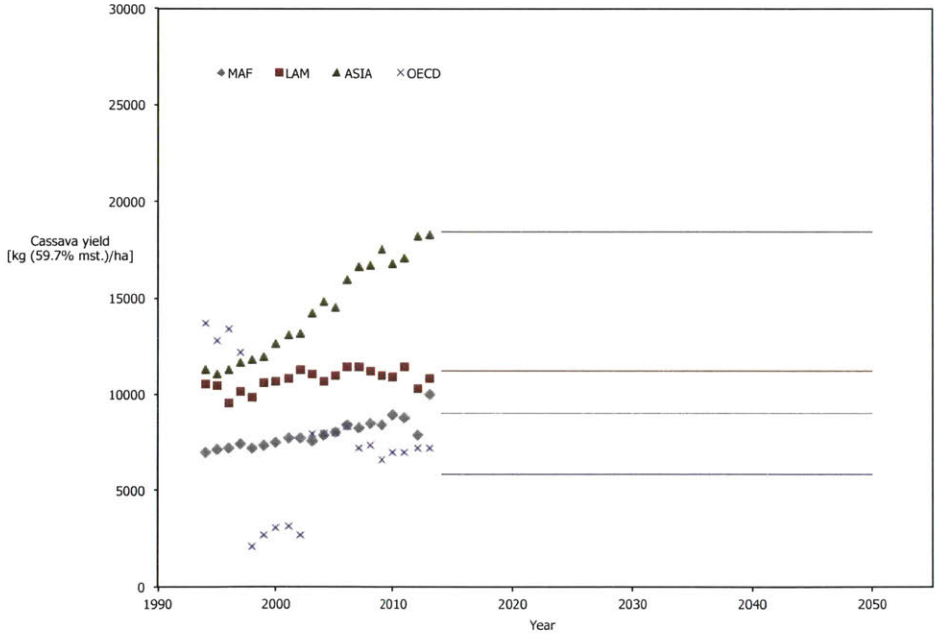

Figure 39: Low cassava yield extrapolation to 2050.

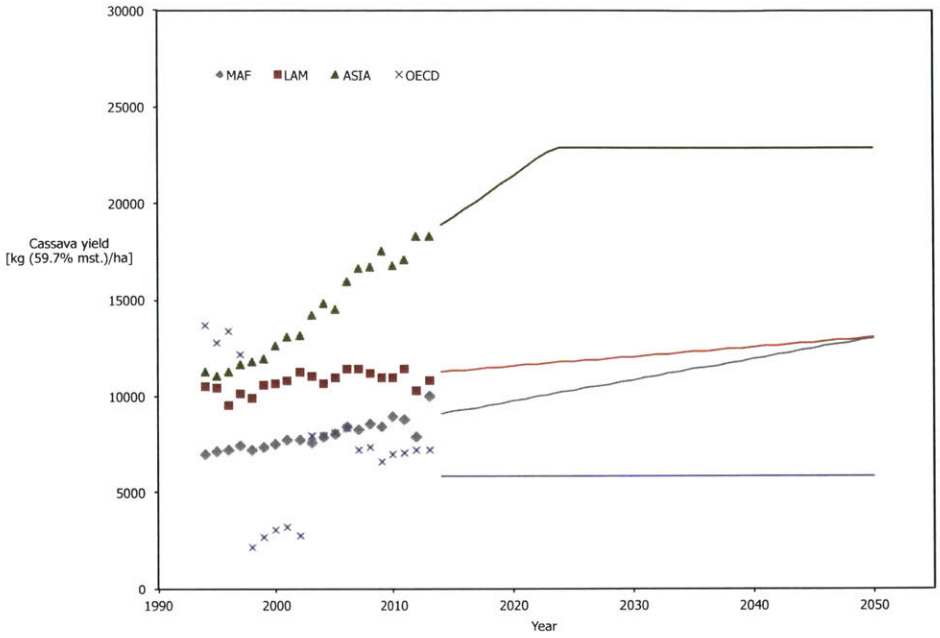

Figure 40: Mid cassava yield extrapolation to 2050.

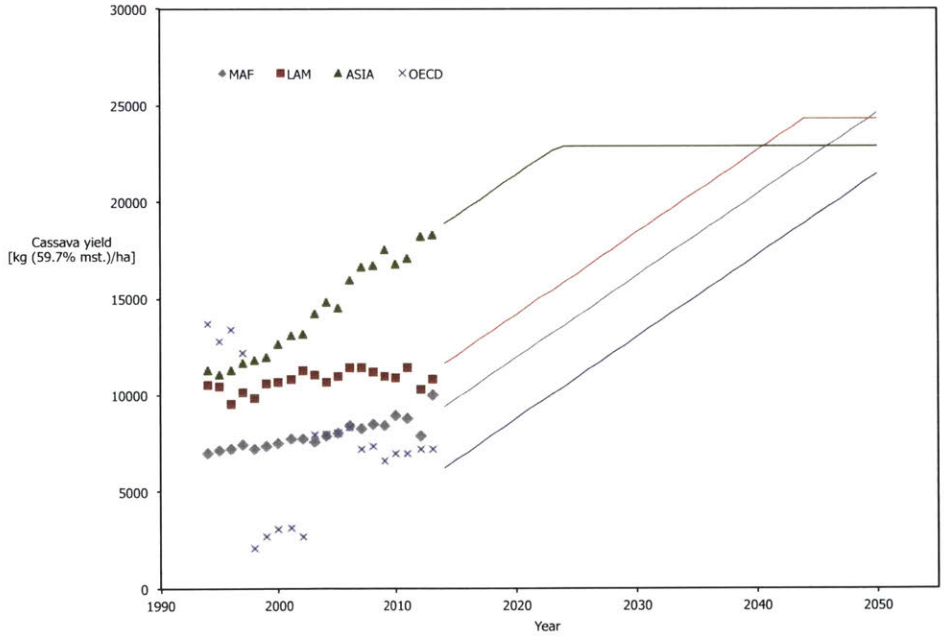

Figure 41: High cassava yield extrapolation to 2050.

Land availability for energy crop cultivation

The Land Use Harmonization (LUH) database is leveraged to assess potential land availability in 2050 [239] Hurtt et al. (2011). The LUH database is a compilation of the outputs of the Integrated Assessment Models (IAM) used to develop the Representative Concentration Pathways (RCP) for IPCC AR5. 2050 global land use is described in terms of five categories at a resolution of 0.5° x 0.5°: cropland, pastureland, urban land, primary land and secondary land. Primary land is defined as land undisturbed by human activities since 1700AD. Secondary land is defined as land previously disturbed by human activities since 1700AD and in the process of recovery. The total global land areas under each of the categories, and key references for the four RCPs, are shown in Table 23 [240-244].

Table 23: Breakdown of land use types and key references in 2050 RCP land use scenarios.

IAM (RCP)	Cropland [Mha]	Pastureland [Mha]	Urban land [Mha]	Primary land [Mha]	Secondary land [Mha]	Key reference
IMAGE (RCP 2.6)	1775	3127	51	3641	3335	van Vuuren et al. (2011)
GCAM (RCP 4.5)	1184	2745	51	3862	4086	Thomson et al. (2010) Thomson et al. (2011)
AIM (RCP 6.0)	1525	2369	119	3755	4161	Masui et al. (2011)
MESSAGE (RCP 8.5)	1597	3459	117	3366	3389	Riahi et al. (2011)

This analysis assumes the primacy of land requirements for food and feed production, human development, and eco-system protection in 2050, meaning that land areas projected for these uses are assumed to be unavailable for energy crop cultivation. Therefore, it is assumed *a priori* that cropland and urban land areas from the LUH data are unavailable for energy crop cultivation. An exception applies where the IAMs used to develop the RCP LUH scenarios include an endogenous estimation of primary energy from energy crops in 2050. In order to avoid the inconsistency of building off of land use data that already accounts for energy crop cultivation, the cropland assumed to be used for energy crop cultivation in the IAMs (specifically in IMAGE (RCP 2.6) and GCAM (RCP 4.5)) is assumed to be available for energy crop cultivation in this analysis. The percentage of total cropland used for energy crop cultivation in the IAMs is 13.4% in IMAGE (RCP 2.6) and 15.4% in GCAM (RCP 4.5).

The potential availability of excess pastureland for energy crop cultivation is evaluated under 3 assumptions: 0%, 10% and 20% availability. *Ceteris paribus*, if livestock production is not to be affected by energy crop cultivation, this assumption implies increased average grazing intensity. Therefore, the impact on grazing intensity of using pastureland for energy crop cultivation is quantified here. Global ruminant livestock production estimates for 2050 are taken from Alexandratos & Bruinsma (2012), which assumes 2.1% annual GDP growth from 2006, and a global population of 9.1 billion in 2050 [39]. This data is scaled to reflect analogous ruminant livestock production estimates for 2050 under the IPCC AR5 shared socio-economic pathways (SSP) on the basis of Tropical Livestock Units (TLU) per capita as a function of GDP per capita. The implied linear relationship between regional GDP per capita, and regional livestock production per capita, is shown graphically in Figure 42.

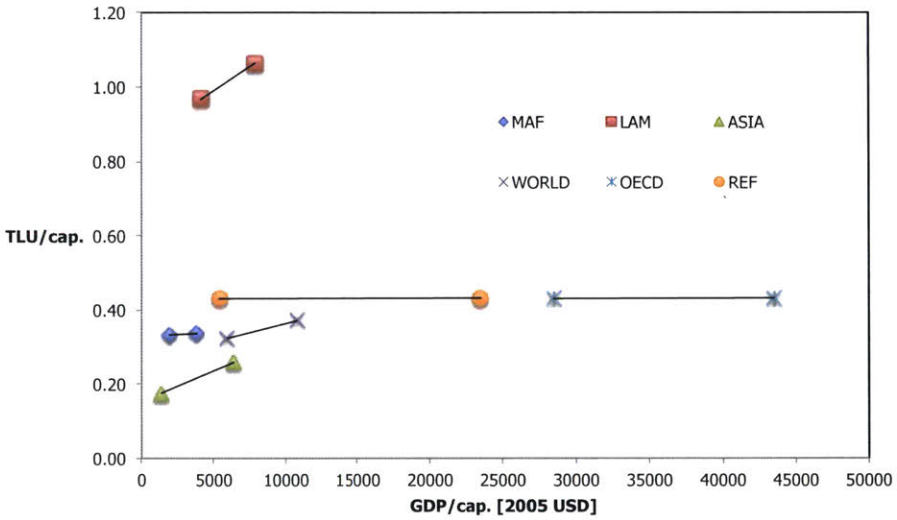

Figure 42: Relationship between GDP and livestock production per capita, in 2006 and 2050, from Alexandratos & Bruinsma (2012). For each world region the left data point is representative of 2006, and the right data point is representative of 2050.

Using the derived relationship between wealth, population and ruminant livestock production; the AR5 SSP projections for GDP and population in 2050; and the pastureland estimates from the 4 RCP scenarios, the resulting grazing intensity is calculated assuming 0%, 10% and 20% pastureland availability for energy crop cultivation, shown in Table 24.

Table 24: Global average implied grazing intensity under RCP 2050 LUH scenarios, AR5 SSPs, and pastureland availability assumptions [TLU/ha].

	RCP6					RCP3					RCP5					RCP9				
	SSP1	SSP2	SSP3	SSP4	SSP5	SSP1	SSP2	SSP3	SSP4	SSP5	SSP1	SSP2	SSP3	SSP4	SSP5	SSP1	SSP2	SSP3	SSP4	SSP5
0%	1.73	1.65	1.60	1.62	1.95	1.31	1.25	1.21	1.23	1.48	1.49	1.43	1.38	1.40	1.68	1.18	1.13	1.10	1.11	1.33
10%	1.92	1.84	1.78	1.80	2.16	1.45	1.39	1.35	1.37	1.64	1.65	1.59	1.53	1.56	1.87	1.31	1.26	1.22	1.24	1.48
20%	2.16	2.07	2.00	2.03	2.43	1.63	1.57	1.51	1.54	1.84	1.86	1.78	1.73	1.75	2.10	1.48	1.42	1.37	1.39	1.67

This analysis also assumes that land areas protected for biodiversity, conservation, and other ecosystems benefits are unavailable for conversion to cultivation of energy crops. The World Database of Protected Areas (WDPA) is used to exclude Ramsar Convention wetlands, World Heritage Convention areas, UNESCO-MAB biosphere reserves, ASEAN heritage lands, Natura2000 lands and nationally protected lands [245].

Finally, the agro-climatic suitability of land for energy crop cultivation is quantified in terms of a crop-specific suitability index ($0 \leq SI \leq 100$), calculated by the GAEZ model under the assumption of advanced-input, rainfed crop cultivation. Land areas that are below a minimum suitability threshold, defined as a suitability of "medium", "good" or "high" ($SI >$ 40, 55 or 70, respectively) are excluded for energy crop cultivation, depending on the calculated scenario. Minimum suitability thresholds of "medium", "good" and "high" are associated with the high, mid, and low bioenergy availability scenarios.

Residue and waste feedstocks

Crop residues

The availability of bioenergy from crop residues is estimated based on food and energy crop production. Alexandratos & Bruinsma (2012) provide a projection of the mix of food crop categories to be produced in 2050 (see table 4.12 of that reference), however this projection is made only for a single set of GDP and population growth assumptions [39]. This data is used to establish the relationship between GDP per capita and caloric intake per capita,

shown in Figure 43, in order to map region-specific food and feed crop production projections to the AR5 SSP scenarios [32]. These are added to the energy crop production from this analysis, to estimate total crop production from which crop residues could be generated.

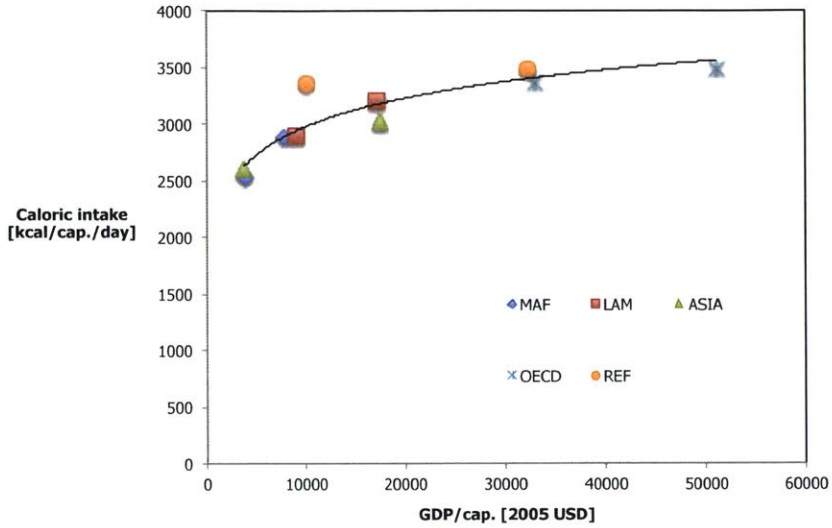

Figure 43: Relationship between GDP per capita and caloric intake per capita, in 2006 and 2050, from Alexandratos & Bruinsma (2012). For each world region the left data point is representative of 2006, and the right data point is representative of 2050.

Subsequently, Lal (2005) is used to estimate the ratio of residue to primary crop production, shown in Table 25 [33].

Table 25: Residue to primary crop ratio, adapted from Lal (2005).

Crop	Ratio of dry residue to primary crop
Wheat	1.5
Rice (paddy)	1.5
Maize	1
Pulses	1
Barley	1.5
Sorghum	1.5
Millet	1.5
Rape seed	1.5
Groundnuts	1
Sunflower	1
Sugarcane	0.25

In order to be consistent with the analysis approach of primacy of land use for other uses mentioned above, a residue removal rate that does not adversely impact global food or feed availability via soil degradation is assumed. The percentage of crop residues that can be removed without causing erosion or soil carbon and nutrient loss depends on many factors, such as climatic region, type of soil, topography of the land, and type of crop. One existing aggregated value from the academic literature indicates that up to 33% of crop residues may be removed without causing erosion or soil carbon and nutrient loss, however recent work indicates that the maximum sustainable removal rate may be up to 75% if certain management practices, such as cover cropping, are used [34,35]. This analysis assumes three removal rate scenarios of 20%, 35% and 50%, globally.

In addition, agricultural residues that would be used for other purposes, such as fodder and bedding for livestock, cultivation of fungi, or other horticultural uses, are not considered available in our analysis. Searle & Malins (2013) estimate that these agricultural uses could account for 5-30% of total available residues, therefore we assume that 70-95% of removed residues are available for bioenergy uses [36]. Three scenarios for net crop residue availability are shown in Table 26.

Table 26: Net residue availability scenarios.

	Residue removal rate	Residues not used for other purposes	Net residue availability
Low	20.0%	70.0%	14.0%
Mid	35.0%	82.5%	28.9%
High	50.0%	95.0%	47.5%

Forestry residues

The availability of residues from logging and wood processing is based on the potential supply of industrial roundwood and woodfuel in 2050 from plantations, non-forest trees, and forests previously disturbed by human activity. This corresponds to *ecological potential* as defined by Smeets & Faaij (2007), shown in Table 27 [37].

Table 27: 2050 supply of harvested wood, adapted from Smeets & Faaij (2007).

	Plantations [EJ/yr]	Non-forest trees [EJ/yr]	Previously disturbed forests [EJ/yr]	Total [EJ/yr]
Industrial roundwood	9.8	-	16.5	26.3
Woodfuel	2.9	12.5	4.8	20.2
Total	12.7	12.5	21.3	46.5

The availability of wood logging residues from plantations and forests is calculated on the basis of the residue fraction of the harvested wood, and the recoverable fraction of the residue fraction. The residue fraction is assumed to range between 71% and 32% [36,37], and the recoverable fraction is assumed to range between 50% and 25% [37]. The availability of wood processing residues is calculated on the basis of the residue fraction of the processed wood, the recoverable fraction of the residue fraction, and the fraction of recoverable residues unused for other purposes. The residue fraction is assumed to range between 70% and 30% [37], the recoverable fraction is assumed to range between 75% and 33% [37], and the fraction unused for other purposes is assumed to range between 50% and 10% [38].

Table 28: Available fraction of forestry residues.

	Logging residues			Processing residues			
	Residue fraction	Recoverable fraction	Net available fraction	Residue fraction	Recoverable fraction	Fraction unused for other purposes	Net available fraction
Low	32%	25%	8.0%	30%	33%	10%	1.0%
Mid	52%	38%	19.3%	50%	54%	30%	8.1%
High	71%	50%	35.5%	70%	75%	50%	26.3%
Note	Only available from plantations and forests			Only available from industrial roundwood			

Combining the estimates of 2050 forestry supply and available residue fractions, three scenarios defined for the availability of forestry residues in 2050, shown in Table 29.

Table 29: Net availability of forestry residues in 2050.

	Logging residues [EJ/yr]	Processing residues [EJ/yr]	Total [EJ/yr]
Low	2.7	0.3	3.0
Mid	6.6	2.1	8.7
High	12.1	6.9	19.0

Waste FOG

The availability of waste fats, oils and greases (FOG) is estimated based on the generation of tallow and animal fats from livestock slaughtering and processing. 2050 livestock production is estimated using Alexandratos & Bruinsma (2012) projections, scaled to the AR5 SSP scenarios in the manner described in the above section on pastureland availability. Tallow extraction and rendered tallow fractions are estimated from the sources shown in Table 30 [40-42]. In addition, this analysis assumes 30-70% of potentially available waste FOG cannot be considered due to their use in the oleo-chemical and animal feed production industries.

Table 30: Available fraction of waste FOG from livestock slaughtering and processing.

		Cattle	Sheep	Pigs	Poultry	Sources
	By-product fraction	27.5%	17.0%	4.0%	29.1%	Jayathilakan et al. (2012) Lopez et al. (2010)
	Rendered tallow fraction from byproducts	27.8%	24.0%	24.0%	20.3%	Lopez et al. (2010) Niederl et al. (2006)
	Fraction unused for oleochemical and feed production	30-70%				-
Net waste FOG availability from carcass weight	**Low**	2.3%	1.2%	0.3%	1.8%	
	Mid	3.8%	2.0%	0.5%	3.0%	
	High	5.4%	2.9%	0.7%	4.1%	

Schematic representation of modeling approach

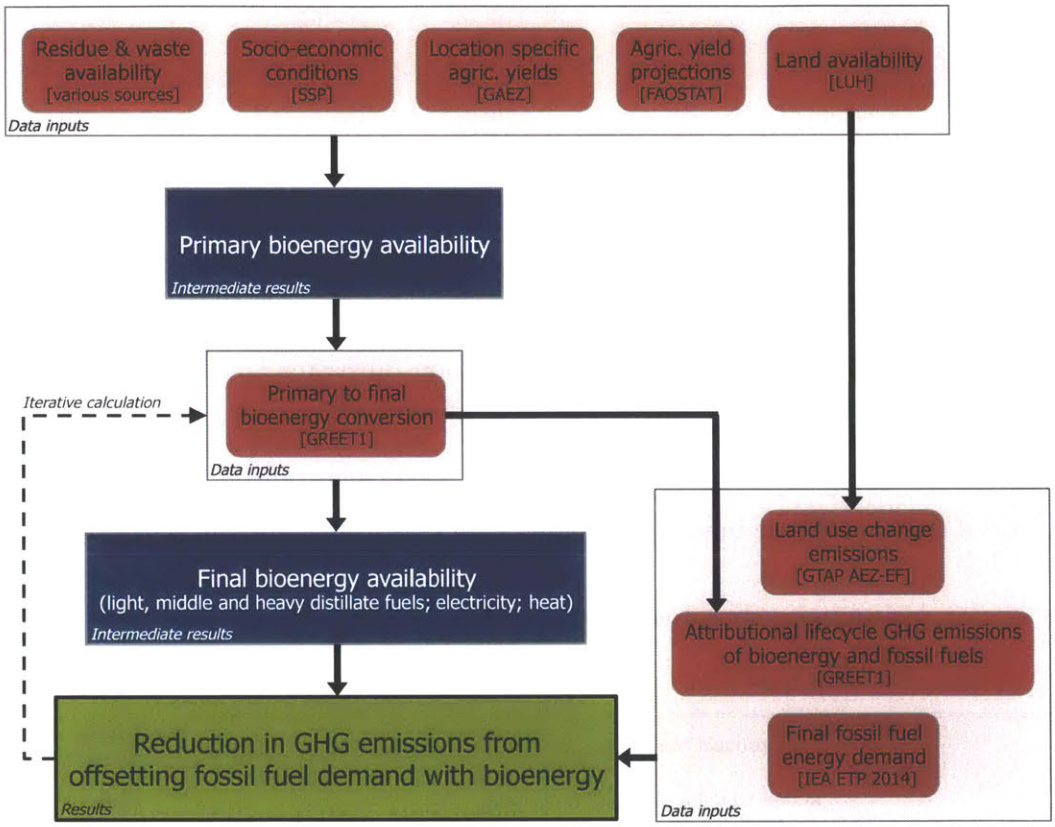

Figure 44: A schematic representation of the modeling approach for this analysis. The red items represent data inputs from the indicated sources; blue rectangles represent calculated intermediate results; the green box represents final results; the black arrows represent flows of data and information; and the dashed arrow represents the iterative step in the analysis required to maximize the calculated reductions in GHG emissions.

Results for a 20-year LUC emissions amortization period

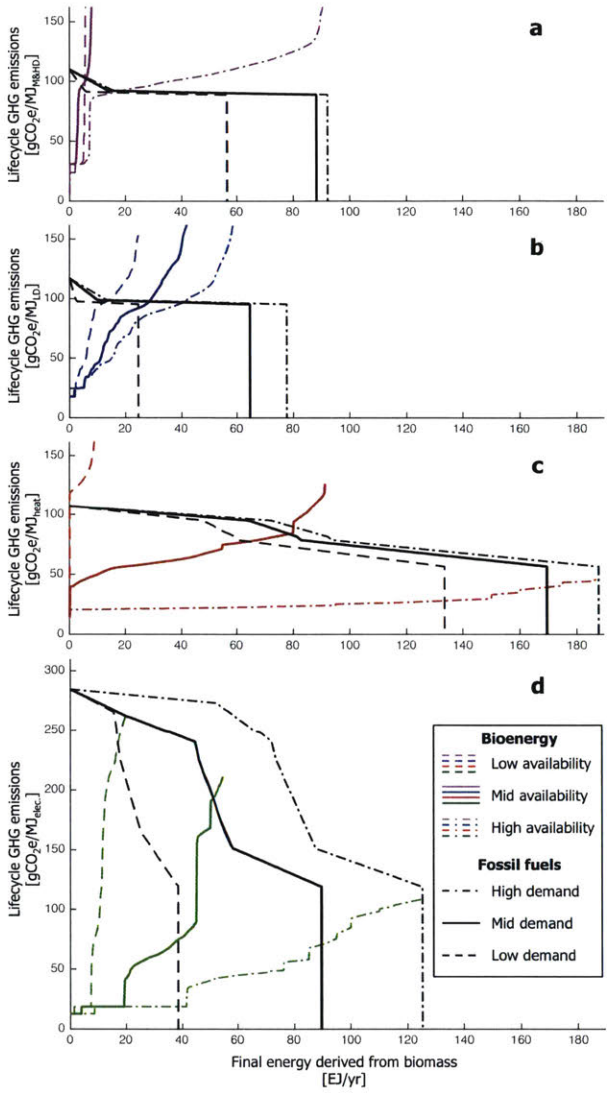

Figure 45: Availability and specific lifecycle GHG emissions of final bioenergy compared to fossil fuel-derived final energy demand and emissions in 2050, allocated to maximize GHG emissions reductions. Panel a shows biomass-derived (magenta) and petroleum-derived (black) middle and heavy distillate (M&HD) liquid fuels. Panel b shows biomass-derived (blue) and petroleum-derived (black) light distillate (LD) liquid fuels. Panel c shows biomass-derived heat final energy (red), compared to coal-, oil-, and natural gas-derived heat (black). Panel d shows biomass-derived electricity (green), compared to for coal-, oil-, and natural gas-derived electricity (black). The colored bioenergy curves in each panel correspond to the three bioenergy availability scenarios, and the black fossil fuel curves correspond to the three fossil fuel demand scenarios (low, mid and high corresponding to 2°C, 4°C and 6°C temperature change scenarios from IEA ETP, respectively [27]). The bioenergy availability curves shown here use a 20-year LUC emissions amortization period, as opposed to the 30-year LUC emissions amortization period used in Figure 4.

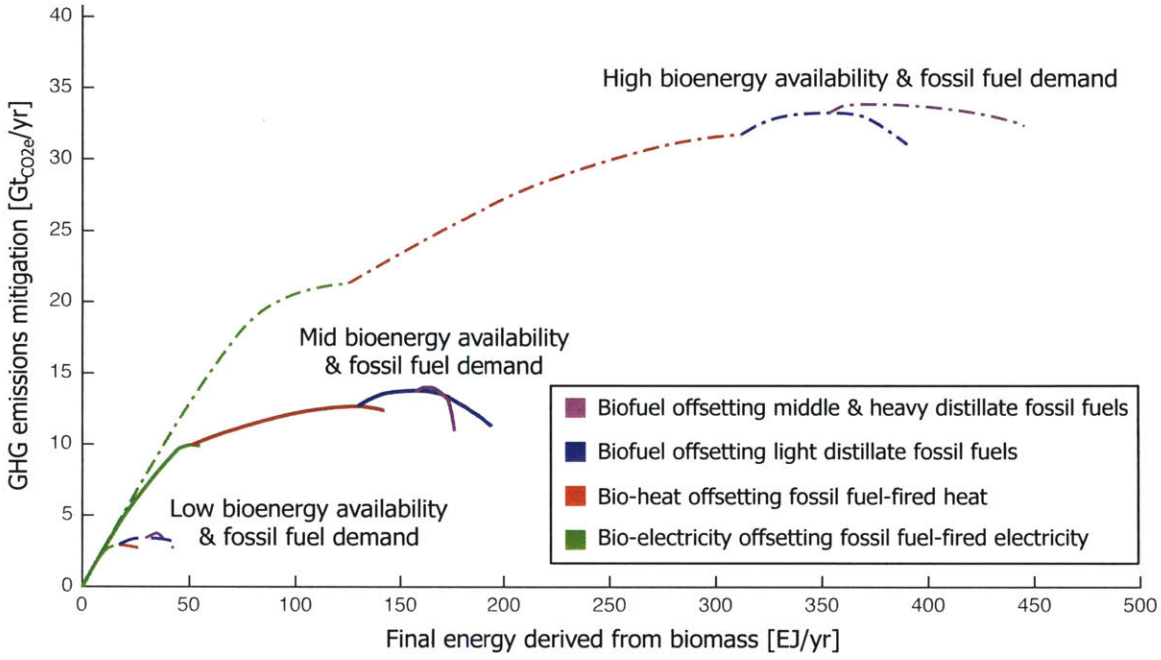

Figure 46: Deployment of biomass-derived final energy versus cumulative GHG emissions mitigation. The maximum of each curve represents the level of final bioenergy deployment for the indicated final energy end-use that maximizes GHG emissions reductions. The dashed lines denote the combination of the low bioenergy availability and fossil fuel demand scenarios, the solid lines denote the combination of the mid bioenergy availability and fossil fuel demand scenarios, and the dash-dot lines denote the combination of the high bioenergy availability and fossil fuel demand scenarios. The results shown here use a 20-year LUC emissions amortization period, as opposed to the 30-year LUC emissions amortization period used in Figure 5.

Table 31: Bioenergy allocation and deployment to maximize GHG emissions reductions. Primary bioenergy availability, final bioenergy deployment, and the reduction in LC GHG emissions are compared against 2050 final energy demand for combustion-generated electricity and heat, and liquid transportation fuels from fossil fuels, and the associated LC GHG emissions. The results shown here use a 20-year LUC emissions amortization period, as opposed to the 30-year LUC emissions amortization period used in Table 8.

2050 scenario					Bioenergy allocation & deployment													
					Primary energy		Final energy						Maximum GHG emissions reduction					
Fossil fuel demand scenario	Global demand for fossil fuel elec., heat, and liquid transp. fuels	LC GHG emissions from fossil fuels	Primary bioenergy avail.		Total	Propoortion of total avail.	Elec.	Heat	LD fuels	M&HD fuels	Total	Offset of final energy demand	Elec.	Heat	LD fuels	M&HD fuels	Total	Reduction in LC GHG emissions
	[EJ/yr]	[Gt_{CO2e}/yr]		[EJ/yr]	[EJ/yr]	[%]	[EJ/yr]					[%]	[Gt_{CO2e}/yr]					[%]
Low	253	26.8	Low	112	60	53%	17.2	0.0	12.2	5.2	35	14%	2.9	0.0	0.5	0.4	3.8	14%
			Mid	368	191	52%	27.7	90.3	24.7	5.8	148	59%	5.4	4.5	0.8	0.4	11.0	41%
			High	794	229	29%	23.0	133.7	24.7	9.8	191	75%	5.5	8.3	1.2	0.6	15.6	58%
Mid	412	47.1	Low	112	68	60%	19.8	0.0	18.6	0.5	39	9%	3.0	0.0	0.9	0.0	3.9	8%
			Mid	368	236	64%	51.1	78.6	28.1	5.9	164	40%	9.9	2.7	1.1	0.2	14.0	30%
			High	794	546	69%	89.9	169.7	40.6	63.9	364	88%	14.9	10.3	1.5	1.3	28.0	59%
High	483	59.6	Low	112	72	65%	21.8	0.0	18.7	0.5	41	8%	3.2	0.0	1.0	0.0	4.1	7%
			Mid	368	250	68%	75.0	39.3	28.2	6.1	149	31%	14.1	0.9	1.1	0.2	16.3	27%
			High	794	553	70%	125.0	187.6	40.8	18.6	372	77%	21.3	10.5	1.5	0.6	33.9	57%

Table 32: Average GHG mitigation effectiveness of bioenergy end-uses in 2050. This is defined as the ratio of maximum GHG emissions reduction, and total final energy, from biomass-derived electricity, heat, light distillate (LD) fuels, and middle & heavy distillate (M&HD) fuels. The ratio of effectiveness of electricity and heat to liquid fuels is shown in the rightmost column. The results shown here use a 20-year LUC emissions amortization period, as opposed to the 30-year LUC emissions amortization period assumed to generate the results in Table 9.

Fossil fuel demand scenario	Bioenergy availability	Average effectiveness [Gt_{CO2e}/EJ]						Ratio of elec. & heat to liquid fuels effectiveness
		Elec.	Heat	Biomass-fired elec. & heat	LD fuels	M&HD fuels	All liquid biofuels	
Low	Low	0.17	-	0.17	0.04	0.07	0.05	3.6
	Mid	0.19	0.05	0.08	0.03	0.07	0.04	2.1
	High	0.24	0.06	0.09	0.05	0.06	0.05	1.7
Mid	Low	0.15	-	0.15	0.05	0.01	0.05	3.1
	Mid	0.19	0.03	0.10	0.04	0.04	0.04	2.5
	High	0.17	0.06	0.10	0.04	0.02	0.03	3.6
High	Low	0.15	-	0.15	0.05	0.01	0.05	2.9
	Mid	0.19	0.02	0.13	0.04	0.04	0.04	3.3
	High	0.17	0.06	0.10	0.04	0.03	0.04	2.9

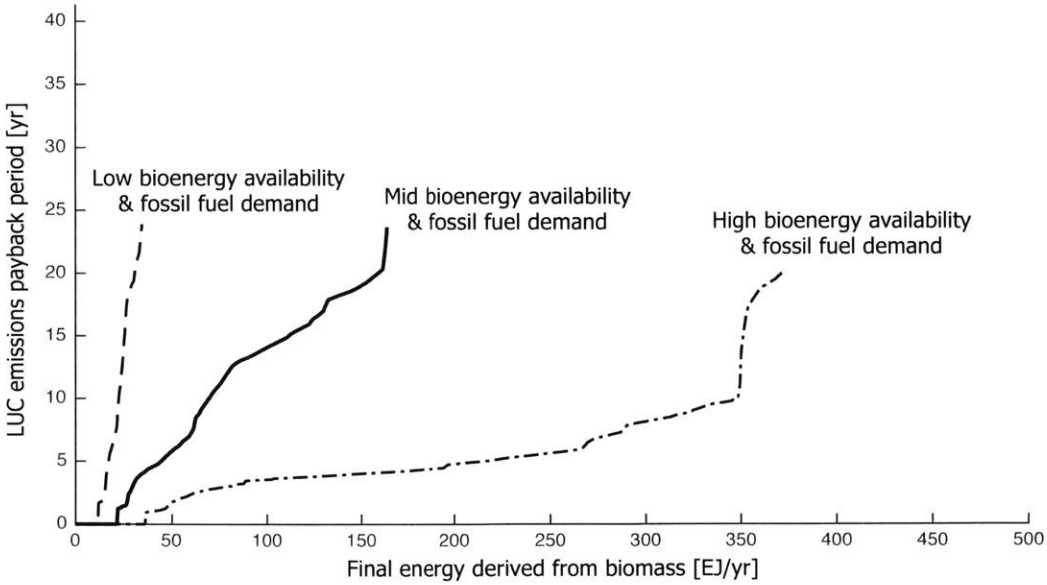

Figure 47: Deployment of biomass-derived final energy versus payback period for LUC emissions. The end point of each curve in the figure represents the level of final bioenergy deployment that maximizes GHG emissions reductions for that scenario combination of bioenergy and fossil fuel curves. The results shown here were generated assuming a 20-year LUC emissions amortization period, as opposed to the 30-year LUC emissions amortization period assumed to generate the results in Figure 6.

Results assuming 50% land req. for expansion of agricultural production

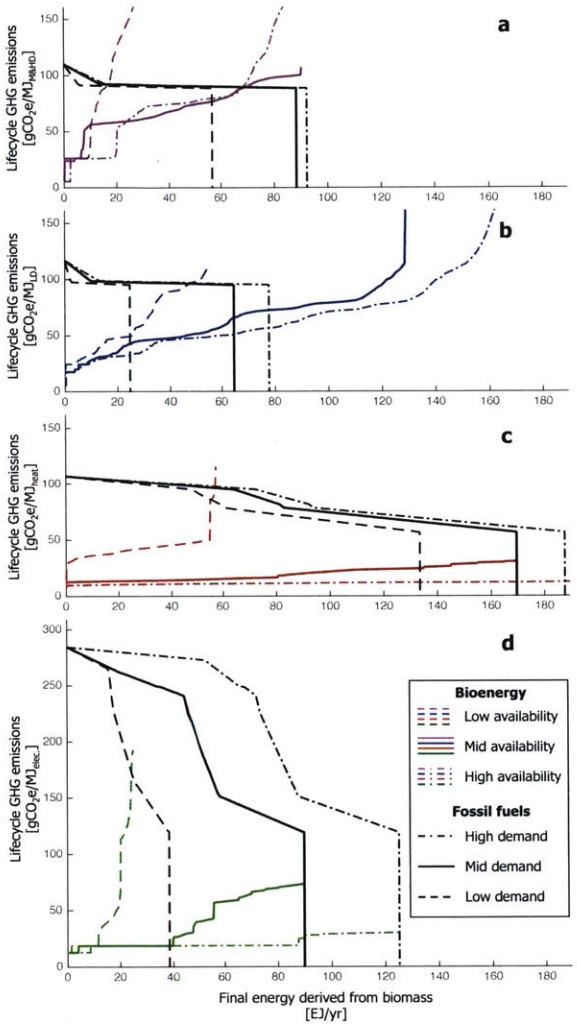

Figure 48: Availability and specific lifecycle GHG emissions of final bioenergy compared to fossil fuel-derived final energy demand and emissions in 2050, allocated to maximize GHG emissions reductions. Panel a shows biomass-derived (magenta) and petroleum-derived (black) middle and heavy distillate (M&HD) liquid fuels. Panel b shows biomass-derived (blue) and petroleum-derived (black) light distillate (LD) liquid fuels. Panel c shows biomass-derived heat final energy (red), compared to coal-, oil-, and natural gas-derived heat (black). Panel d shows biomass-derived electricity (green), compared to for coal-, oil-, and natural gas-derived electricity (black). The colored bioenergy curves in each panel correspond to the three bioenergy availability scenarios, and the black fossil fuel curves correspond to the three fossil fuel demand scenarios (low, mid and high corresponding to 2°C, 4°C and 6°C temperature change scenarios from IEA ETP, respectively [27]). The bioenergy availability curves shown here assume biomass land area requirements that are 50% of those in the results shown in Figure 4, in order to quantify the sensitivity of the results to the potential for intensification of agricultural production.

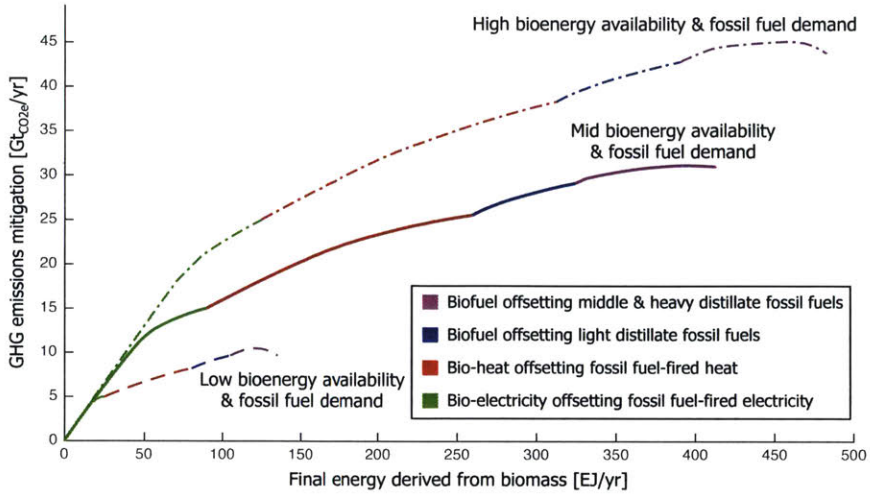

Figure 49: Deployment of biomass-derived final energy versus cumulative GHG emissions mitigation. The maximum of each curve represents the level of final bioenergy deployment for the indicated final energy end-use that maximizes GHG emissions reductions. The dashed lines denote the combination of the low bioenergy availability and fossil fuel demand scenarios, the solid lines denote the combination of the mid bioenergy availability and fossil fuel demand scenarios, and the dash-dot lines denote the combination of the high bioenergy availability and fossil fuel demand scenarios. The results shown here assume biomass land area requirements that are 50% of those in the results shown in Figure 5, in order to quantify the sensitivity of the results to the potential for intensification of agricultural production.

Table 33: Bioenergy allocation and deployment to maximize GHG emissions reductions. Primary bioenergy availability, final bioenergy deployment, and the reduction in LC GHG emissions are compared against 2050 final energy demand for combustion-generated electricity and heat, and liquid transportation fuels from fossil fuels, and the associated LC GHG emissions. The results shown here assume biomass land area requirements that are 50% of those in the results shown in Table 8, in order to quantify the sensitivity of the results to the potential for intensification of agricultural production.

			Final energy		Maximum GHG emissions reduction	
	Global demand for fossil fuel elec., heat, and liquid transp. fuels	LC GHG emissions from fossil fuels	Total	Offset of final energy demand	Total	Reduction in LC GHG emissions
Scenario	[EJ/yr]	[Gt_{CO2e}/yr]	[EJ/yr]	[%]	[Gt_{CO2e}/yr]	[%]
Low bioenergy availability and fossli fuel demand	253	26.8	121	48%	10.5	39%
Mid bioenergy availability and fossli fuel demand	412	47.1	394	96%	31.3	66%
High bioenergy availability and fossli fuel demand	483	59.6	459	95%	45.3	76%

Appendix B

Table 34: MSP results broken out by capital cost (CapEx), feedstock operating costs (feedstock OpEx) and non-feedstock operating costs (non-feedstock OpEx). All values in $USD_{2012}/liter_{MD}$

		CapEx	Feedstock OpEx	Non-feedstock OpEx	Total MSP
Sugarcane AF	Low	0.28	0.21	0.12	0.61
	Base	0.52	0.80	0.24	1.56
	High	0.75	1.49	0.38	2.63
Corn grain AF	Low	0.24	0.43	0.17	0.84
	Base	0.39	1.06	0.30	1.75
	High	0.70	2.30	0.65	3.65
Switchgrass AF	Low	0.56	0.12	0.42	1.09
	Base	1.10	0.38	0.82	2.30
	High	3.00	1.24	2.06	6.30

References

1. Intergovernmental Panel on Climate Change (IPCC) (2014). *Climate change 2014: synthesis report summary for policymakers.* Retrieved from: https://www.ipcc.ch/pdf/assessment-report/ar5/syr/AR5_SYR_FINAL_SPM.pdf

2. Myhre, G., Shindell, D., Breon, F.-M., Collins, W., Fuglestvedt, J., Huang, J., Koch, D., Lamarque, J.-F., Lee, D., Mendoza, B., Nakajima, T., Robock, A., Stephens, G., Takemura, T. & Zhang, H. (2013). Anthropogenic and natural radiative forcing. In *Climate change 2013: The physical science basis. Contribution of Working Group I to the Fifth Assessment Report of the Intergovernmental Panel on Climate Change (659-740).* Cambridge, UK: Cambridge University Press.

3. Smil, V. (2004). World history and energy. In Cleveland, C.J. (Ed.), *Encyclopedia of energy, vol. 6 (549-561).* Elsevier.

4. United States Department of Energy Bioenergy Technology Office (US DoE BETO) (2015) About the Bioenergy Technologies Office: growing America's energy future. Retrieved from: http://energy.gov/eere/bioenergy/about-bioenergy-technologies-office-growing-americas-energy-future

5. European Commission (EC) (2014) State of play on the sustainability of solid and gaseous biomass used for electricity, heating and cooling in the EU. (Working document of European Commission Staff, Brussels) Retrieved from: https://ec.europa.eu/energy/en/topics/renewable-energy/biomass

6. Wang, M., Wu, M. & Huo, H. (2007). Life-cycle energy and greenhouse gas emission impacts of different corn ethanol plan types. *Environmental Research Letters, 2(2),* DOI: 10.1088/1748-9326/2/2/024001

7. Huo, H., Wang, M., Bloyd, C. & Putsche, V. (2009). Life-cycle assessment of energy use and greenhouse gas emissions of soybean-derived biodiesel and renewable fuels. *Environmental Science & Technology, 43(3),* 750-756. DOI: 10.1021/es8011436

8. Farrell, A.E., Plevin, R.J., Turner, B.T., Jones, A.D., O'Hare, M. & Kammen, D.M. (2006) Ethanol can contribute to energy and environmental goals. *Science, 311(5760),* 506-508. DOI: 10.1126/science.1121416

9. Stratton, R.W., Wong, H.M. & Hileman, J.I. (2011). Quantifying variability in life cycle greenhouse gas inventories of alternative middle distillate transportation fuels. *Environmental Science & Technology, 45(10),* 4637-4644. DOI: 10.1021/es102597f

10. Wang, M., Han, J., Cai, H. & Elgowainy, A. (2012) Well-to-wheels energy use and greenhouse gas emissions of ethanol from corn, sugarcane and cellulosic biomass for US use. *Environ Res Lett* 7(4): 045905.

11. Staples, M.D., Malina, R., Olcay, H., Pearlson, M.N., Hileman, J.I., Boies, A. & Barrett, S.R.H. (2014) Lifecycle greenhouse gas footprint and minimum selling price of renewable diesel and

jet fuel from fermentation and advanced fermentation production technologies. *Energy & Environmental Science, 7(5),* 1545-1554. DOI: 10.1039/C3EE43655A

12. Edwards, R., Hass, H., Larive, J.-F., Lonza, L., Maas, H., Rickeard, D., Godwin, S., Hamje, H., Krasenbrink, A., Nelson, R. & Rose, K.D. (2014). *JEC well-to-wheels analysis: well-to-wheels analysis of future automotive fuels and powertrains in the European context.* (Technical report EUR 26236EN prepared by the European Commission Joint Research Centre, Ispra, Italy) Retrieved from: http://iet.jrc.ec.europa.eu/about-jec/sites/iet.jrc.ec.europa.eu.about-jec/files/documents/wtw_report_v4a_march_2014_final_333_rev_140408.pdf

13. Elgowainy A., Han, J., Poch, L., Wang, M., Vyas, A., Mahalik, M. & Rousseau, A. (2010) *Well-to-wheels analysis of energy use and greenhouse gas emissions of plug-in hybrid electric vehicles.* (Technical report ANL/ESD/10-1 prepared at Argonne National Laboratory, Lemont, IL) Retrieved from: http://www.afdc.energy.gov/pdfs/argonne_phev_evaluation_report.pdf

14. Burnham, A., Han, J., Clark, C.E., Wang, M., Dunn, J.B. & Palou-Rivera, I. (2012). Life-cycle greenhouse gas emissions of shale gas, natural gas, coal and petroleum. *Environmental Science & Technology, 46(2),* 619-627. DOI: 10.1021/es201942m

15. Searchinger, T., Heimlich, R., Houghton, R.A., Dong, F., Elobeid, A., Fabiosa, J., Tokgoz, S., Hayes, D. & Yu, T-.H. (2008) Use of US croplands for biofuels increases greenhouse gases through emissions from land-use change. *Science, 319(5867),* 1238-1240. DOI: 10.1126/science.1151861

16. Hertel, T., Golub, A.A., Jones, A.D., O'Hare, M., Plevin, R.J. & Kammen, D.M. (2010). Effects of US maize ethanol on global land use and greenhouse gas emissions: estimating market-mediated responses. *BioScience, 60(3),* 223-231. DOI: 10.1525/bio.2010.60.3.8

17. Plevin, R.J., O'Hare, M., Jones, A.D., Torn, M.S. & Gibbs, H.K. (2010). Greenhouse gas emissions from biofuels' indirect land use change are uncertain but may be much greater than previously estimated. *Environmental Science & Technology, 44(21),* 8015-8021. DOI: 10.1021/es101946t

18. Fargione, J., Hill, J., Tilman, D., Polasky, S. & Hawthorne, P. (2008). Land clearing and the biofuel carbon debt. *Science, 319,* 1235-1237. DOI: 10.1126/science.1152747

19. Winjum, J.K., Brown, S. & Schlamadinger, B. (1998). Forest harvest and wood products: sources and sinks of atmospheric carbon dioxide. *Forest Science, 44(2),* 272-284.

20. West, T.O., Marland, G., King, A.W., Post, W.M., Jain, A.K. & Andrasko, K. (2004). Carbon management response curves: estimates of temporal soil carbon dynamics. *Environmental Management, 33(4),* 507-518. DOI: 10.1007/s00267-003-9108-3

21. Fischer, G. & Schrattenholzer, L. (2001). Global bioenergy potentials through 2050. *Biomass & Bioenergy, 20(3),* 151-159. DOI: 10.1016/S0961-9534(00)00074-X

22. Hoogwijk, M., Faaij, A., Eickhout, B., de Vries, B. & Turkenburg W (2005). Potential of biomass energy out to 2100, for four IPCC SRES land-use scenarios. *Biomass Bioenergy, 29(4),* 225-257. DOI: 10.1016/j.biombioe.2005.05.002

23. Field, C.B., Campbell, J.E. & Lobell, D.B. (2008). Biomass energy: the scale of the potential resource. *Trends in Ecology & Evolution, 23(2),* 65-72. DOI: 10.1016/j.tree.2007.12.001

24. Ros, J., Olivier, J., Notenboom, J., Croezen, H. & Bergsma, G. (2012). *Sustainability of biomass in a bio-based economy.* (Technical report 500143001 of the PBL Netherlands Environmental Assessment Agency, The Hague, NL) Retrieved from: http://www.pbl.nl/sites/default/files/cms/publicaties/PBL-2012-Sustainability-of-biomass-in-a-BBE-500143001_0.pdf

25. Searle, S. & Malins, C. (2015). A reassessment of global bioenergy potential in 2050. *GCB Bioenergy, 7(2),* 328-336. DOI: 10.1111/gcbb.12141

26. Slade, R., Bauen, A. & Gross, R. (2014). Global bioenergy resources. *Nature Climate Change, 4(2),* 99-105. DOI: 10.1038/nclimate2097

27. International Energy Agency (IEA) (2014). *Energy Technology Perspectives 2014.* (Annual report prepared by IEA, Paris) Retrieved from: http://www.iea.org/etp/etp2014/

28. Food and Agricultural Organization of the United Nations Statistical Service (FAOSTAT) (2016) *Database of historical areal crop yields.* Retrieved from: http://faostat3.fao.org/home/E [Accessed August 20, 2016]

29. International Institute for Applied Systems Analysis (IIASA) (2016). *Global agro-ecological zones (GAEZ) model.* (Model developed by IIASA, Laxenburg, Austria) Retrieved from: http://www.gaez.iiasa.ac.at/

30. University of Maryland (2016). *Land use harmonization (LUH) project of future land use projections.* (Database developed by University of Maryland, College Park, Maryland) Retrieved from: http://luh.umd.edu/

31. Gibbs, H., Yui, S. & Plevin, R. (2014). *New estimates of soil and biomass carbon stocks for global economic models.* (GTAP Technical Paper No. 33, Purdue University, West Lafayette, IN) Retrieved from: https://www.gtap.agecon.purdue.edu/resources/download/6688.pdf

32. International Institute for Applied Systems Analysis (IIASA) (2016a) *SSP Database.* (Database maintained by IIASA, Laxenburg, Austria) Retrieved from: https://secure.iiasa.ac.at/web-apps/ene/SspDb/dsd?Action=htmlpage&page=about#regiondefs

33. Lal, R. (2005) World crop residues production and implications of its use as a biofuel. *Environment International, 31(4),* 575-584. DOI: 10.1016/j.envint.2004.09.005

34. Andrews, S.S. (2006). *Crop residue removal for biomass energy production: effects on soils and recommendations.* (White paper prepared for US Department of Agriculture, Natural Resource Conservation Service, Washington, DC) Retrieved from: http://www.nrcs.usda.gov/Internet/FSE_DOCUMENTS/nrcs142p2_053255.pdf

35. Pratt, M.R., Tyner, W.E., Muth Jr., D.J. & Kladivko, E.J. (2014). Synergies between cover crops and corn stover removal. *Agricultural System, 130,* 67-76. DOI: 10.1016/j.agsy.2014.06.008

36. Searle, S.Y. & Malins, C.J. (2014). Will energy crop yields meet expectations? *Biomass & Bioenergy, 65,* 3-12. DOI: 10.1016/j.biombioe.2014.01.001

37. Smeets, E.M.W. & Faaij, A.P.C. (2007). Bioenergy potentials from forestry in 2050: an assessment of the drivers that determine the potentials. *Climatic Change, 81(3),* 353-390. DOI: 10.1007/s10584-006-9163-x

38. McKeever, D.B. (2002). *Inventories of woody residues and solid wood waste in the United States* (White paper prepared for the US Department of Agriculture Forest Service, Forest Product Laboratory, Washington, DC) Retrieved from: http://originwww.fpl.fs.fed.us/documnts/pdf2004/fpl_2004_mckeever002.pdf

39. Alexandratos, N. & Bruinsma, J. (2012). *World agriculture towards 2030/2050: the 2012 revision.* (ESA working paper no. 12-03 prepared for UN FAO, Rome, Italy) Retrieved from: http://www.fao.org/docrep/016/ap106e/ap106e.pdf

40. Jayathilakan, K., Sultana, K., Radhakrishna, K. & Bawa, A.S. (2012). Utilization of byproducts and waste materials from meat, poultry and fish processing industries: a review. *Journal of Food Science Technology, 49(3),* 278-293. DOI: 10.1007/s13197-011-0290-7

41. Lopez, D.E., Mullins, J.C. & Bruce, D.A. (2010). Energy life cycle assessment for the production of biodiesel from rendered lipids in the United States. *Industrial & Engineering Chemistry Research, 49(5),* 2419-2432. DOI: 10.1021/ie900884x

42. Niederl, A. & Narodoslawsky, M. (2006). Ecological evaluation of processes based on by-products or waste from agriculture: life cycle assessment of biodiesel from tallow and used vegetable oil. In: *Feedstocks for the Future*, eds. Bozell JJ, Patel MK (American Chemical Society, Washington DC), pp. 239-252.

43. International Energy Agency (IEA) (2015). CO_2 emissions from fuel combustion: highlights. (Annual report prepared by IEA, Paris) Retrieved from: http://www.iea.org/publications/freepublications/publication/CO2EmissionsFromFuelCombustionHighlights2015.pdf

44. The Greenhouse Gases, Regulated Emissions, Energy Use in Transportation Model (GREET 1 2015) (2015). (Model developed by Argonne National Laboratory, Lemont, IL) Retrieved from: https://greet.es.anl.gov/greet_1_series

45. International Energy Agency (IEA) (2014a) *World Energy Outlook 2014.* (Annual report prepared by IEA, Paris) Retrieved from: https://www.iea.org/bookshop/477-World_Energy_Outlook_2014

46. United States Environmental Protection Agency (US EPA) (2010). *Regulation of fuels and fuel additives: changes to renewable fuel standard program; final rule.* (Federal register. 40 CFR Part 80, pp. 14669-15320.) Retrieved from: https://www.epa.gov/renewable-fuel-standard-program/regulations-and-volume-standards-under-renewable-fuel-standard

47. European Commission (EC) (2009) *Directive 2009/28/EC of the European Parliament and of the Council of 23 April 2009 on the promotion of the use of energy from renewable sources and amending and subsequently repealing Directives 2001/77/EC and 2003/30/EC.* (Document 32009L0028, Procedure2008/0016/COD) Retrieved from: http://eur-lex.europa.eu/legal-content/en/ALL/?uri=CELEX%3A32009L0028

48. Food and Agricultural Organization of the United Nations Statistical Service (FAOSTAT) (2016a) *Global arable land area and area harvested.* Retrieved from: http://fenix.fao.org/faostat/beta/en/#data/RL

49. Daioglou, V., Stehfest, E., Wicke, B., Faaij, A. & van Vuuren, D.P. (2015). Projections of the availability and cost of residues from agriculture and forestry. *GCB Bioenergy, 8(2),* 456-470. DOI: 10.1111/gcbb.12285

50. Trivedi, P., Malina, R. & Barrett, S.R.H. (2015). Environmental and economic tradeoffs of using corn stover for liquid fuels and power production. *Energy & Environmental Science, 8(5),* 1428-1437. DOI: 10.1039/c5ee00153f

51. Steubing, B., Zah, R. & Ludwig, C. (2012). Heat, electricity or transportation? The optimal use of residual and waste biomass in Europe from and environmental perspective. *Environmental Science & Technology, 46(1),* 164-171. DOI: 10.1021/es202154k

52. Campbell, J.E. & Lobell, D.B. & Field, C.B. (2009). Greater transportation energy and GHG offsets from bioelectricity than ethanol. *Science, 324(5930),* 1055-1057. DOI: 10.1126/science.1168885

53. International Energy Agency (IEA) (2012). *Technology roadmap: bioenergy for heat and power.* (Technical report prepared by IEA, Paris) Retrieved from: http://www.iea.org/publications/freepublications/publication/technology-roadmap-bioenergy-for-heat-and-power-.html

54. European Environment Agency (EEA) (2008). *Maximising the environmental benefits of Europe's bioenergy potential.* (Technical report no. 10/2008 prepared by EEA, Copenhagen) Retrieved from: http://www.eea.europa.eu/publications/technical_report_2008_10

55. Dray, L., Evans, A., Reynolds, T. & Schaefer, A. (2010). Mitigation of aviation emissions of carbon dioxide. *Transportation Research Record, 2177,* 17-26. DOI: 10.3141/2177-03

56. Hileman, J.I., De la Rosa Blanco, E., Bonnefoy, P.A. & Carter, N.A. (2013). The carbon dioxide challenge facing aviation. *Progress in Aerospace Science, 63,* 84-95. DOI: 10.1016/j.paerosci.2013.07.003

57. Sgouridis, S., Bonnefoy, P.A. & Hansman, R.J. (2011). Air transportation in a carbon constrained world: long-term dynamics of policies and strategies for mitigating the carbon footprint of commercial aviation. *Transportation Research Part A Policy & Practice, 45(10),* 1077-1091. DOI: 10.1016/j.tra.2010.03.019

58. Lal, R. (2008). Carbon sequestration. *Philosophical Transactions of the Royal Society B, 363,* 815-830. DOI: 10.1098/rstb.2007.2185

59. Hileman, J.I., Ortiz, D.S., Bartis, J.T., Wong, H.M., Donohoo, P.E., Weiss, M.A. & Waitz, I.A. (2009). *Near-term feasibility of alternative jet fuels* (Technical report prepared for the RAND Corporation, Santa Monica, CA) Retrieved from: http://www.rand.org/pubs/technical_reports/TR554.html

60. Bond, J.Q., Upadhye, A.A., Olcay, H., Tompsett, G.A., Jae, J., Xing, R., Alonso, D.M., Wang, D., Zhang, T., Kumar, R., Foster, A., Sen, S.M., Maravelias, C.T., Malina, R., Barrett, S.R.H., Lobo, R., Wyman, C.E., Dumesic, J.A. & Huber, G.W. (2014). Production of renewable jet fuel range alkanes and commodity chemicals from integrated catalytic processing of biomass. *Energy & Environmental Science, 7,* 1500-1523. DOI: 10.1039/c3ee43846e

61. Cox, K., Renouf, M., Dargan, A., Turner, C. & Klein-Marcuschamer, D. (2014). Environmental life cycle assessment (LCA) of aviation biofuels from microalgae, Pongamia pinnata, and sugarcane molasses. *Biofuels, Bioproducts & Biorefining, 8(4),* 579-593. DOI: 10.1002/bbb.1488

62. Fan, J., Shonnard, D.R., Kalnes, T.N., Johnsen, P.B. & Rao, S. (2013). A life cycle assessment of pennycress (Thlaspi arvense L.) –derived jet fuel and diesel. *Biomass & Bioenergy* 55: 87-100. DOI: 10.1016/j.biombioe.2012.12.040

63. Seber, G., Malina, R., Pearlson, M.N., Olcay, H., Hileman, J.I. & Barrett, S.R.H. (2014). Environmental and economic assessment of producing hydroprocessed jet and diesel fuel from waste oils and tallow. *Biomass & Bioenergy, 67,* 108-118. DOI: 10.1016/j.biombioe.2014.04.024

64. Shonnard, D.R., Williams, L. & Kalnes, T.B. (2010). Camelina-derived jet fuel and diesel: sustainable advanced biofuels. *Environmental Progress & Sustainable Energy, 29(3),* 382-392. DOI: 10.1002/ep.10461

65. Pearlson, M.N., Wollersheim, C.W. & Hileman, J.I. (2013). A techno-economic review of hydroprocessed renewable esters and fatty acids for jet fuel production. *Biofuels, Bioproducts & Biorefining, 7(1),* 89-96. DOI: 10.1002/bbb.1378

66. Langeveld, J.W.A., Dixon, J., van Keulen, H. & Quist-Wessel, P.M.F. (2014). Analyzing the effect of biofuel expansion on land use in major producing countries: evidence of increased multiple cropping. *Biofuels, Bioproducts & Biorefining, 8(1),* 49-58. DOI: 10.1002/bbb.1432

67. Wigmosta, M.K., Coleman, A.M., Skaggs, R.J., Huesemass, M.H. & Lane, L.J. (2011). National microalgae biofuel production potential and resource demand. *Water Resources Research, 47(3),* 1-13. DOI: 10.1029/2010WR009966

68. Rose, S.K., Kriegler, E., Bibas, R., Calvin, K., Popp, A., van Vuuren, D.P. & Weyant, J. (2014). Bioenergy in energy transformation and climate management. *Climatic Change, 123(3),* 477-493. DOI: 10.1007/s10584-013-0965-3

69. Humpenoeder, F., Popp, A., Dietrich, J.P, Klein, D., Lotze-Campen, H., Bonsch, M., Bodirsky, B.L., Weindl, I., Stevanovic, M. & Mueller, C. (2014). Investigating afforestation and bioenergy CCS as climate change mitigation strategies. *Environmental Research Letters, 9(6),* 1-13. DOI: 10.1088/1748-9326/9/6/064029

70. Azar, C., Johansson, D.J.A. & Mattsson, N. (2013). Meeting global temperature targets – the role of bioenergy with carbon capture and storage. *Environmental Research Letters, 8(3),* 1-8. DOI: 10.1088/1748-9326/8/3/034004

71. International Energy Agency (IEA) (2016). *CO_2 emissions from fuel combustion: highlights.* (Technical report prepared at OECD/IEA, Paris) Retrieved from: https://www.iea.org/publications/freepublications/publication/CO2EmissionsfromFuelCombustion_Highlights_2016.pdf

72. United States Environmental Protection Agency (US EPA) (2016). Renewable Fuel Standard (RFS2): Final rule additional resources. Retrieved from: https://www.epa.gov/renewable-fuel-standard-program/renewable-fuel-standard-rfs2-final-rule-additional-resources

73. United States Energy Information Administration (US EIA) (2016). Short-term energy outlook: US liquid fuels. Retrieved from: http://www.eia.gov/outlooks/steo/report/us_oil.cfm

74. Renewable Energy Policy Network for the 21st Century (2016). Renewables 2016 global status report. Retrieved from: http://www.ren21.net/wp-content/uploads/2016/10/REN21_GSR2016_FullReport_en_11.pdf

75. United States Environmental Protection Agency (US EPA) (2016a). Fuels registration, reporting, and compliance help: 2015 Renewable Fuel Standard data. Retrieved from: https://www.epa.gov/fuels-registration-reporting-and-compliance-help/2015-renewable-fuel-standard-data

76. International Civil Aviation Organization (ICAO) (2013). *Present and future trends in aircraft noise and emissions.* (Working paper A38-WP/26 presented to the 38th assembly of the Committee for Aviation Environmental Protection) Retrieved from: http://www.icao.int/Meetings/a38/Documents/WP/wp026_en.pdf

77. Owen, B., Lee, D.S. & Lim, L. (2010) Flying in the future: aviation emissions scenarios to 2050. *Environmental Science & Technology, 44,* 2255-2260. DOI: 10.1021/es902530z

78. The World Bank (2016). GDP growth (annual %). Retrieved from: http://data.worldbank.org/indicator/NY.GDP.MKTP.KD.ZG?end=2015&locations=1W&start=2004

79. International Air Transport Association (IATA) (2016). Fact sheet industry statistics. Retrieved from: http://www.iata.org/pressroom/facts_figures/fact_sheets/Documents/fact-sheet-industry-facts.pdf

80. Kar, R., Bonnefoy, P.A. & Hansman, R.J. (2010). Dynamics of implementation of mitigating measures to reduce CO_2 emissions from commercial aviation. (Technical report no. ICAT-2010-01 prepared at MIT, Cambridge, MA) Retrieved from: https://dspace.mit.edu/bitstream/handle/1721.1/56268/Kar_et_al_ICAT_Report.pdf

81. International Civil Aviation Organization (ICAO) (2016). *Resolution A39-3: Consolidated statement of continuing ICAO policies and practices related to environmental protection – global market-based measure (MBM).* (Assembly resolution A39-3 adopted by ICAO, Montreal, Canada). Retrieved from: http://www.icao.int/environmental-protection/Documents/Resolution_A39_3.pdf

82. United States Energy Information Administration (US EIA) (2016a). US aviation gasoline all sales/deliveries by prime supplier. Retrieved from: http://www.eia.gov/dnav/pet/hist/LeafHandler.ashx?n=pet&s=c400000001&f=a

83. United States Energy Information Administration (US EIA) (2016b). US kerosene-type jet fuel all sales/deliveries by prime supplier. Retrieved from: http://www.eia.gov/dnav/pet/hist/LeafHandler.ashx?n=pet&s=c500000001&f=a

84. Waterland, L.R., Venkatesh, S. & Unnasch, S. (2003). *Safety and performance assessment of ethanol/diesel blends (e-diesel).* (Technical report NREL/SR-540-34817 prepared for the National Renewable Energy Laboratory, Golden, CO).

85. ElMekawy, A., Diels, L., De Wever, H. & Pant, D. (2013). Valorization of cereal based biorefinery byproducts: reality and expectations. *Environmental Science & Technology, 47(16),* 9014-9027. DOI: 10.1021/es402395g

86. ElMekawy, A., Diels, L., Bertin, L., De Wever, H. & Pant, D. (2014). Potential biovalorization techniques for olive mill biorefinery wastewater. *Biofuels, Bioproducts & Biorefining, 8(2),* 283-293. DOI: 10.1002/bbb.1450

87. ASTM International. (2016). *ASTM D7566-16b Standard Specification for Aviation Turbine Fuel Containing Synthesized Hydrocarbons.* Retrieved from: https://doi.org/10.1520/D7566-16B

88. Limayem, A. & Ricke, S.C. (2012). Lignocellulosic biomass for bioethanol production: current perspectives, potential issues and future prospects. *Progress in Energy and Combustion Science, 38,* 449-467. DOI: :10.1016/j.pecs.2012.03.002

89. Singh, A., Pant, D. & Olsen, S.I. (2013). *Life cycle assessment of renewable energy sources.* London, UK: Springer-Verlag.

90. Singh, A., Pant, D., Korres, N.E., Nizami, A.S., Prasad, S. & Murphy, J.D. (2010). Key issues in life cycle assessment of ethanol production from lignocellulosic biomass: challenges and perspectives. *Bioresource Technology, 101(13),* 5003-5012. DOI: 10.1016/j.biortech.2009.11.062

91. Wang, M., Huo, H. & Arora, S. (2010). Methods of dealing with co-products of biofuels in life-cycle analysis and consequent results within the US context. *Energy Policy, 39(10),* 5726-5736. DOI: 10.1016/j.enpol.2010.03.052

92. Patel, A.D., Meesters, K., den Uil, H., de Jong, E., Blok, K. & Patel, M.K. (2012). Sustainability assessment of novel chemical processes at early stage: application to biobased processes. *Energy & Environmental Science, 5,* 8430-8444. DOI: 10.1039/C2EE21581K

93. Wang, L., Littlewood, J. & Murphy, R.J. (2013). Environmental sustainability of bioethanol production from wheat straw in the UK. *Renewable and Sustainability Energy Reviews, 28,* 715-725. DOI: 10.1016/j.rser.2013.08.031

94. Reap, J., Roman, F., Duncan, S. & Bras, B. (2008). A survey of unresolved problems in life cycle assessment: Parts I and II. *The International Journal of Life Cycle Assessment, 13.* DOI: 10.1007/s11367-008-0008-x, 10.1007/s11367-008-0009-9

95. von der Assen, N., Jung, J. & Bardow, A. (2013). Life-cycle assessment of carbon dioxide capture and utilization: avoiding the pitfalls. *Energy & Environmental Science, 6,* 2721-2734. DOI: 10.1039/C3EE41151F

96. Lobo, P.C., Jaguaribe, E.F., Rodrigues, J. & da Rocha, F.A.A. (2007). Economics of alternative sugar cane milling options. *Applied Thermal Engineering, 27,* 1405-1413. DOI: 10.1016/j.applthermaleng.2006.10.023

97. Ensinas, A.V., Nebra, S.A., Lozano, M.A. & Serra, L.M. (2007). Analysis of process steam demand reduction and electricity generation in sugar and ethanol production from sugarcane. *Energy Conversion and Management, 48,* 2978-2987. DOI: 10.1016/j.enconman.2007.06.038

98. Murphy, J.D. & McKeogh, E. (2004). Technical, economic and environmental analysis of energy production from municipal solid waste. *Renewable Energy, 29,* 1043-1057. DOI: 10.1016/j.renene.2003.12.002

99. United States Department of Energy (US DoE) (2016). *Ethanol production and distribution.* Retrieved from: http://www.afdc.energy.gov/fuels/ethanol_production.html

100. Wang, M., Saricks, C. & Wu, M. (1999). Fuel ethanol produced from Midwest US corn: help or hindrance to the vision of Kyoto? *Journal of the Air & Waste Management Association, 49,* 756-772. DOI: 10.1080/10473289.1999.10463846

101. Mei, F. (2006). *Mass and energy balance for a corn-to-ethanol plant.* (Masters thesis submitted to Washington University, St. Louis, MO). Retrieved from: http://crelonweb.eec.wustl.edu/theses/Masters/Fan%20Mei%20-Master%20thesis.pdf

102. Shapouri, H., Duffield, J.A. & Wang, M. (2002). *The energy balance of corn ethanol: an update.* (Agricultural economic report no. 814 prepared for US Department of Agriculture, Washington, DC). Retrieved from: https://greet.es.anl.gov/files/5dfmot4h

103. Mueller, S. (2008). *Detailed report: 2008 national dry mill corn ethanol survey.* (Technical report prepared at the University of Illinois at Chicago Energy Resources Center, Chicago, IL). Retrieved from: http://ethanolrfa.3cdn.net/2e04acb7ed88d08d21_99m6idfc1.pdf

104. Kwiatkowski, J.R., McAloon, A.J., Taylor, F. & Johnston, D.B. (2006). Modeling the process and costs of fuel ethanol production by the corn dry-grind process. *Industrial Crops and Products, 23,* 288-296. DOI: 10.1016/j.indcrop.2005.08.004

105. Phillips, S., Aden, A., Jechura, J., Dayton, D. & Eggerman, T. (2007). *Thermochemical ethanol via indirect gasification and mixed alcohol synthesis of lignocellulosic biomass.* (Technical report NREL/TP-510-41168 prepared at the National Renewable Energy Laboratory, Golden, CO). Retrieved from: http://energy.gov/sites/prod/files/2014/03/f14/41168.pdf

106. Kumar, D. & Murthy, G.S. (2011). Impact of pretreatment and downstream processing technologies and economics and energy in cellulosic ethanol production. *Biotechnology for Biofuels, 4(27),* DOI: 10.1186/1754-6834-4-27

107. Tao, L., Aden, A., Elander, R.T., Pallabolu, V.R., Lee, Y.Y., Garlock, R.J., Balan, V., Dale, B.E., Kim, Y., Mosier, N.S., Ladisch, M.R., Falls, M., Holtzapple, M.T., Sierra, R., Shi, J., Ebrik, M.A., Redmond, T., Yang, B., Wyman, C.E., Hames, B., Thomas, S. & Warner, R.E. (2011). Process and technoeconomic analysis of leading pretreatment technologies for lignocellulosic ethanol production using switchgrass. *Bioresource Technology, 102,* 11105-11114. DOI: 10.1016/j.biortech.2011.07.051

108. Wyman, C.E., Dale, B.E., Elander, R.T., Holtzapple, M., Ladisch, M.R. & Lee, Y.Y. (2005). Coordinated development of leading biomass pretreatment technologies. *Bioresource Technology, 96,* 1959-1966. DOI: 10.1016/j.biortech.2005.01.010

109. Aden, A., Ruth, M., Ibsen, K., Jechura, J., Neeves, K., Sheehan, J., Wallace, B., Montague, L., Slayton, A. & Lukas, J. (2002). *Lignocellulosic biomass to ethanol process design and economics utilizing co-current dilute acid prehydrolysis and enzymatic hydrolysis for corn stover.* (Technical report NREL/TP-510-32438 prepared at the National Renewable Energy Laboratory, Golden, CO). Retrieved from: http://energy.gov/sites/prod/files/2014/03/f14/32438.pdf

110. Humbird, D., Davis, R., Tao, L., Kinchin, C., Hsu, D., Aden, A., Schoen, P., Lukas, J., Olthof, B., Worley, M., Sexton, D. & Dudgeon, D. (2011). *Process design and economics for biochemical conversion of lignocellulosic biomass to ethanol: dilute acid pretreatment and enzymatic hydrolysis of corn stover.* (Technical report NREL/TP-510-32438 prepared at the National Renewable Energy Laboratory, Golden, CO). Retrieved from: http://www.nrel.gov/docs/fy11osti/47764.pdf

111. Domalski, E.S., Jobe Jr., T.L. & Milne, T.A. (1986) *Thermodynamic data for biomass conversion and waste incineration.* (Technical report prepared for the US Department of Energy, Washington, DC). Retrieved from: http://www.nrel.gov/docs/legosti/old/2839.pdf

112. Quaak, P., Knoef, H. & Stassen, H. (1999). *Energy from biomass: a review of combustion and gasification technologies.* (Technical paper no. 422 prepared by the World Bank, Washington, DC). Retrieved from: http://documents.worldbank.org/curated/en/936651468740985551/Energy-from-biomass-a-review-of-combustion-and-gasification-technologies

113. Staples, M.D. (2011). *Personal communication with Dr. Hussain Abidi, post-doctoral researcher at MIT.* Email received on November 28, 2011.

114. United States Patent Application Publication (2013). *Bioprocess and microbe engineering for total carbon utilization in biofuel production.* (Patent application no. US2011/0177564A21 filed by Prof. Gregory Stephanopoulos)

115. United States Patent Application Publication (2013). *Method and compositions for enhanced production of fatty aldehydes and fatty alcohols.* (Patent application no. US2013/0035513 filed by Dr. Zhihao Hu)

116. Dugar, D. & Stephanopoulos, G. (2011). Relative potential of biosynthetic pathways for biofuels and bio-based products. *Nature Biotechnology, 29,* 1074-1078. DOI: 10.1038/nbt.2055

117. Najafpour, G.D. (2007). *Biochemical engineering and biotechnology.* Elsevier B.V., Chapters 3 & 6

118. Couper, J.R., Penney, W.R., Fair, J.R. & Walas, S.M. (2012). *Chemical process equipment.* Elsevier Inc., Chapter 10.

119. Vasudevan, V., Stratton, R.W., Pearlson, M.N., Jersey, G.R., Beyene, A.G., Weissman, J.C., Rubino, M. & Hileman, J.I. (2012). Environmental performance of algal biofuel technology options. *Environmental Science & Technology, 46(4),* 2451-2459. DOI: 10.1021/es2026399

120. Sheehan, J., Camobreco, V., Duffield, J., Graboski, M. & Shapouri, H. (1998). *Life cycle inventory of biodiesel and petroleum diesel for use in an urban bus.* (Technical report NREL/SR-580-24089 prepared at the National Renewable Energy Laboratory, Golden, CO). Retrieved from: http://www.nrel.gov/docs/legosti/fy98/24089.pdf

121. Vaswani, S. (2010). *Biofuels from algae.* (Technical report no. 278 prepared by SRI Consulting). Retrieved from: https://www.ihs.com/pdf/RP278_toc_173691110917062932.pdf

122. Minnesota Technical Assistance Program (MnTAP) (2008). *Ethanol benchmarking and best practices.* (Technical report).

123. Hu, Q., Sommerfeld, M., Jarvis, E., Ghirardi, M., Posewitz, M., Seibert, M. & Darzins, A. (2008). Microalgal triacylglycerols as feedstocks for biofuel production: perspectives and advances. *The Plant Journal, 54,* 621-639. DOI: 10.1111/j.1365-313X.2008.03492.x

124. Staples, M.D. (2012). *Personal communication with Kevin Weiss, CEO of Byogy Renewable Inc.* Email received on August 8, 2012.

125. Staples, M.D. (2012). *Personal communication with Glenn Johnston, VP of Regulatory Affairs for Gevo Inc.* Email received on March 21, 2012.

126. Asia-Pacific Economic Co-operation Energy Working Group (2010). *Biofuel costs, technologies and economics in APEC economies.* (Technical report APEC#210-RE-01.21). Retrieved from: http://publications.apec.org/publication-detail.php?pub_id=1121

127. Goldemberg, J. (2008). The Brazilian biofuels industry. *Biotechnology for Biofuels, 1(6).* DOI: 10.1186/1754-6834-1-6

128. Urbanchuk, J. (2010). *Current state of the US ethanol industry.* (Technical report prepared by Cardno ENTRIX for the US Department of Energy, Washington, DC). Retrieved from: http://www1.eere.energy.gov/bioenergy/pdfs/current_state_of_the_us_ethanol_industry.pdf

129. Wallace, R., Ibsen, K., McAloon, A. & Yee, W. (2005). *Feasibility study for co-locating and integrating ethanol production plants from corn starch and lignocellulosic feedstocks.* (Technical report NREL/TP-510-37092 prepared at the National Renewable Energy Laboratory, Golden, CO). Retrieved from: http://www.nrel.gov/docs/fy05osti/37092.pdf

130. Bain, R.L. (2007). *World biofuels assessment.* (Technical report NREL/MP-510-42467 prepared at the National Renewable Energy Laboratory, Golden, CO). Retrieved from: http://www.nrel.gov/docs/fy08osti/42467.pdf

131. Handwerk, G.E. & Gary, J.H. (2001). *Petroleum refining: technology and economics (4th ed.).* New York, NY: CRC Press.

132. United States Energy Information Administration (US EIA) (2013). *US natural gas industrial price.* Retrieved from: http:// www.eia.gov/dnav/ng/hist/n3035us3m.htm

133. Shapouri, H. & Salassi, M. (2006). *The economic feasibility of ethanol production from sugar in the United States.* (Technical report prepared at the US Department of Agriculture). Retrieved from: http://www.usda.gov/oce/reports/energy/EthanolSugarFeasibilityReport3.pdf

134. Index Mundi (2013). *Sugar monthly price – US cents per pound.* Retrieved from: http:// www.indexmundi.com/commodities/?commodity1/4sugar

135. da Rosa, A. (2009) *Fundamentals of renewable energy processes (3rd ed.).* Elsevier.

136. Index Mundi (2013). *Maize (corn) daily price.* Retrieved from: http://www.indexmundi.com/ commodities/?commodity1/4corn

137. Perlack, R.D. & Stokes, B.J. (2011). *US billion-ton update: biomass supply for a bioenergy and bioproducts industry.* (Technical report ORNL/TM-2011/224 prepared at the Oakridge National Laboratory, Oak Ridge, TN). Retrieved from: http://energy.gov/sites/prod/files/2015/01/f19/billion_ton_update_0.pdf

138. United States Energy Information Administration (US EIA) (2013a). *Petroleum and other liquids.* Retrieved from: http://www.eia.gov/ petroleum/data.cfm

139. Lapola, D.M., Schaldach, R., Alcamo, J., Bondeau, A., Koch, J., Koelking, C. & Priess, J.A. (2010). Indirect land-use changes can overcome carbon savings from biofuels in Brazil. *Proceeding of*

the National Academy of Sciences of the United States of America, 107(8), 3388-3393. DOI: 10.1073/pnas.0907318107

140. United States Department of Agriculture (US DoA). (2013). *National Agricultural Statistics Service.* Retrieved from: http://www.nass.usda.gov/

141. Wullschleger, S.D., Davis, E.B., Borsuk, M.E., Gunderson, C.A. & Lynd, L.R. (2010). Biomass production in switchgrass across the United States: database description determinants of yield. *Agronomy Journal, 102(4),* 1158-1168. DOI: 10.2134/agronj2010.0087

142. United States Energy Information Agency (US EIA) (2016c). *US Gulf Coast Kerosene-Type Jet Fuel Spot Price FOB.* Available: https://www.eia.gov/dnav/pet/hist/LeafHandler.ashx?n=pet&s=eer_epjk_pf4_rgc_dpg&f=m

143. United States Energy Information Agency (US EIA) (2016d). *International energy outlook 2016: petroleum and other liquid fuels.* (Technical report DOE/EIA-0484(2016) prepared at the US Department of Energy) Retrieved from: http://www.eia.gov/outlooks/ieo/liquid_fuels.cfm

144. Seabra, J.E.A., Macedo, I.C., Chum, H.L., Faroni, C.E. & Sarto, C.A. (2011). Life cycle assessment of Brazilian sugarcane products: GHG emissions and energy use. *Biofuels, bioproducts & biorefining, 5(5),* 519-532. DOI: 10.1002/bbb.289

145. Hsu, D.D., Inman, D., Heath, G.A., Wolfrum, E.J., Mann, M.K., Aden, A. (2010). Life cycle environmental impacts of selected US ethanol production and use pathways in 2022. *Environmental Science & Technology, 44(13),* 5289-5297. DOI: 10.1021/es100186h

146. Aden, A., Foust, T. (2009). Technoeconomic analysis of the dilute sulfuric acid and enzymatic hydrolysis process for the conversion of corn stover to ethanol. *Cellulose, 16(4),* 535-545. DOI: 10.1007/s10570-009-9327-8

147. Nagarajan, S., Chou, S.K., Cao, S., Wu, C. & Zhou, Z. (2013). An updated comprehensive techno-economic analysis of algae biodiesel. *Bioresource Technology, 145,* 150-156. DOI: 10.1016/j.biortech.2012.11.108

148. Bann, S.J., Malina, R., Staples, M.D., Suresh, P., Pearlson, M., Tyner, W.E., Hileman, J.I., & Barrett, S.R.H. (2016). The costs of production of alternative jet fuel: a harmonized stochastic assessment. *Bioresource Technology, 277,* 179-187. DOI: 10.1016/j.biortech.2016.12.032

149. Suresh, P. (2016). *Environmental and economic assessment of transportation fuels from municipal solid waste* (Masters thesis submitted to the Massachusetts Institute of Technology). Retrieved from DSpace@MIT.

150. Staples, M.D., Olcay, H., Malina, R., Trivedi, P., Pearlson, M.N., Strzepek, K., Paltsev, S.V., Wollersheim, C. & Barrett, S.R.H. (2013). Water consumption footprint and land requirements of large-scale alternative diesel and jet fuel production. *Environmental Science & Technology, 47,* 12557-12565. DOI: 10.1021/es4030782

151. Hoekman, S.K. (2009). Biofuels in the US – challenges and opportunities, *Renewable Energy, 34,* 14-22. DOI: 10.1016/j.renene.2008.04.030

152. Stratton, R.W., Wolfe, P.J. & Hileman, J.I. (2011). Impact of aviation non-CO2 combustion effects on the environmental feasibility of alternative jet fuels. *Environmental Science & Technology, 45,* 10736-10743. DOI: 10.1021/es2017522

153. ARGUS Media Ltd. (2013). *Argus white paper: Argus RINs prices.* Retrieved from: http://www.argusmedia.com/~/media/files/pdfs/white-paper/argus-rins-prices-2013.pdf/?la=en

154. United States Energy Information Agency (US EIA) (2015). *Annual energy outlook 2015 with projections to 2040.* Retrieved from: https://www.eia.gov/forecasts/archive/aeo15/pdf/0383(2015).pdf

155. United States Government Interagency Working Group on Social Cost of Carbon (2015). *Technical update of the social cost of carbon for regulatory impact analysis – under Executive Order 12866.* Retrieved from: https://www.whitehouse.gov/sites/default/files/omb/inforeg/scc-tsd-final-july-2015.pdf

156. Chen, X. & Khanna, M. (2012). Explaining the reductions in US corn ethanol processing costs: testing competing hypotheses. *Energy Policy, 44,* 153-159. DOI: 10.1016/j.enpol.2012.01.032

157. Hettinga, W.G., Junginger, H.M., Dekker, S.C., Hoogwijk, M., McAloon, A.J., & Hicks, K.B. (2009). Understanding the reductions in US corn ethanol production costs: an experience curve approach. *Energy Policy, 37,* 190-203. DOI: 10.1016/j.enpol.2008.08.002

158. van den Wall Bake, J.D., Junginger, M., Faaij, A., Poot, T. & Walter, A. (2009). Explaining the experience curve: cost reductions of Brazilian ethanol from sugarcane. *Biomass and Bioenergy, 33,* 644-658. DOI: 10.1016/j.biombioe.2008.10.006

159. Goldemberg, J., Teixeira Coelho, S., Nastari, P.M. & Lucon, O. (2004). Ethanol learning curve – the Brazilian experience. *Biomass and Bioenergy, 26,* 301-304. DOI: 10.1016/S0961-9534(03)00125-9

160. Berghout, N.A. (2008). *Technological learning in the German biodiesel industry.* (Masters thesis submitted to Utrecht University, Netherlands) Retrieved from https://www.researchgate.net/publication/235704228_Technological_learning_in_the_German_biodiesel_industry_An_experience_curve_approach_to_quantify_reductions_in_production_costs_energy_use_and_greenhouse_gas_emissions.

161. Nogueira, L.A.H., Capaz, R.S., Souza, S.P. & Seabra, J.E.A. (2016). Biodiesel program in Brazil: learning curve over ten years (2005-2015). *Biofuels, Bioproducts and Biorefining, 10(6),* 728-737. DOI: 10.1002/bbb.1718

162. Stratton, R.W., Wong, H.M. & Hileman, J.I. (2010). Life cycle greenhouse gas emissions from alternative jet fuels. (Technical report no. PARTNER-COE-2010-001 prepared at MIT, Cambridge, MA). Retrieved from: http://web.mit.edu/aeroastro/partner/reports/proj28/partner-proj28-2010-001.pdf

163. Olcay, H., Seber, G., Malina, R., & Barrett, S.R.H. (2013). *Life cycle analysis for fully-synthetic jet fuel production.* (Technical Final Report for Phase I and II of Continuous Lower Energy, Emissions and Noise (CLEEN) program).

164. Mahashabde, A., Wolfe, P., Ashok, A., Dorbian, C., He, Q., Fan, A., Lukachko, S., Mozdzanowska, A., Wollersheim, C., Barrett, S.R.H., Locke, M., & Waitz, I.A. (2011). Assessing the

environmental impacts of aircraft noise and emissions. *Progress in Aerospace Sciences, 47(1),* 15-52. DOI: 10.1016/j.paerosci.2010.04.003

165. Hasselmann, K., Hasselman, S., Giering, R., Ocana, V., & Storch, H.V. (1997). Sensitivity study of optimal CO2 emission paths using a simplified structural integrated assessment model (SIAM). *Climatic Change, 37(2),* 345-386. DOI: 10.1023/A:1005339625015

166. Nordhaus, W.D. (1992). *The 'DICE' model: background and structure of a dynamic integrated climate-economy model of the economics of global warming.* Cowles Foundation Discussion Papers 1009. Retrieved from: http://cowles.yale.edu/sites/default/files/files/pub/d10/d1009.pdf

167. Nordhaus, W.D. (2008). *A question of balance: Weighing the options on global warming policies.* New Haven, CT: Yale University Press.

168. Wolfe, P. (2012). *Aviation environmental policy effects on national- and regional-scale air quality, noise, and climate impacts.* (Masters thesis submitted to the Massachusetts Institute of Technology). Retrieved from DSpace@MIT.

169. United States Office of Management and Budget (US OMB). (2016). *Circular A-94 Appendix C, Revised November 2015, Discount rates for cost-effectiveness, lease purchase, and related analyses.* Available: https://www.whitehouse.gov/omb/circulars_a094/a94_appx-c

170. Mishan E.J., & Quah E. (2007). *Cost–benefit analysis.* New York, NY: Routledge.

171. Withers, M.R., Malina, R., Gilmore, C.K., Gibbs, J.M., Trigg, C., Wolfe, P.J., Trivedi, P., & Barrett, S.R.H. (2014). Economic and environmental assessment of liquefied natural gas as a supplemental aircraft fuel. *Progress in Aerospace Sciences, 66,* 17-36. http://dx.doi.org/10.1016/j.paerosci.2013.12.002

172. Ford, G.S. (2011). An investigation into the relationship of retail gas prices on oil company profitability. *Applied Economics, 43(27),* 4033-4041. DOI: 10.1080/00036841003781486

173. United States Government Accountability Office (US GAO). (2013). *Corporate Income Tax: Effective Tax Rates Can Differ Significantly from the Statutory Rate* (GAO-13-520). Available: http://gao.gov/assets/660/654957.pdf

174. Jongschaap, R.E.E., Corre, W.J., Bindraban, P.S. & Brandenburg, W.A. (2007). *Claims and facts on jatropha curcas L.* (Technical report 158 prepared by Plant Research International, Wageningen UR, Netherlands) Retrieved from: http://edepot.wur.nl/41683

175. English, B.C., De La Torre Ugarte, D.G., Hellwinckel, C., Jensen, K.L., Menard, R.J., West, T.O. & Clark, C.D. (2010). *Implications of energy and carbon policies for the agriculture and forestry sectors.* (Technical report prepared at the University of Tennessee, TN). Retrieved from: http://beag.ag.utk.edu/pub/UTReportNov19.pdf

176. Biggs, L. & Giles, D. (2013). *Current and future agricultural practices and technologies which affect fuel efficiency.* (Technical report IEE/09/764/SI2.558250 prepared for the European Commission, Brussels). Retrieved from: https://ec.europa.eu/energy/intelligent/projects/sites/iee-projects/files/projects/documents/efficient20_review_of_agricultural_practices_and_technologies_en.pdf

177. Minnesota Project (2010). *Energy efficient farms: identifying the proper improvements.* (Technical report prepared for the Office of Energy Security, Minnesota Department of Commerce, MN). Retrieved from: http://www.cleanenergyresourceteams.org/sites/default/files/Farm_EE_ProperImprovementsGuide.pdf

178. United States Department of Agriculture Economic Research Service (USDA ERS) (2014) *Fertilizer use and price, 1960-2012 dataset.* Retrieved from: http://www.ers.usda.gov/data-products/fertilizer-use-and-price.aspx

179. Rosas, F. (2011). *World fertilizer model – the WorldNPK model.* (Working paper 11-WP 520, Iowa State University, Center for Agricultural and Rural Development, Ames, IA) Retrieved from: http://www.card.iastate.edu/products/publications/pdf/11wp520.pdf

180. Pradhan, A., Shrestha, D.S., McAloon, A., Yee, W., Haas, M., Duffield, J.A., Shapouri, H. (2011). Energy life-cycle assessment of soybean biodiesel revisited. *Transactions of the ASABE, 54(3),* 1031-1039.

181. Hoy, R., Rohner, R., Liska, A., Luck, J., Isom, L. & Keshwani, D. (2014). *Agricultural industry advanced vehicle technology: benchmark study for reduction in petroleum use.* (Technical report INL/EXT-14-33118, Idaho National Laboratory, Idaho Falls, ID) Retrieved from: https://avt.inl.gov/sites/default/files/pdf/agindustry/AgIndustryAVTbenchmarkStudy.pdf

182. United Kingdom Department for Environment, Food & Rural Affairs (UK DEFRA) (2013). *British survey of fertilizer practice 2013 – annual report.* (Technical report for UK government, London, UK) Retrieved from: https://www.gov.uk/government/uploads/system/uploads/attachment_data/file/301474/fertiliser use-report2013-08apr14.pdf

183. Malaysian Palm Oil Board (MPOB) (2014). *Oil palm & the environment (updated March 2014).* Official portal of the MPOB. Retrieved from: http://www.mpob.gov.my/palm-info/environment/520-achievements

184. Goh, K.J. & Hardter, R. (2003). General oil palm nutrition, in: *Oil palm: management for large and sustainable yields.* Fairhurst, T.H. & Hardter, R. (eds.), Switzerland, PPI, pp. 191-230.

185. Ludin, N.A., Bakri, M.A.M., Kamaruddin, N., Sopian, K., Deraman, M.S., Hamid, N.H., Asim, N. & Othman, Y. (2014). Malaysian oil palm plantation sector: exploiting renewable energy toward sustainable production. *Journal of Cleaner Production, 65,* 9-15.

186. Whitaker, M. & Heath, G. (2009). *Life cycle assessment of the use of jatropha biodiesel in Indian locomotives.* (Technical report NREL/TP-6A2-44428, National Renewable Energy Laboratory). Retrieved from: http://www.nrel.gov/docs/fy09osti/44428.pdf

187. FACT Foundation (2010). *The jatropha handbook: from cultivation to application.* (Technical report prepared for the Dutch Ministry of Environment, Netherlands). Retrieved from: http://www.jatropha.pro/PDF%20bestanden/FACT_Foundation_Jatropha_Handbook_2010.pdf

188. Macedo, I.C., Seabra, J.E.A. & Silva, J.E.A.R. (2008). Greenhouse gas emissions in the production and use of ethanol from sugarcane in Brazil: the 2005/2006 averages and a prediction for 2020. *Biomass & Bioenergy, 32,* 582-595. DOI: 10.1016/j.biombioe.2007.12.006

189. Mulkey, V.R., Owens, V.N. & Lee, D.K. (2006). Management of switchgrass-dominated conservation reserve program lands for biomass production in South Dakota. *Crop Science, 46(2),* 712-720. DOI: 10.2135/cropsci2005.04-0007

190. Thomson, A.M., Izarrualde, R.C., West, T.O., Parrish, D.J., Tyler, D.D. & Williams, J.R. (2009). *Simulating potential switchgrass production in the United States.* (Technical report PNNL-19072, Pacific Northwest National Laboratory, Richland, WA). Retrieved from: http://www.globalchange.umd.edu/data/publications/PNNL-19072-USSwitchgrass.pdf

191. Hess, J.R., Kenney, K.L., Ovard, L.P., Searcy, E.M. & Wright, C.T. (2009). *Commodity-scale production of an infrastructure-compatible bulk solid from herbaceous lignocellulosic biomass.* (Technical report INL/EXT-09-17527, Idaho National Laboratory, Idaho Falls, ID). Retrieved from: https://bioenergy.inl.gov/Reports/Uniform%20Format%20Bioenergy%20Feedstock.pdf

192. Giuntoli, J., Agostini, A., Edwards, R. & Marelli, L. (2015). *Solid and gaseous bioenergy pathways: input values and GHG emissions.* (Technical report EUR 27215 EN, European Union Joint Research Centre, Brussels, Belgium). Retrieved from: https://ec.europa.eu/energy/sites/ener/files/documents/Solid%20and%20gaseous%20bioenergy%20pathways.pdf

193. Grasso, F.V., Montoya, P.A., Camusso, C.C. & Maroto, B.G. (2012). Improvement of soybean oil solvent extraction through enzymatic pretreatment. *International Journal of Agronomy, 2012,* DOI: 10.1155/2012/543230

194. Shahidi, F. (1990). *Canola and rapeseed: production, chemistry, nutrition and processing technology.* New York, NY: Springer US.

195. Malaysian Economic Transformation Programme (2014). EPP 4: increasing oil extraction rate. (Technical report to the Malaysian Economic Transformation Programme) Retrieved from: http://etp.pemandu.gov.my/Palm_Oil-@-Palm_Oil_-%E2%97%98-_Rubber_-_EPP_4-;_Increasing_the_Oil_Extraction_Rate_(OER).aspx

196. System Dynamics Society (2016). Introduction to system dynamics. *Website of the System Dynamics Society.* Retrieved from: http://www.systemdynamics.org/what-is-s/

197. Sterman, J. (2000). *Business dynamics: systems thinking and modeling for a complex world.* Boston, MA: Irwin McGraw-Hill.

198. Feng, Y.Y, Chen, S.Q. & Zhang, L.X. (2013). System dynamics modeling for urban energy consumption and CO2 emissions: A case study of Beijing, China. *Ecological Modeling, 252,* 44-52. DOI: 10.1016/j.ecolmodel.2012.09.008

199. Hsu, C.-W. (2012). Using a system dynamics model to assess the effects of subsidies and feed-in tariffs on solar PV installations. *Applied Energy, 100,* 205-217.

200. Keith, D.R. (2014). Natural gas pathways and alternative-fuel vehicle diffusion in the US automotive fleet. *Proceedings of the 2014 International System Dynamics Society Conference,* Albany, NY.

201. Shafiei, E., Davidsdottir, B., Leaver, J., Stefansson, H., Asgeirsson, E.I. & Keith, D.R. (2016). Analysis of supply-push strategies governing the transition to biofuel vehicles in a market-oriented renewable energy system. *Energy, 94,* 409-421. DOI: 10.1016/j.energy.2015.11.013

202. Vimmerstedt, L.J., Bush, B. & Peterson, S.O. (2015). Dynamic modeling of learning in emerging energy industries: the example of advanced biofuels in the United States. Paper presented at the *33rd International Conference of the System Dynamics Society*, Cambridge, MA, July 19-23, 2015.

203. Newes, E., Inman, D. & Bush, B. (2011). Understanding the developing cellulosic biofuels industry through dynamic modeling, in: *Economic effects of biofuel production.* Dos Santos Bernardes, M.A. (ed.), InTech. DOI: 10.5772/17090.

204. McDonald, A. & Schrattenholzer, L. (2001). Learning rates for energy technologies. *Energy Policy, 29,* 255-261. DOI: 10.1016/S0301-4215(00)00122-1

205. Papineau, M. (2006). An economic perspective on experience curves and dynamic economies in renewable energy technologies. *Energy Policy, 34(4),* 422-432. DOI: 10.1016/j.enpol.2004.06.008

206. Roberts, M.J. & Schlenker, W. (2013). Identifying supply and demand elasticities of agricultural commodities: implications for the US ethanol mandate. *American Economic Review, 103(6),* 2265-2295. DOI: 10.1257/aer.103.6.2265

207. Ahlgren, S. & Di Lucia, L. (2014). Indirect land use changes of biofuel production: a review of modeling efforts and policy developments in the European Union. *Biotechnology for Biofuels, 7(35),* DOI: 10.1186/1754-6834-7-35

208. Winchester, N., Malina, R., Staples, M.D. & Barrett, S.R.H. (2015). The impact of advanced biofuels on aviation emissions and operations in the US. *Energy Economics, 49,* 482-491. DOI: 10.1016/j.eneco.2015.03.024

209. Wadud, Z. (2015). Imperfect reversibility of air transport demand: Effects of air fare, fuel prices and price transmission. *Transportation Research Part A, 72,* 16-26. DOI: 10.1016/j.tra.2014.11.005

210. Koopmans, C. & Lieshout, R. (2016). Airline cost changes: To what extent are they passed through to the passenger. *Journal of Air Transport Management, 53,* 1-11. DOI: 10.1016/j.jairtraman.2015.12.013

211. Smyth, M. & Pearce, B. (2008). *Air travel demand.* (International Air Transport Association Economics Briefing No. 9) Retrieved from: http://www.iata.org/publications/economic-briefings/air_travel_demand.pdf

212. Ross, S.M. (2014). Variations on Brownian motion. In *Introduction to Probability Models (11th ed.)* (612-614). Amsterdam: Elsevier.

213. United States Energy Information Agency (US EIA) (2016e). *Global consumption of jet fuel.* Retrieved from: http://www.eia.gov/beta/international/data/browser/#/?pa=0000000000g&c=ruvvvvvfvtvnvv1urvvvvfvvvvvvfvvvou20evvvvvvvvvvnvvuvo&ct=0&tl_id=5-A&vs=INTL.63-2-AFG-TBPD.A&ord=SA&cy=2013&vo=0&v=H&start=1980&end=2014

214. United States Department of Energy (US DoE) (2016). *2016 billion-ton report Vol. 1.* Retrieved from: http://energy.gov/sites/prod/files/2016/08/f33/BillionTon_Report_2016_8.18.2016.pdf

215. Index Mundi (2016a). *No. 11 sugar futures end of day settlement price.* Retrieved from: http://www.indexmundi.com/Commodities/?commodity=sugar

216. Index Mundi (2016b). *Crude palm oil future end of day settlement price.* Retrieved from: http://www.indexmundi.com/commodities/?commodity=palm-oil

217. Index Mundi (2016c). *Rapeseed oil monthly price – US dollars per metric ton.* Retrieved from: http://www.indexmundi.com/commodities/?commodity=rapeseed-oil

218. Index Mundi (2016d). *Soybean oil futures end of day settlement price.* Retrieved from: http://www.indexmundi.com/commodities/?commodity=soybean-oil

219. Index Mundi (2016e). *Corn futures end of day settlement price.* Retrieved from: http://www.indexmundi.com/Commodities/?commodity=corn

220. Index Mundi (2016f). *Sorghum monthly price – US dollars per metric price.* Retrieved from: http://www.indexmundi.com/commodities/?commodity=sorghum

221. The Boeing Company (2015). *Boeing and sustainable aviation biofuel development.* (Press release by the Boeing Company, Seattle, WA). Retrieved from: http://www.boeing.com/resources/boeingdotcom/principles/environment/pdf/Backgrounder_Boeing_biofuel.pdf

222. United States Environmental Protection Agency (US EPA) (2015a). *Advancing sustainable materials management: facts and figures 2013.* (Technical report EPA530-R-15-002) Retrieved from: https://www.epa.gov/sites/production/files/2015-09/documents/2013_advncng_smm_rpt.pdf

223. Barrett, S.R.H., Yim, S.H.L., Gilmore, C.K., Murray, L.T., Kuhn, S.R., Tai, A.P.K., Yantosca, R.M., Byun, D.W., Ngan, F., Li, X., Levy, J.I., Ashok, A., Koo, J., Wong, H.M., Dessens, O., Balasubramanian, S., Fleming, G.G., Pearlson, M.N., Wollersheim, C., Malina, R., Arunachalam, S., Binkowski, F.S., Leibensperger, E.M., Jacob, D.J., Hileman, J.I. & Waitz, I.A. (2012). Public health climate, and economic impacts of desulfurizing jet fuel. *Environmental Science & Technology, 46,* 4275-4282. DOI: 10.1021/es203325a

224. Speth, R., Rojo, C., Malina, R. & Barrett, S.R.H. (2015). Black carbon emission reductions from combustion of alternative jet fuels. *Atmospheric Environment, 105,* 37-42. DOI: 10.1016/j.atmosenv.2015.01.040

225. Caiazzo, F., Malina, R., Staples, M.D., Wolfe, P.J., Yim, S.H.L. & Barrett, S.R.H. (2014). Quantifying the climate impacts of albedo changes due to biofuel production: a comparison with biogeochemical effects. *Environmental Research Letters, 9(2),* DOI: 10.1088/1748-9326/9/2/024015

226. Silalertruksa, T., Gheewala, S.H., Huenecke, K. & Fritsche, U.R. (2012). Biofuels and employment effects: implications for socio-economic development in Thailand. *Biomass & Bioenergy, 46,* 409-418. DOI: 10.1016/j.biombioe.2012.07.019

227. Walter, A., Dolzan, P., Quildran, O., de Oliveira, J.G., da Silva, C., Piacente, F. & Segerstedt, A. (2011). Sustainability assessment of bio-ethanol production in Brazil considering land use change, GHG emissions and socio-economic aspects. *Energy Policy, 39(10),* 5703-5716. DOI: 10.1016/j.enpol.2010.07.043

228. Brown, S.P.A. & Huntington, H.G. (2008). Energy security and climate change protection: complementarity or tradeoff? *Energy Policy, 36(9),* 3510-3513. DOI: 10-1016/j.enpol.2008.05.027

229. World Bank (2015). *State and Trends of Carbon Pricing 2015.* (Technical report prepared by the World Bank and Ecofys for the World Bank, Washington, DC). Retrieved from: http://documents.worldbank.org/curated/en/636161467995665933/pdf/99533-REVISED-PUB-P153405-Box393205B.pdf

230. Koh, L.P. & Ghazoul, J. (2008). Biofuels, biodiversity, and people: Understanding the conflicts and finding opportunities. *Biological Conservation, 141,* 2450-2460. DOI: 10.1016/j.biocon.2008.08.005

231. McLaughlin, S.B. & Walsh, M.E. (1998). Evaluating environmental consequences of producing herbaceous crops for bioenergy. *Biomass & Bioenergy, 14(4),* 317-324.

232. Zilberman, D., Hochman, G., Rajagopal, D., Sexton, S. & Timilsina, G. (2012). The impact of biofuels on commodity prices: assessment of findings. *American Journal of Agricultural Economics,* 1-7. DOI: 10.1093/ajae/aas037

233. Pimentel, D., Marklein, A., Toth, M.A., Karpoff, M.N., Paul, G.S., McCormack, R., Kyriazis, J. & Krueger, T. (2009). Food versus biofuels: environmental and economic costs. *Human Ecology, 37(1).* DOI: 10.1007/s10745-009-9215-8

234. Edwards, M.R. & Trancik, J.E. (2014). Climate impacts of energy technologies depend on emissions timing. *Nature Climate Change, 4,* 347-352. DOI: 10.1038/nclimate2204

235. Withers, M.R., Malina, R., Barrett, S.R.H. (2015). Carbon, climate, and economic breakeven times for biofuel from woody biomass from managed forests. *Ecological Economics, 112,* 45-52. DOI: 10.1016/j.ecolecon.2015.02.004

236. International Institute for Applied Systems Analysis (IIASA) (2012). *Global Agro-ecological Zones (GAEZ v3.0) model documentation.* (Model documentation prepared by IIASA, Laxenburg, Austria) Retrieved from: http://www.gaez.iiasa.ac.at/docs/GAEZ_Model_Documentation.pdf

237. Grassini, P., Eskridge, K.M. & Cassman, K.G. (2013). Distinguishing between yield advances and yield plateaus in historical crop production trends. *Nature Communications, 4,* 1-11. DOI: 0.1038/ncomms3918

238. Achten W.M.J., Verchot, L., Franken, Y.J., Mathijs, E., Singh, V.P., Aerts, R. & Muys, B. (2008). Jatropha bio-diesel production and use. *Biomass & Bioenergy, 32(12),* 1063-1084. DOI: 10.1016/j.biombioe.2008.03.003

239. Hurtt G.C., Chini, L.P., Frolking, S., Betts, R.A., Feddema, J., Fischer, G., Fisk, J.P., Hibbard, K., Houghton, R.A., Janetos, A., Jones, C.D., Kindermann, G., Kinoshita, T., Goldewijk, K.K., Riahi, K., Shevliakova, E., Smith, S., Stehfest, E., Thomson, A., Thornton, P., van Vuuren, D.P. & Wang, Y.P. (2011) Harmonization of land-use scenarios for the period 1500-2100: 600 years of global gridded annual land-use transitions, wood harvest, and resulting secondary lands. *Climatic Change, 109(1),* 117-161. DOI: 10.1007/s10584-011-0153-2

240. van Vuuren D.P., Stehfest, E., den Elzen, M.G.J., Kram, T., van Vliet, J., Deetman, S., Isaac, M., Goldewijk, K.K., Hof, A., Beltran, A.M., Oostenrijk, R. & van Ruijven, B. (2011). RCP2.6:

Exploring the possibility to keep global mean temperature increase below 2°C. *Climatic Change* 109(1): 95-116. DOI: 10.1007/s10584-011-0152-3

241. Thomson, A.M., Calvin, K.V., Chini, L.B., Hurtt, G., Edmonds, J.A., Bond-Lamberty, B., Frolking, S., Wise, M.A., & Janetosa, A.C. (2010). Climate mitigation and the future of tropical landscapes. *Proceedings of the National Academy of Sciences of the United States of America, 107(46),* 19633-19638. DOI: 10.1073/pnas.0910467107

242. Thomson, A.M., Calvin, K.V., Smith, S.J., Kyle, G.P., Volke, A., Patel, P., Delgado-Arias, S., Bond-Lamberty, B., Wise, M.A., Clarke, L.E. & Edmonds, J.A. (2011). RCP4.5: a pathway for stabilization of radiative forcing by 2100. *Climatic Change, 109(1),* 77-94. DOI: 10.1007/s10584-011-0151-4

243. Masui T., Matsumoto, K., Hijoka, Y., Kinoshita, T., Nozawa, T., Ishiwatari, S., Kato, E., Shukla, P.R., Yamagata, Y. & Kainuma, M. (2011). An emissions pathway for stabilization at 6 Wm^{-2} radiative forcing. *Climatic Change, 109(1),* 59-76. DOI: 10.1007/s10584-011-0150-5

244. Riahi K., Rao, S., Krey, V., Cho, C., Chirkov, V., Fischer, G., Kindermann, G., Nakicenovic, N. & Rafaj, P. (2011). RCP8.5 – A scenario of comparatively high greenhouse gas emissions. *Climatic Change, 109(1),* 33-57. DOI: 10.1007/s10584-011-0149-y

245. World Database of Protected Areas (WDPA) (2016). *WDPA dataset.* (Database developed by United Nations Environmental Programme's World Conservation Monitoring Centre) Retrieved from: https://www.protectedplanet.net/